

**T.C.**

**ISTANBUL GEDİK UNIVERSITY  
INSTITUTE OF GRADUATE STUDIES**



**INNOVATIVE NUMERICAL APPROACHES BASED ON TRADITIONAL  
SLOPE STABILITY ANALYSIS METHODS**

**MASTER'S THESIS**

**Ersin YILDIZ**

**Civil Engineering Department**

**Civil Engineering Master's Program with Thesis**

**JANUARY 2021**  
**T.C.**  
**ISTANBUL GEDİK UNIVERSITY**  
**INSTITUTE OF GRADUATE STUDIES**



**INNOVATIVE NUMERICAL APPROACHES BASED ON TRADITIONAL  
SLOPE STABILITY ANALYSIS METHODS**

**MASTER'S THESIS**

**Ersin YILDIZ**  
**181282004**

**Civil Engineering Department**

**Civil Engineering Master's Program with Thesis**

**Thesis Advisor: Asst. Prof. Dr. Mert TOLON**

**JANUARY 2021**



## YEMİN METNİ

Yüksek Lisans tezi olarak sunduğum “Innovative Numerical Approaches based on Traditional Slope Stability Analysis Methods” adlı çalışmanın, tezin proje safhasından sonuçlanmasına kadarki bütün süreçlerde bilimsel ahlak ve geleneklere aykırı düşecek bir yardıma başvurulmaksızın yazıldığını ve yararlandığım eserlerin Bibliyografya’da gösterilenlerden oluştuğunu, bunlara atıf yapılarak yararlanılmış olduğunu belirtir ve onurumla beyan ederim. (15/01/2021)

Ersin YILDIZ





*I would like to thank my dear wife, children and family for their support.*

## **FOREWORD**

The construction industry is developing technology and gaining quality. It is well known that with the population increases in cities, the land values in cities also increases. Innovative solutions are developed as a solution to these problems. Therefore, geotechnical engineering finds a place in slope stability in this perspective. At this point, the stability of slopes is examined to minimize the risk of slope failures. In many important cases in terms of loss of life and property loss, the slope stability phenomena are critical for civil engineers both in the design and the practical areas. According to the literature, it is known that slope stability has been calculated by classical methods until today and that there is not much research about soil behaviour. Knowing the soil and choosing the right method reduces costs and improves safety. Thus, it was deemed appropriate to develop innovative methods in slope stability and investigate stability criteria. The research will be conducted for not a specific area or site; the developed software code will also be applied for any area or site. In this research, slope stability methods will be investigated, and appropriate software will be developed using the Matlab code. Therefore, slope stability criteria will be determined effectively to maximize the results' short calculation times and reliability. In particular, I would like to thank my thesis supervisor, who is Asst. Prof. Dr. Mert TOLON for his valuable information and help, my family who support me, and finally Istanbul Gedik University for help and information.

January 2021

Ersin YILDIZ  
(Civil Engineer)

## ÖNSÖZ

İnşaat sektörü her geçen gün yeni teknoloji geliştiriyor ve kalite kazanıyor. Ayrıca, şehirlerde nüfus arttıkça şehirlerdeki arazi değerlerinin de arttığı bilinmektedir. Bu sorunlara çözüm olarak yenilikçi çözümler geliştirilmektedir. Dolayısıyla geoteknik mühendisliği bu perspektifte şev stabilitesinde kendine yer bulmaktadır. Bu noktada şevin kırılma riskini en aza indirmek için şevlerin stabilitesi incelenir. Can ve mal kaybı açısından birçok önemli durumda, şev stabilitesi fenomeni inşaat mühendisleri için hem tasarım hem de uygulama alanlarında kritik bir konudur. Literatüre göre şev stabilitesinin günümüze kadar klasik yöntemlerle hesaplandığı ve zemin davranışı ile ilgili pek fazla araştırma yapılmadığı bilinmektedir. Zemini bilmek ve doğru yöntemi seçmek, maliyeti düşürür ve güvenliği artırır. Bu nedenle şev stabilitesinde yenilikçi yöntemler geliştirmek ve stabilite kriterlerini araştırmak uygun görülmüştür. Araştırma belirli bir alan veya saha için yapılmayacaktır; geliştirilen yazılım kodu sayesinde herhangi bir alan veya geometri için uygulanabilecektir. Bu araştırmada şev stabilitesi yöntemleri araştırılacak ve Matlab kodu kullanılarak uygun yazılım geliştirilecektir. Böylece, sonuçların kısa sürede hesaplanması ve güvenilirliğini maksimize etmek için şev stabilitesi kriterleri etkin bir şekilde belirlenecektir. Özellikle tez danışmanım Dr. Öğr. Ü. Mert TOLON'a değerli bilgileri ve yardımları için, beni destekleyen aileme ve son olarak İstanbul Gedik Üniversitesi'ne yardım ve bilgileri için teşekkürlerimi sunarım.

Ocak 2021

Ersin YILDIZ  
İnşaat Mühendisi

## CONTENTS

	<u>Page</u>
<b>FOREWORD</b> .....	<b>iii</b>
<b>ÖNSÖZ</b> .....	<b>iv</b>
<b>CONTENTS</b> .....	<b>v</b>
<b>SYMBOLS</b> .....	<b>vii</b>
<b>ABBREVIATIONS</b> .....	<b>ix</b>
<b>TABLE LIST</b> .....	<b>x</b>
<b>FIGURE LIST</b> .....	<b>xi</b>
<b>ABSTRACT</b> .....	<b>xiv</b>
<b>ÖZET</b> .....	<b>xv</b>
<b>1. INTRODUCTION</b> .....	<b>1</b>
1.1 General .....	1
1.2 Objectives .....	2
1.3 Format of the Thesis .....	2
<b>2. LITERATURE REVIEW</b> .....	<b>3</b>
2.1 Introduction .....	3
2.2 History of Slope stability.....	3
2.3 Slope Stability Terminology .....	5
2.4 Slope Stability Parameters .....	6
2.5 Landslide Classification .....	9
2.5.1 Falls .....	10
2.5.2 Toppling .....	11
2.5.3 Slide .....	11
2.5.4 Spread.....	12
2.5.5 Flow .....	14
2.5.6 Complex moments .....	15
2.6 Factors Affecting Mass Movements .....	15
2.7 Types of Slope Failure Modes .....	16
2.7.1 Total stability stress .....	17
2.7.2 Effective stability stress .....	18
2.8 Factors Affecting Slope Stability Analysis .....	20
2.8.1 Failure plane geometry.....	20
2.8.2 Non-homogeneity of soil layers .....	22
2.8.3 Tension crack .....	22
2.8.4 Dynamic loading .....	23
2.9 Limit Equilibrium Analysis.....	24
2.9.1 Cullman method .....	26
2.9.2 Fellenius method (Swedish slice method) .....	26
2.9.3 Bishop and simplified bishop method.....	28
2.9.4 Jambu method .....	30
2.9.5 Spencer method.....	33



2.9.6 Morgenstern-Price method.....	35
2.10 Finite Element Aided Stress Method .....	38
2.10.1 Numerical method and shear strength reduction (SSR) technique .....	39
2.11 Software Used For Slope Stability .....	40
2.11.1 Matlab software.....	45
2.11.2 Slope stability analyses with matlab .....	46
<b>3. DEVELOPED MODEL.....</b>	<b>47</b>
3.1 Input of Data.....	49
3.1.1 Geometry created with the developed model.....	49
3.1.2 Loading with developed model.....	50
3.1.3 Check error list in developed model .....	52
3.2 Dynamic Loading .....	52
3.2.1 Pseudo-static analysis .....	52
3.2.2 Pseudo-static coefficient chosen .....	54
3.2.3 Pseudo-static load in developed model.....	55
3.3 Displacement Calculation .....	55
3.3.1 Newmark sliding block analysis .....	55
3.3.2 Newmark sliding block analysis in developed model.....	59
3.4 General Limit Equilibrium (GLE).....	60
3.4.1 Moment balance safety factor, $F_m$ .....	67
3.4.2 Force balance safety factor, $F_f$ .....	67
3.4.3 Normal force on slice base, $N$ .....	67
3.4.4 Inter-slice forces, $E$ , and $X$ .....	68
3.4.5 Method chosen in the developed model.....	70
3.5 Getting the most critical circle .....	71
3.5.1 Calculating the most critical circle with the developed model .....	72
<b>4. CODE VERIFICATION RESULTS AND DISCUSSION.....</b>	<b>74</b>
4.1 Program Test Examples .....	74
4.1.1 Method chosen with developed model.....	74
4.1.2 Comparison with cases from literature .....	85
<b>5. CONCLUSIONS AND RECOMMENDATIONS.....</b>	<b>97</b>
<b>REFERENCES.....</b>	<b>101</b>
<b>APPENDICES .....</b>	<b>106</b>
<b>RESUME.....</b>	<b>114</b>

## SYMBOLS

$\gamma_{unsat}$	: dry unit weight
$\gamma_{sat}$	: wet unit weight
<b>E50ref</b>	: triaxial loading stiffness
<b>Eoedref</b>	: odometer loading stiffness
<b>Euref</b>	: triaxial loading-unloading stiffness
<b>Fh</b>	: creates the horizontal inertia force.
<b>Fv</b>	: creates the vertical inertia force.
<b>M</b>	: stress-dependent value of stiffness
<b>C</b>	: cohesion
$\phi$	: angle of internal friction
$\psi$	: dilatation angle
<b>OCR</b>	: over-consolidation rate
<b>R</b>	: reduction factor
$\gamma_{unsat}$	: dry unit weight
$\gamma$	: unit volume weight
<b>E</b>	: Modulus of Elasticity
$\nu$	: Poisson Ratio
<b>c</b>	: Cohesion
$\psi$	: Dilatation Angle
$\phi'$	: internal friction angle
$\beta$	: slice base length
<b>H</b>	: slope height
<b>Hw</b>	: water height
<b>kh</b>	: lateral force coefficient
<b>Hb</b>	: distance from heel to solid ground
<b>N</b>	: base normal force = $W \cos\alpha$
<b>W</b>	: weight of the sliding mass.
<b>S<sub>DS</sub></b>	: short-period design spectral acceleration coefficient.
<b>S<sub>T</sub></b>	: short-period design spectral acceleration coefficient.
<b>u</b>	: pore water pressure acting on the base of the slice
<b>b</b>	: slice width
<b>ac</b>	: The critical acceleration
<b>ky</b>	: the horizontal coefficient
$\sigma_n$	: total stress
$\delta$	: Refers to the total displacement on the slope.
<b>N</b>	: the total normal force on the base of the slice
<b>Sm</b>	: the shear force mobilized on the base of each slice
<b>E</b>	: the horizontal interslice normal forces. Subscripts given as L and R indicate the left and right directions of the slice, respectively.
<b>X</b>	: the vertical interslice shear forces. Subscripts given as L and R indicate the left and right directions of the slice, respectively.
<b>D</b>	: an external point load.

- kW** : the horizontal seismic load applied through the centroid of each slice.
- R** : is the radius of the circular sliding surface. Moment arm associated with moving shear force,  $S_m$  for sliding surface shape in any slice
- f** : the perpendicular offset of the normal force from the center of rotation or from the center of moments. A positive slope (a slope facing left) is assumed to be positive at the distances  $f$  to the left of the center of rotation and negative to the right of the center of rotation. The sign rule is reversed for positive slopes.
- x** : the horizontal distance from the centerline of each slice to the center of rotation or to the center of moments.
- e** : vertical distance from the center of gravity of each slice to the moment point.
- d** : perpendicular distance from the center of gravity of each slice to the moment point.
- h** : the vertical distance from the center of the base of each slice to the uppermost line in the geometry (i.e., generally ground surface).
- a** : the perpendicular distance from the resultant external water force to the center of rotation or to the center of moments. The L and R subscripts designate the left and right sides of the slope, respectively.
- A** : the resultant external water forces. The L and R subscripts designate the left and right sides of the slope, respectively.
- $\omega$**  : angle of point load with horizontal. This angle is determined by counterclockwise from the positive x-axis.
- $\alpha$**  : the angle between the tangent to the center of the base of each slice and the horizontal. The sign convention is as follows. When the angle slopes in the same direction as the overall slope of the

## **ABBREVIATIONS**

<b>FEA</b>	: Finite Elements Analysis
<b>LEM</b>	: Limit Equilibrium Method
<b>SSR</b>	: Safety Reduction Factor
<b>GWL</b>	: Groundwater Level
<b>rf</b>	: The Reaction Force Value
<b>sf</b>	: The Slipping Force Value
<b>FS</b>	: Factor of Safety
<b>FOS</b>	: Factor of Safety
<b>M-P</b>	: Morgenstern-Price Method



## TABLE LIST

	<u>Page</u>
<b>Table 2.1</b> : Advised values of soil parameters for LEM. ....	8
<b>Table 2.2</b> : Mohr-Coulomb parameters for LEM program. ....	8
<b>Table 2.3</b> : The order of effects of parameters for slope failure.....	9
<b>Table 2.4</b> : Types of landslides of the shortened version of Varnes's classification of inclination motions. ....	10
<b>Table 2.5</b> : Methods of stability analysis. ....	21
<b>Table 2.6</b> : Comparison of existing analysis methods.....	25
<b>Table 2.7</b> : Software used in slope stability analysis. ....	41
<b>Table 2.8</b> : Software used in the market.....	45
<b>Table 3.1</b> : Pseudo-static results of slope failure effect of an earthquake.....	54
<b>Table 3.2</b> : Comparison of limit equilibrium analysis in terms of moment and force balance.....	61
<b>Table 3.3</b> : Parameters with the known solution in safety factor calculation.....	64
<b>Table 3.4</b> : Parameters with an unknown solution in safety factor calculation.....	65
<b>Table 4.1</b> : Slope height and soil parameters. ....	74
<b>Table 4.2</b> : Slope height and soil parameters. ....	74
<b>Table 4.3</b> : Slope height and soil parameters. ....	85
<b>Table 4.4</b> : Slope height and soil parameters. ....	85
<b>Table 5.1</b> : Summary of FOS outputs.....	98
<b>Table 5.2</b> : Regression statistics. ....	99

## FIGURE LIST

	<u>Page</u>
<b>Figure 2.1</b> : The terminology used to define slopes and its geometry .....	6
<b>Figure 2.2</b> : The ideal material's modulus of elasticity .....	6
<b>Figure 2.3</b> : Mohr-Coulomb material's modulus of elasticity .....	7
<b>Figure 2.4</b> : Slope Geometry model developed for ANN .....	9
<b>Figure 2.5</b> : Falls on the slopes .....	11
<b>Figure 2.6</b> : Toppling on the slopes.....	11
<b>Figure 2.7</b> : Slide on the slopes .....	12
<b>Figure 2.8</b> : Spread on the slopes .....	13
<b>Figure 2.9</b> : Lateral expansion movement in rock .....	13
<b>Figure 2.10</b> : Lateral expansion movement in soil.....	14
<b>Figure 2.11</b> : Flow on the slopes .....	15
<b>Figure 2.12</b> : The complex moment on the slopes .....	15
<b>Figure 2.13</b> : Effective stress below groundwater level.....	17
<b>Figure 2.14</b> : Effective stress below groundwater level graphic.....	17
<b>Figure 2.15</b> : Over consolidated clay. Shear properties of Mohr-Coulomb failure envelopes corresponding to clay.....	18
<b>Figure 2.16</b> : Plasticity Index .....	19
<b>Figure 2.17</b> : Liquid Limit.....	20
<b>Figure 2.18</b> : Circular and non-circular failure surfaces .....	21
<b>Figure 2.19</b> : The minimum FOS variation with the stress crack depth for the fixed $c$ & $\phi'$ .....	23
<b>Figure 2.20</b> : Slope stability analysis methods.....	25
<b>Figure 2.21</b> : Cullman surface failure .....	26
<b>Figure 2.22</b> : Forces acting on a slice and force polygon in the Swiss slice method.....	27
<b>Figure 2.23</b> : Force polygons that are belonging to slices according to the Fellenius method .....	28
<b>Figure 2.24</b> : Forces acting on the slice .....	29
<b>Figure 2.25</b> : Free and force polygon of the object for Bishop's Simplified method .....	30
<b>Figure 2.26</b> : Bishop's Simplified factor of safety.....	31
<b>Figure 2.27</b> : Jambu factor .....	31
<b>Figure 2.28</b> : Free and force polygon of the object for Janbu's method.....	32
<b>Figure 2.29</b> : Janbu's Simplified factor of safety.....	33
<b>Figure 2.30</b> : Free and force polygon of the object for Spencer's method .....	34
<b>Figure 2.31</b> : Spencer factor of safety .....	34
<b>Figure 2.32</b> : Calculation of the security number provides both equilibrium equations in the Spencer method using different $\lambda$ values.....	35
<b>Figure 2.33</b> : Morgenstern-Price method, according to the force function types between slices. ....	36

<b>Figure 2.34</b> : Free and force polygon of the object for M&P's method .....	37
<b>Figure 2.35</b> : Alpha interslice force vs. distance for the M-P method .....	37
<b>Figure 2.36</b> : Comparison of Bishop and M-P methods .....	38
<b>Figure 3.1</b> : Input and output in developed model. ....	47
<b>Figure 3.2</b> : Calculation algorithm in the developed model.....	48
<b>Figure 3.3</b> : Input geometry in developed model. ....	50
<b>Figure 3.4</b> : Loading in developed model. ....	51
<b>Figure 3.5</b> : Water loading in developed model.....	51
<b>Figure 3.6</b> : Check error list in developed model.....	52
<b>Figure 3.7</b> : The loads acting on the triangular fracture surface in pseudo-static loading .....	53
<b>Figure 3.8</b> : Pseudo-static loading in developed model. ....	55
<b>Figure 3.9</b> : a) Sliding Block b)Newmark analysis algorithm .....	56
<b>Figure 3.10</b> : Newmark analysis algorithm in the developed model.....	59
<b>Figure 3.11</b> : Critical acceleration calculation. ....	60
<b>Figure 3.12</b> : Forces that are acting on a slice in a circular sliding circle.....	63
<b>Figure 3.13</b> : Forces that are acting on a slice in a circular sliding non-circle.....	63
<b>Figure 3.14</b> : Comparison of Bishop and M-P methods.....	66
<b>Figure 3.15</b> : Morgenstern-Price (1965) method, according to the force function types between slices.....	69
<b>Figure 3.16</b> : Using the half sine force function with two different lambda values.....	70
<b>Figure 3.17</b> : Method chosen in the developed model. ....	71
<b>Figure 3.18</b> : Grid search pattern .....	72
<b>Figure 3.19</b> : The rectangle is shown in the developed model.....	73
<b>Figure 4.1</b> : SlopeME input of properties: Case 1.....	75
<b>Figure 4.2</b> : SlopeME input of creat slide: Case 1. ....	76
<b>Figure 4.3</b> : SlopeME output of running: Case 1. ....	77
<b>Figure 4.4</b> : SlopeME output of internal forces for slice number 2: Bishop.....	78
<b>Figure 4.5</b> : SlopeME output of internal forces for slice number 2: M&P. ....	78
<b>Figure 4.6</b> : SLOPE/W output of toe failure: Case 1 .....	79
<b>Figure 4.7</b> : SlopeME output of toe failure: Case 1. ....	79
<b>Figure 4.8</b> : SlopeME input of properties: Case 2.....	80
<b>Figure 4.9</b> : SlopeME input of creat slide: Case 2. ....	81
<b>Figure 4.10</b> : SlopeME input of running: Case 2. ....	82
<b>Figure 4.11</b> : SlopeME output of internal forces for slice number 2: Bishop.....	83
<b>Figure 4.12</b> : SlopeME output of internal forces for slice number 2: M&P .....	83
<b>Figure 4.13</b> : SLOPE/W output of toe failure: Case 2 .....	84
<b>Figure 4.14</b> : SlopeME output of toe failure: Case 2. ....	84
<b>Figure 4.15</b> : SlopeME input of properties: Case 3.....	86
<b>Figure 4.16</b> : SlopeME input of creat slide: Case 3. ....	87
<b>Figure 4.17</b> : SlopeME input of running: Case 3. ....	88
<b>Figure 4.18</b> : SlopeME output of internal forces for slice number 10: Bishop.....	88
<b>Figure 4.19</b> : SlopeME output of internal forces for slice number 10: M&P .....	89
<b>Figure 4.20</b> : SLOPE/W output of FOS: Case 3 .....	90
<b>Figure 4.21</b> : SlopeME output of FOS: Case 3. ....	90
<b>Figure 4.22</b> : SlopeME input of properties: Case 4.....	91
<b>Figure 4.23</b> : SlopeME input of creat slide: Case 4. ....	92
<b>Figure 4.24</b> : SlopeME input of running: Case 4. ....	93
<b>Figure 4.25</b> : SlopeME output of internal forces for slice number 10: Bishop.....	94

<b>Figure 4.26</b> : SlopeME output of internal forces for slice number 10: M&P .....	94
<b>Figure 4.27</b> : SLOPE/W output of FOS: Case 4 .....	95
<b>Figure 4.28</b> : SlopeME output of FOS: Case 4. ....	95
<b>Figure 5.1</b> : Line alignment drawing for FOS.....	99





## INNOVATIVE NUMERICAL APPROACHES BASED ON TRADITIONAL SLOPE STABILITY ANALYSIS METHODS

### ABSTRACT

Within the scope of this study, it aimed to develop software licensed by Istanbul Gedik University by writing code with Matlab and the licensed programs used in the sector for the solution of the slope stability problem, which is a problem of geotechnical engineering. This research will start by examining slope stability analysis methods. A calculation model can be created by taking the soil profile parameters from the drilling data and entering these data. The necessary drillings in the case area and the obtained laboratory data are presented for the samples examined. The working area should consist of at least one soil layer. Soil parameters can be entered separately for each layer created. The underground water level can also be entered optionally. Limit Equilibrium Method (LEM) has been chosen for the calculation analysis method. Computing LEM calculations with a computer increase the probability of reliability. Thanks to the software, many possibilities are explored in a short time. The calculations were made by selecting geometries in the literature and theses. According to the previously determined results, the overlap of security factors is the main purpose of the software to be developed. The software will investigate the stability of the slopes and the error level and decide whether it is safe or not. The software can be further developed to calculate the analysis of slopes with different geometries and soil parameters. Slope stability analysis results with different geometries in the literature will be compared with the developed software, and the proximity of safety factors will be compared. It is aimed to provide the software to the service of users by providing user-friendly and reliable qualities. In the later stages, some additions will be made, and it is planned to add features to improve unsafe slopes. These will be made available as structural additions.

**Keywords:** *Matlab, geotechnical model, slope stability, slip plane, limit equilibrium method.*

## GELENEKSEL ŞEV STABİLİTESİ ANALİZ YÖNTEMLERİNE DAYALI YENİLİKÇİ SAYISAL YAKLAŞIMLAR

### ÖZET

Bu çalışma kapsamında, geoteknik mühendisliğinin bir sorunu olan şev stabilitesi probleminin çözümü için, sektörde kullanılan lisanslı programların yanı sıra, Matlab ile kod yazılarak İstanbul Gedik Üniversitesi lisanslı bir yazılım geliştirmek amaçlanmıştır. Bu araştırma da ilk olarak şev stabilitesi analizi yöntemleri incelenerek başlayacaktır. Zemin profili ile ilgili parametreler sondaj verilerinden alınarak ve bu veriler girilerek hesap modeli oluşturulabilmektedir. Vaka bölgesinde gerekli sondajları yapılan ve elde edilen laboratuvar verileri incelenen örnekler için kullanılacaktır. Çalışma alanı en az bir zemin katmanından oluşmalıdır. Oluşturulan her katman için zemin parametreleri ayrı ayrı girilebilmektedir. Yer altı su seviyeside opsiyonel olarak girilebilmektedir. Hesap analiz yöntemi için Limit denge yöntemi (LEM) seçilmiştir. LEM hesaplarının bilgisayar yardımıyla hesaplanması güvenilirlik olasılığını arttırmaktadır. Yazılımlar sayesinde kısa sürede çok sayıda olasılıklar incelenmektedir. Hesaplar literatürde ve tezlerde yer alan geometriler seçilerek yapılmıştır. Önceden belli olan sonuçlara göre, güvenlik faktörlerinin birbiriyle örtüşmesi, geliştirilecek olan yazılımın asıl amacıdır. Yazılım şevlerin stabilitesini hata seviyesini araştırarak ve güvenli olup olmadığına karar verir nitelikte olacaktır. Yazılım daha da geliştirilerek farklı geometri ve toprak parametrelerine sahip şevlerin analizini de hesaplayabilecektir. Geliştirilen yazılım ile literatürde bulunan farklı geometrilere sahip şev stabilite analiz sonuçları karşılaştırılacak ve güvenlik faktörlerinin yakınlığı kıyaslanacaktır. Yazılımın kullanıcı dostu, güvenilir niteliklerinin sağlanması ile, kullanıcıların hizmetine sunulması hedeflenmektedir. Daha sonraki aşamalarda ise bazı eklentiler yapılarak, güvenli olmayan şevlerin iyileştirilmesine yönelik, özelliklerin eklenmesi düşünülmektedir. Bunlar yapısal eklemeler olarak sunulacaktır.

**Anahtar Kelimeler:** *Matlab, geoteknik model, şev stabilitesi, kayma düzlemi, limit denge yöntemi.*

# 1. INTRODUCTION

## 1.1 General

In slope stability, external loads such as soils (fill), buildings, earthquakes, and precipitation are the most critical parameters. The safety factor is the ratio of soil shear strength to shear stress (Duncan, 1996). This ratio is called the safety factor. If this ratio is greater than 1, it is considered safe. If it is less than 1, it is considered unsafe. In slope stability analysis, there is a fractured circle based on total stress. The importance of slice methods increased in the mid-1900s. The calculation steps of the slope analysis were expanded and merged under the name of the Limit Equilibrium Method (LEM). In this method, the slope is divided into slices on a circle. As a result of the different acceptance of slices' interaction with each other, different methods were born (Bishop 1950 and Spencer 1967). However, Finite Element Methods (FEM) has gained importance recently. The most important advantage of this method is the variable safety factor acceptance (SSR). In this way, the deformations that occur on the slopes are known closer to reality. However, deformations cannot be known in LEM methods. There is a fixed safety factor in the LEM method (Griffiths and Lane, 1999).

In the latest research articles, more complex methods are tried to be presented in slope stability analysis. For example, the effect of rainfall on underground flow and slope stability was investigated by Shao et al. (2015). It was conceived as a double-pass model to analyze the effect of precipitation events on slope stability for both saturated and unsaturated soils. It is not always possible to solve these complex problems with the finite element method (FEM).

Additionally, artificial intelligence (AI) is another matter. People had the opportunity to transfer their previous experiences or the experiences of others to the machines. The increasing number of applications and processes experts use in our daily life; web searches, budget models, computer games, auto processors, etc., applications of AI methods are just a few of the best known (Tolon 2007).

MATLAB code is a code written to determine the factor of safety for different sliding surfaces. This code was developed with the Limit Equilibrium Method, Bishop, Jambu, Spencer, Morgenstern & Price, and Wrap methods were used. These approaches generally calculate normal, and shear stresses along the failure plane. The safety factor is the ratio of shear strength to finite element shear stress calculated from the mobilized normal stress and Mohr-Coulomb parameters.

## **1.2 Objectives**

The aim of this study is to analyze a model with a semi-analytical approach. The main objectives of this thesis are;

- 1- Solution methods will be investigated in slope stability analysis; the safety factor concept will be examined.
- 2- The developed limit equilibrium model's results will be compared with the most used model, which is the Finite Element Method (FEM).
- 3- The software and solution method will be proven by reliable software (Geoslope, Talren, Geo5, etc.) that is preferred to use by practitioners.
- 4- Displacement calculations will be made according to the Newmark sliding block theory. Thanks to the parameters obtained from the recorded earthquake records, displacement can be calculated with improved formulas.
- 5- As a result of the software being user-friendly and reliable, it is aimed to be offered to users.
- 6- In the later stages, it is planned to add features to improve unsafe slopes.

## **1.3 Format of the Thesis**

Chapter 1 discusses the introduction of slope stability problems. A comprehensive literature review of slope stability is described in Chapter 2. The calculation methods will be explained in detail in Chapter 3. The details of the developed software, the assumptions used, methods, and the software interface will be introduced in detail. In Chapter 4, comparisons with other software and literature examples will be presented. A comparison will be made at the end of the chapter. There are discussions and suggestions in Chapter 5.

## **2. LITERATURE REVIEW**

### **2.1 Introduction**

People have struggled with the stability of the slope from the past to the present. Looking at the slopes' history, people have used both natural slopes and filler slope as living spaces. Natural slopes have been affected by natural events like earthquakes, erosion, flood, volcanic, wind, etc., in the service phase. The filler slopes might be formed by human and environmental factors. Slopes have been used in the past as a safety area because of war or optional reasons. Due to the increasing population density and value of the property, it has started to be used for structuring. Due to the topography of Turkey, the deaths and financial losses are seen as relatively high. When slopes are used as cultivated areas, they cause some damage due to loss of stability.

### **2.2 History of Slope stability**

The milestones of geotechnical science was created in 1773 by Coulomb. Coulomb actually formed the cornerstones of soil mechanics. This concept is the cohesion and friction angle ingrained and cohesive soils. In practice, as the cohesion and refraction angle ( $c$  and  $\phi$ ) have different meanings, Coulomb researched the concept of friction angle in coarse and cohesive soils. Coulomb disquisitioned the shear state of the soil mass at a point and examined the shear wedge balance. The balance here is achieved by the soil's weight, the forces affecting the sliding surface, and the wall's response. Coulomb's research was the basis of such studies of acceptance of the sliding surface. Later in 1856, Rankine transformed the equilibrium problem of soil mass into one of the practical methods. In 1886, Cullman graphically transformed the same conditions.

After that, the landslide problem has started to increase in importance day by day. In the early part of the 20th century, roads in Germany and Sweden shifted, later on, the

famous Panama Canal. The efforts of engineers to uncover the slopes have emerged. The French engineer Collin researched this and investigated that there were fractures along a curve (Çamlıbel, 1982).

In 1913, financial losses were experienced due to slope failures. The Statens Järn- och Gruvindustriella Geotekniska Kommission in Sweden and the Society of Civil Engineers in the United States were established in these years. These organizations researched landslide problems and proposed the necessary methods. Peterson (1955) determined that the sliding surface is a circular cylinder. Later, this concept was supported by Fellenius and achieved successful results. Fellenius published the “Slope Stability Analysis” method, which includes cohesion and internal friction angle in *Erdstatische Berechnungen* (1927).

Later, Terzaghi (1950) researched far-going in soil mechanics for slopes. Gilboy, Krey, Frontard, Resal, Caquot, Jaky designed the landslides as graphical and analytical methods. Rendulic (1935) investigated the shear plane as a logarithmic spiral surface. Taylor and Leps (1939) published an article comparing all of these studies (Tekin, 2011).

After this stage, Bishop and Janbu realized that lateral shifts were not taken into account. They have published articles on the slice method. Bishop and Morgenstern (1960), Morgenstern, Morgenstern and Price (1965) later did these researches. While developing methods of analysis, another issue is the development of laboratory methods and minimizing the limits. Especially, Bjerrum and Skempton (1964) found the most successful results.

In this sense, friction circle and slice methods used to determine the shear level give almost the same result. Instead of calculation methods developed to determine the slipping plane, applications comparing the experiments obtained in the laboratory have been investigated. Although the safety factor in the use of these methods is greater than 1, it is seen that landslides still fail.

The reason for failure can be;

- Soils are not homogeneous,
- The same soil layer is crack (especially fissured clays),
- Due to the excessive inclination of slopes, it prevents the soil borehole,
- Drilling carot is not real because it affects laboratory results,

- GWL (groundwater level) is very variable in slopes,
- The effect of human beings on the stability of slopes in changing and developing metropolitan cities (very close to the slope construction, a slope can cause stability problems in the channel, water connections, slope unconscious filling to be used as excavation site, etc.).

For slope stability, the reaction force value (rf) must be larger than the slipping force value (sf). So,

$$\frac{rf}{sf} \gg 1 \quad (2.1)$$

The concept of safety factor will be explained in more detail later on. The safety factor of 1 in the equation is the basis of geotechnical engineering. Depending on the Factor of Safety (FS), slope stability needs to be evaluated, analyzed, and, where necessary, improved.

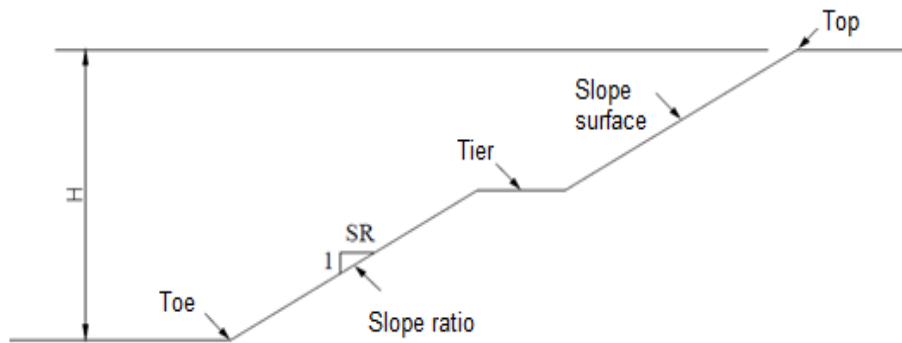
### 2.3 Slope Stability Terminology

In geotechnical engineering, sloping surfaces are called "the slopes" (Önalp ve Arel, 2004). For the first time, they used the terms; for natural slopes "slope", a landslide for slope movements, "slip", "collapse" and "tipping".

The slopes are part of the natural topography. It is seen in two different situations as split slopes and filler slopes. Split slopes are slopes created by excavation. They reveal the natural soil that was once buried. Filler slopes are the slopes created while placing the fill. Cotudo used several typical terms in the definition of the slope like (Cotudo, 2006);

- Slope ratio is the definition of the steepness of the slope., For example, 4:1 is a horizontal slope, while 1:4 is a vertical slope,
- The slope top and slope toe are the starting and ending points of the slope,
- The slope surface is the part between the toe and the top,
- Slope height is the subtraction of the toe level and the top level, and
- Tier is the horizontal part of the slope surface, which is formed for the purpose of providing drainage and stability.

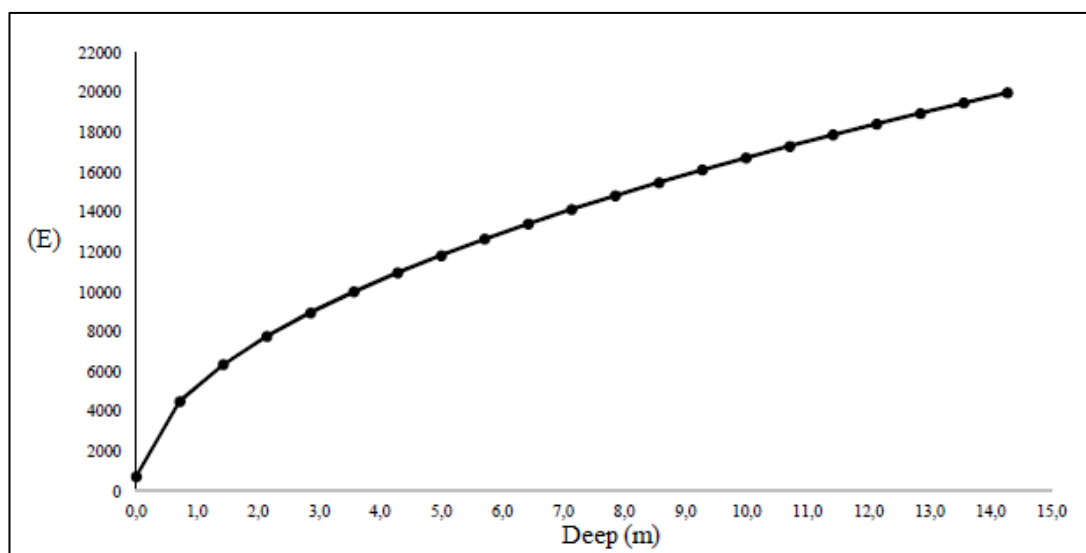
Figure 2.1 shows the toe, top, and tier points of a typical slope geometry.



**Figure 2.1 :** The terminology used to define slopes and its geometry  
**Source:** (Cotudo, 2006).

## 2.4 Slope Stability Parameters

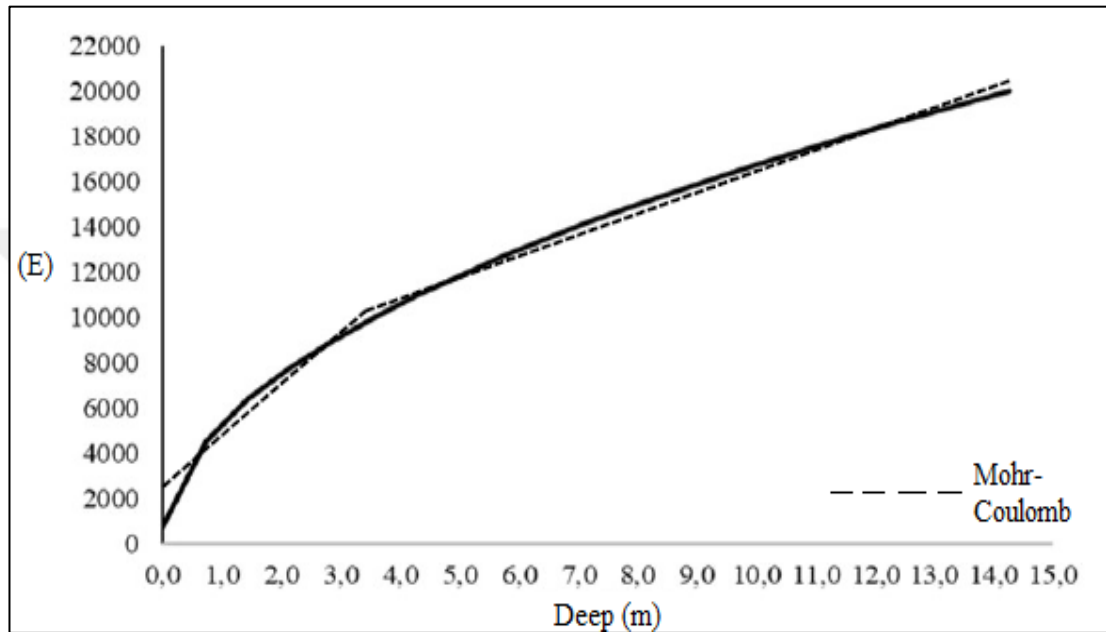
Soil parameters are found by making various experiments or assumptions. The type of experiment to be selected according to the calculation method of geotechnical engineering is decisive. According to Mohr-Coulomb, some of the soil parameters are as follows; Modulus of Elasticity (E), Poisson Ratio ( $\nu$ ), Cohesion (c), Dilatation Angle ( $\psi$ ), dry unit weight, wet unit weight. In fact, the materials are not elastic, and they behave elasto-plastic. Therefore, the number of parameters given above is determined according to the desired purpose. The soil, in particular, has a more complex structure. Each material has a yield limit. After the yield point, the material exhibits plastic behavior. Figure 2.2 shows the Modulus of Elasticity of an ideal material changing with depth.



**Figure 2.2 :** The ideal material's modulus of elasticity  
**Source:** (Sert 2019).



In Mohr-Coulomb material, the modulus of elasticity is obtained by the transformation. Figure 2.3 shows that the Elasticity Modulus is approximately captured in the Mohr-Coulomb model according to the ideal material. Mohr-Coulomb model seems to be a valid method. The Mohr-Coulomb model method is presented in computer software that calculates based on finite elements. This method has been used in many previous studies and articles.



**Figure 2.3 :** Mohr-Coulomb material's modulus of elasticity  
**Source:** (Sert, 2019).

When looking at the studies conducted in slope stability analysis, it is known what the most critical soil parameters are. Besides, the software to be used, and the calculation method of the software is also essential. For example, in limit equilibrium analysis, it is sufficient to know three parameters. These are internal friction angle ( $\phi'$ ), unit volume weight ( $\gamma$ ) and cohesion ( $c'$ ) (Tekin, 2011).

When these parameters are known, analysis can be made for any limit equilibrium method. Sample soil parameters to be used with LEM are given in Table 2.1. Besides, the geometry and environmental effects of slopes with inclined surfaces should be well known.

**Table 2.1** : Advised values of soil parameters for LEM.

Soil Layer	Parameters	Advice
Filler	Internal Friction Angle ( $\phi'$ )	24°
	Cohesion (c')	2 kPa
	Dry Unit Weight	19 kN/m <sup>3</sup>
	Modulus Of Elasticity (E)	10 MPa
Sandstone	Internal Friction Angle ( $\phi'$ )	32°
	Cohesion (c')	5 kPa
	Dry Unit Weight	23 kN/m <sup>3</sup>
	Modulus Of Elasticity (E)	100 MPa

**Source:** (Yıldız and Tolon, 2020).

The parameters to be calculated for LEM in the table above are sufficient. However, in finite element-based analysis, more soil parameters should be known according to the chosen method. According to the Mohr-Coulomb method, Table 2.2 lists the parameters required to be entered for the FEM program.

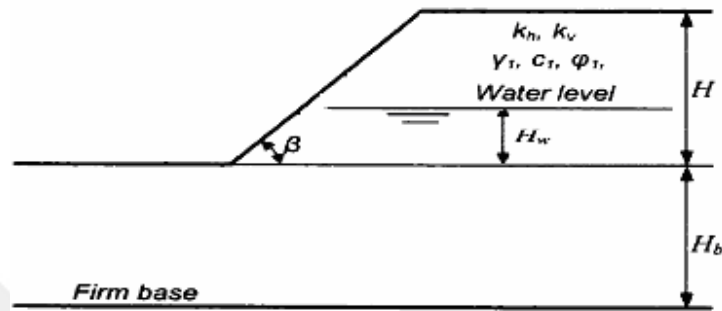
**Table 2.2** : Mohr-Coulomb parameters for LEM program.

Parameter	Symbol	Unit
Material Model	Model	-
Dry Unit Weight	$\gamma_{\text{unsat}}$	kN/m <sup>3</sup>
Wet Unit Weight	$\gamma_{\text{sat}}$	kN/m <sup>3</sup>
Natural State Vacancy Rate	$e_{\text{init}}$	-
Modulus of Elasticity	$E_{50}^{\text{ref}}$	kN/m <sup>2</sup>
Value Of Stiffness Due To Stress	m	-
Internal Friction Angle	( $\phi'$ )	°
Cohesion	( $c_{\text{ref}}'$ )	kN/m <sup>2</sup>
Dilatation Angle	$\psi$	°
Poisson Ratio	$\nu_{\text{ur}}'$	-
Reduction Factor	$R_{\text{int}}$	-

**Source:** (Sert, 2019).

In addition, Tolon (2007) made a study on five different slope geometries. This study is based on artificial neural networks, and the parameters are the ranking of the effect

rates of the parameters that affect the slope stability. The most crucial soil parameter and geometry effects affecting slope failure on a slope were investigated. This work with an artificial neural network is the model that was previously taught; the parameters that affect the failure the most by changing the parameters in a slope were investigated. Here the parameters are;  $\beta$  (slope of the slope), H (slope height), Hw (water height), kh (lateral force coefficient), Hb (distance from heel to firm base).



**Figure 2.4 :** Slope geometry model developed for ANN

Source: (Tolon, 2007).

Tolon (2007) investigated the slope's failure by changing the parameters each time on the slope geometry of 5 different sizes (Table 2.3).

**Table 2.3 :** The order of effects of parameters for slope failure

Order	Model 3	Model 4	Model 5
1	$\beta$ (deg.)	c (kPa)	c (kPa)
2	H (m)	$\beta$ (deg.)	$\beta$ (deg.)
3	Hw (m)	$\phi'$ (deg.)	H (m)
4	kh	H (m)	$\phi'$ (deg.)
5	Hb (m)	kh	kh

Source: (Tolon 2007).

Here, the most important soil parameters that cause breakage according to various slope geometries are given. For Model 3, the parameters causing the break are in order of importance; is H, Hw, kh, and Hb.

## 2.5 Landslide Classification

According to Varnes (1978), there are two types of landslide classification. First, the water content. Then the movement is limited. Moreover, he stated that there are five

different types of motion kinematically. These; falling, tipping, slipping, spreading, flowing, and complex. Material types are; debris, rock, and soil.

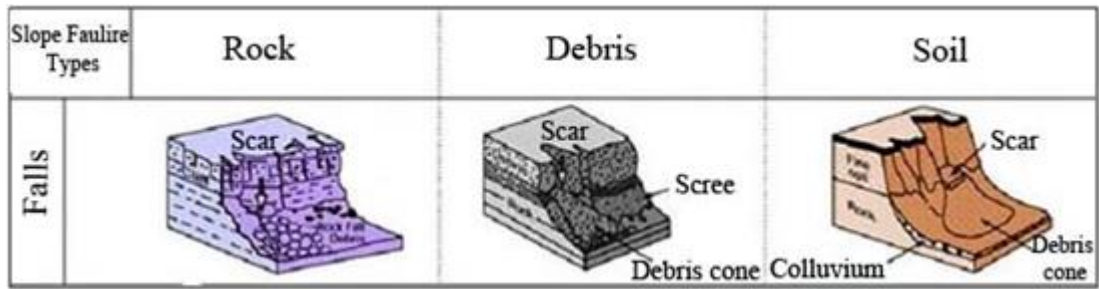
**Table 2.4 :** Types of landslides of the shortened version of Varnes's classification of inclination motions.

TYPE OF MOVEMENT	TYPE OF MATERIAL		
	BEDROCK	ENGINEERING SOILS	
		Predominantly coarse	Predominantly fine
FALLS	Rockfall	Debris fall	Earthfall
TOPPLES	Rock topple	Debris topple	Earth toggle
SLIDES	ROTATIONAL	Rockslope	Debris slide
	TRANSLATIONAL		
LATERAL SPREADS	Rock spread	Debris spread	Earth spread
FLOWS	Rock flow	Debris flow	Earth flow
	(deep creep)	(soil creep)	
COMPLEX	Combination of two or more principal types of movement		

**Source:** (Varnes, 1978).

### 2.5.1 Falls

This is the separation of pieces of rock and/or soil that fall down a slope. A fall is seen where a large mass of soil slides down a slope. That soils slide down a slope and rolls along the sloping slope. They are faults consisting of rock fragments on the slope (Das and Sobhan, 2012). Reasons for this unstable; discontinuity of rocks. In other soils are separated due to fissures local blocks (independent from external effects) fall off by gravity (Ulusay, 2008). Falls are masses of geological materials consisting of sudden movements (Figure 2.5). The soil is separated from steep slopes or rocks. Separation; fracture discontinuities occur with free fall of joints and bearing planes; bouncing and rolling. Falls have been heavily influenced by gravity, mechanical weathering, and the presence of interstitial water (Varnes, 1978). The falls usually occur on steep rock slopes. The triggering factors may be erosion, tree roots, icing, water effect, and earthquake effect.

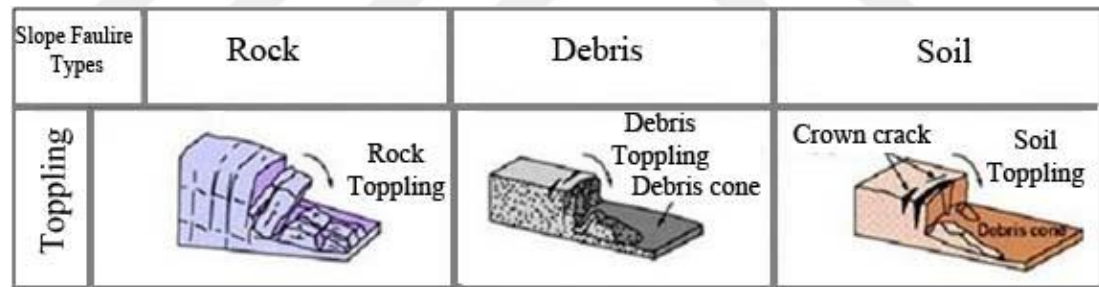


**Figure 2.5 :** Falls on the slopes

Source: (Anaçali, 2015).

### 2.5.2 Toppling

This is the forward rotation of the rock and / or the soil mass about an axis below the displaced mass center of gravity. In a rock or hard clay layer with many discontinuous surfaces, the slope is separated on a crack point near-surface from the main part and turns down (Das and Sobhan, 2012). Various tipping types are available (Figure 2.6). There are three different tipping types: bending, block, and block-bending (Ulusay, 2008). Tipping failures are distinguished by the fluid pressure of a unit or units in the spaces between the units, and by the force of gravity, the units rotate forward around the point of rotation below the units (Varnes, 1978).




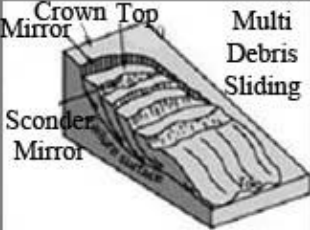
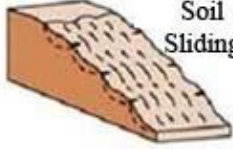
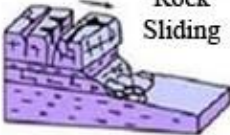
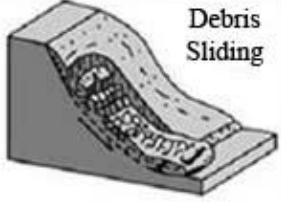
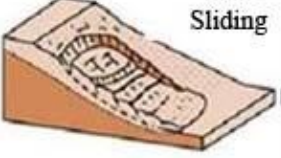
**Figure 2.6 :** Toppling on the slopes

Source: (Anaçali, 2015).

### 2.5.3 Slide

A break occurs on the surface, and then the soil mass moves downward (Das & Sobhan, 2012). For this reason, the critical phenomenon in slope analysis is the instability of slides. Stresses at the sliding failure; zone on a slope, increases on the particular direction's surface. Fracture in this type of imbalances happens like a bow from top to bottom (Ulusay, 2008). The word "landslide" refers to mass movements. The slide is the weakness zone that separates the more stable from the underlying material. There are two slide types; rotary slide and translation slide (Figure 2.7). In a

rotational (circular) slide, the rupture surface is concavely curved upwards. The slide rotates parallel to the floor and roughly around the slide cutter. The landslide mass moves roughly along the planar surface by rotation and backward bending in the translation slide. The units act with each other (Varnes, 1978).

Slope Failure Types		Rock	Debris	Soil
Sliding	Circular	Only Sliding 	Multi Debris Sliding Crown Top Mirror Sconder Mirror 	Successive Soil Sliding 
	Offset (Planar)	Rock Sliding  (*)	Debris Sliding 	Soil Sliding 

**Figure 2.7 :** Slide on the slopes

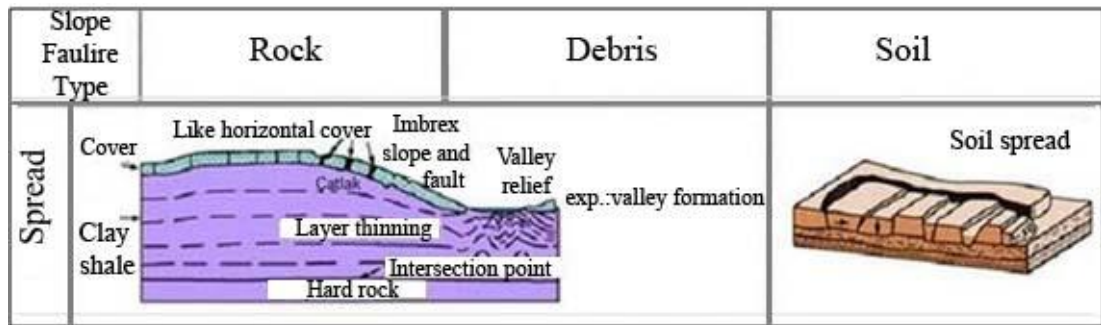
Source: (Anaçali, 2015).

Circular gliding clay, silt, sand, etc., type of soils, stream channels, road slopes, fillings, and highly articulated rock masses and / or highly decomposed rocks occur (Tekin, 2011). Planar slide on a flat or slightly rough surface is the soil's downward movement parallel to the sliding surface. Such movements of mass move relative to circular failures without much deformation (Tekin, 2011). Multiple points of discontinuity or cracked in the soil are also formed, in particular, by the combination of fault or stratification surfaces. It is a type of unstable; that increase in piece masses and filler soils in natural environments or weak soils (Çavumirza, 2018).

#### 2.5.4 Spread

This spread failure is a slide format through motion (Figure 2.8). The abrupt movement of water-laden silt or sand bonds is loaded with a layer of clay or fill. It is a segmented separation of the more robust soil at the top, collapsing along with the layer of weak soils. Running sand layers may occur with liquefaction effect the earthquake. It continues up to the waterway on the slopes. Due to the slopes' low slope, this instability can occur in very large areas (Das and Sobhan, 2012). Spreading is the lateral expansion movement formed by the combination of shear and

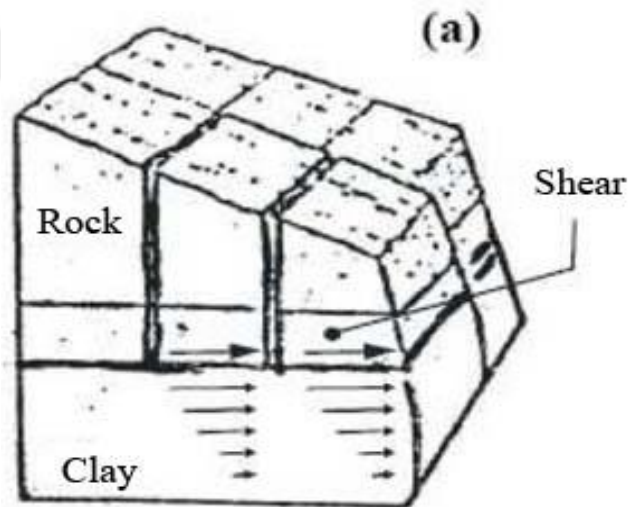
tensile crack movements (Tekin, 2011). Lateral spreading is distinctive because they occur on very soft slopes or flat terrain. The dominant movement style is lateral stretches with sliding or tensile fractures. Fault liquefaction, saturated, loose, cohesionless floors (usually sand and silts) turn from a solid to liquefied state (Varnes, 1978).



**Figure 2.8 :** Spread on the slopes

Source: (Anaçali, 2015).

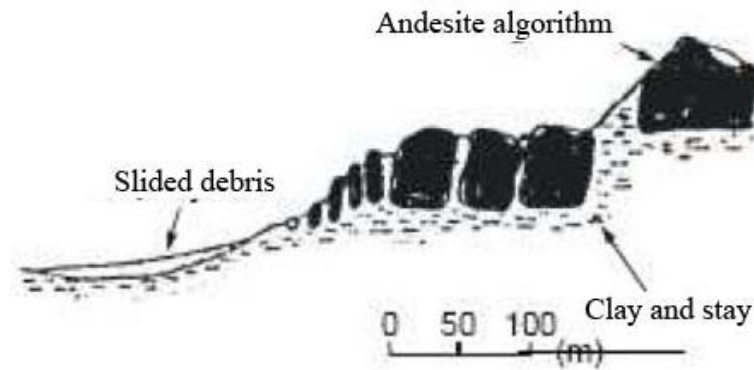
Figure 2.9 shows the blocky rock mass on the clay-like plastic soil moves slowly with cutting defeat.



**Figure 2.9 :** Lateral expansion movement in rock

Source: (Broms, 1975).

Lateral ground spreading is the movement of both materials together towards the rock blocks' slope in a relatively ductile, weak, and fine-grained plastic soil ground at very low velocity, as shown in Figure 2.10.



**Figure 2.10 :** Lateral expansion movement in soil

**Source:** (Broms, 1975).

### 2.5.5 Flow

The soil is like a viscous liquid. It is a downward movement of the soil mass as viscous. Soils act as fluid water and move towards the toe. Flows shown in Figure 2.11 are flowing unit strain in all directions, not through different planes (Das and Sobhan, 2012). Unconsolidated soils, saturated or dry, regardless of speed, just like a viscous material flows along the slope until it reaches equilibrium. It is known to cause significant disasters (Ulusay, 2008).

According to the definition of Varnes (1978), flow types are as follows:

*a. Debris flows;* loose soil, rock, organic matter, air, and water accumulations are the form of mass in which it moves down. Debris flows generally occur with heavy rainfall and rapid snowmelt. Debris streams source areas are generally associated with steep grooves. Debris flow deposits are usually indicated by the presence of debris fans in the troughs. The presence of fires polluting the slopes of the vegetation increases stability.

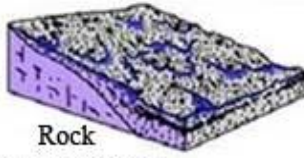

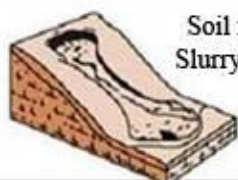
*b. Debris avalanche:* Very fast debris flow.

*c. Earth flow:* Soil flows are in the form of a characteristic "hourglass". The sloping soil becomes liquefied, and when liquefaction is finished, a bowl is formed in the head. It occurs in fine-grained materials or rocks bearing clay under saturated conditions.

*d. Mud flow:* Mud flow. It consists of materials containing at least 50% sand, silt, and fine-grained particles.



e. *Creep*: The slope is an imperceptibly slow, steady, downward movement in the soil formed. Permanent deformations with motion occur with very little cutting force. Usually, there are three types of creep: seasonal, continuous, and progressive.

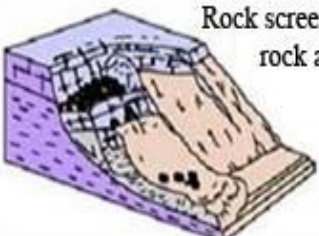
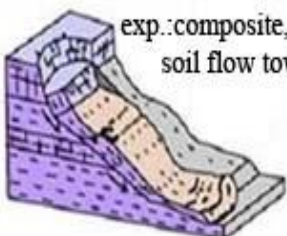
Slope Failure Types	Rock	Debris	Soil
Flow	 <p>Rock flow and ice flow</p>	 <p>Debris flow</p>	 <p>Soil flow Slurry flow</p>

**Figure 2.11** : Flow on the slopes

Source: (Anaçali, 2015).

### 2.5.6 Complex moments

It is a combination of multiple landslides (Figure 2.12). When a type of rock is toppled, it can turn into rock flow and then rockfall. Sludge is, in the clay and silt soils, mixed flow mobilizing landslide.

Slope Failure Types	Rock	Debris	Soil
Complex	 <p>Rock scree toward edge with rock and soil flow</p>	 <p>exp.: composite, non-circular, soil flow toward edge</p>	

**Figure 2.12** : The complex moment on the slopes

Source: (Anaçali, 2015).

## 2.6 Factors Affecting Mass Movements

As a result of the research conducted by Cruden and Varnes in 1993, it was collected under four titles, which are;

- a) Geological causes
  - Properties of materials
  - Damaged, weak, and previously damaged materials

- Non-homogeneity of materials, cracks, etc.
- Poorly graded materials
- Differences in hardness and permeability between different materials

b) Morphological causes

- Tectonic and morphological movements
- Presence of streams close to the slope heel
- Wave-induced erosion or glacier in the slope heel
- Displacement of slope or elevation loads
- Sudden flora change (such as forest fire)

c) Physical causes

- Heavy rains
- Rapid snow melting or icing
- Long-lasting rains
- Earthquakes
- Volcanic eruptions

d) Human-induced causes

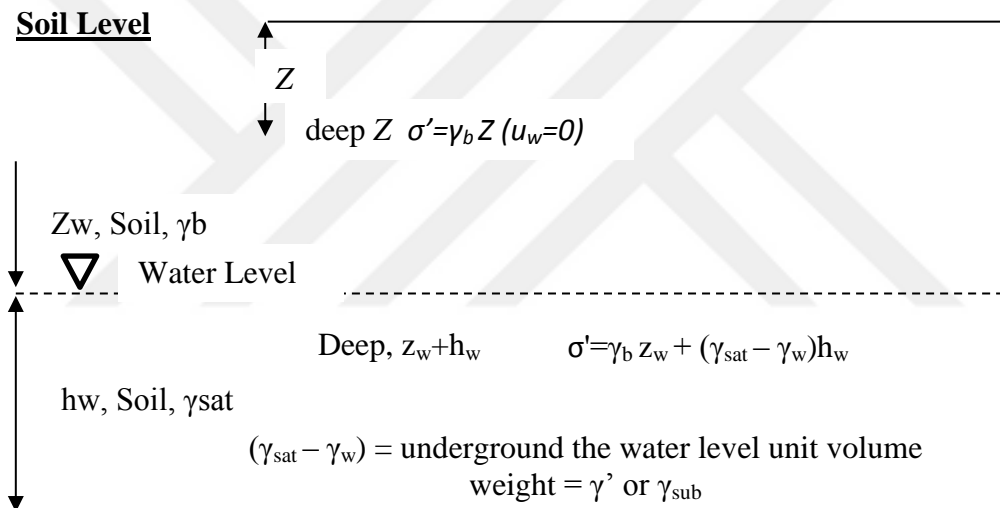
- Excavations at the slope or slope heel
- Additional load to the slope
- Load withdrawal from reservoir
- Destruction of trees
- Irrigation and mining
- Artificial vibrations
- Water leaks

## 2.7 Types of Slope Failure Modes

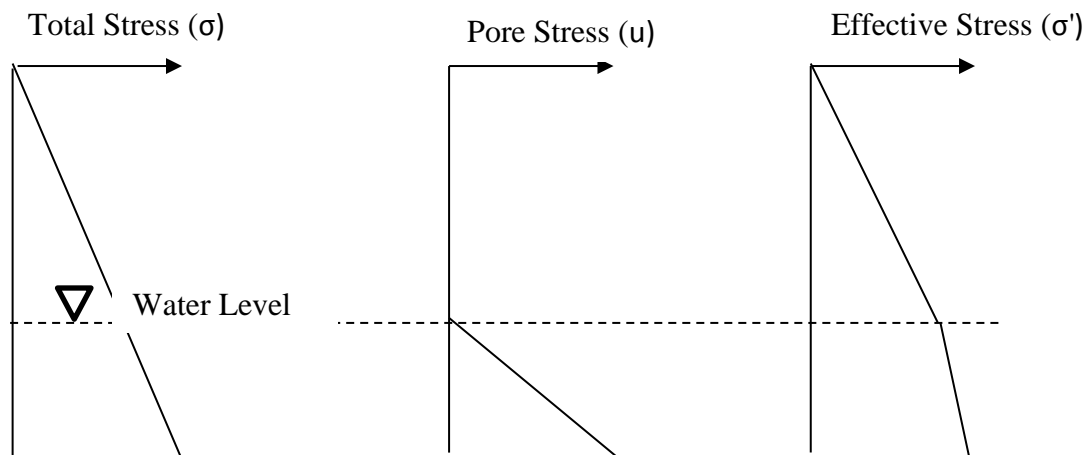
In a stability check, for the safety factor, it is known to be made for two different failure modes. Otherwise, slope; during excavation, it may fail even before the construction is completed. Therefore, to control these slope error modes, the slope's stability should be checked for both total stability stress and effective stability stress (Tolon, 2007).

### 2.7.1 Total stability stress

In the event of a cut on a slope, the total stability conditions apply. The shear stresses that can cause failure in the undrained state are determined for cutting on a cut slope. Total stress, cohesion (c), which is the strength parameter, is used for total stability (Tolon, 2007). The stability calculation is used to examine the short-term stability of clayey slopes or water-saturated sandy slopes. In this approach, the pore water pressure in the soil is also included in the calculations so that short-term ground behavior can be correctly defined. For many soils, effective stress is more effective than total stress. Effective stress is the negative stress caused by the pore water pressure in the grains below the groundwater level. As seen in Figure 2.13, the stress decreases under the water level. In Figure 2.14, the stress differences occurring at the soil level are better understood.



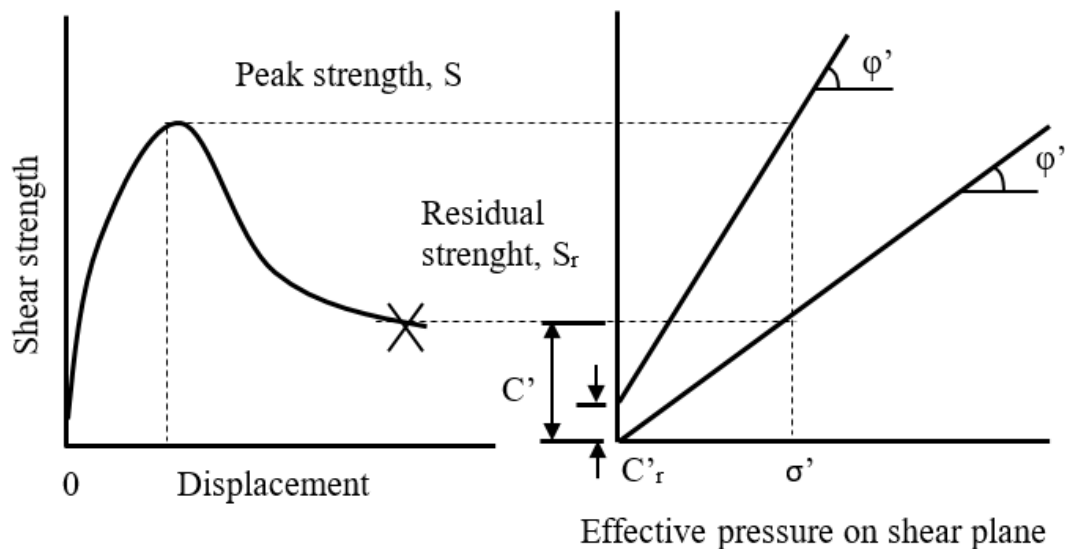
**Figure 2.13 :** Effective stress below groundwater level.



**Figure 2.14 :** Effective stress below groundwater level graphic.

### 2.7.2 Effective stability stress

In natural slopes, long-term stability is encountered and taken into account in calculations. Effective stress analysis methods are used for long term stability analysis of non-fissured and overconsolidated fissured clay. According to effective stress parameters,  $c'$  and  $\phi'$  must be used to calculations the long-term stability problem. Pore water pressure is assumed to be in equilibrium and is determined, taking into account the maximum constant leakage. Skempton (1964) proposed the radial shear strength concept for long-term slope analysis for the calculation of overconsolidated clays. Figure 2.15 shows the shear strength properties of an overconsolidated clay in effective tensile maintenance. Strength parameters are required for stability. Discussions and research on the selection method of its parameters are given by Lowe (1967), Duncan-Dunlop (1969), and Schuster (1968) (Tolon 2007).



**Figure 2.15 :** Over consolidated clay. Shear properties of Mohr-Coulomb failure envelopes corresponding to clay

**Source:** (Feng, 1991).

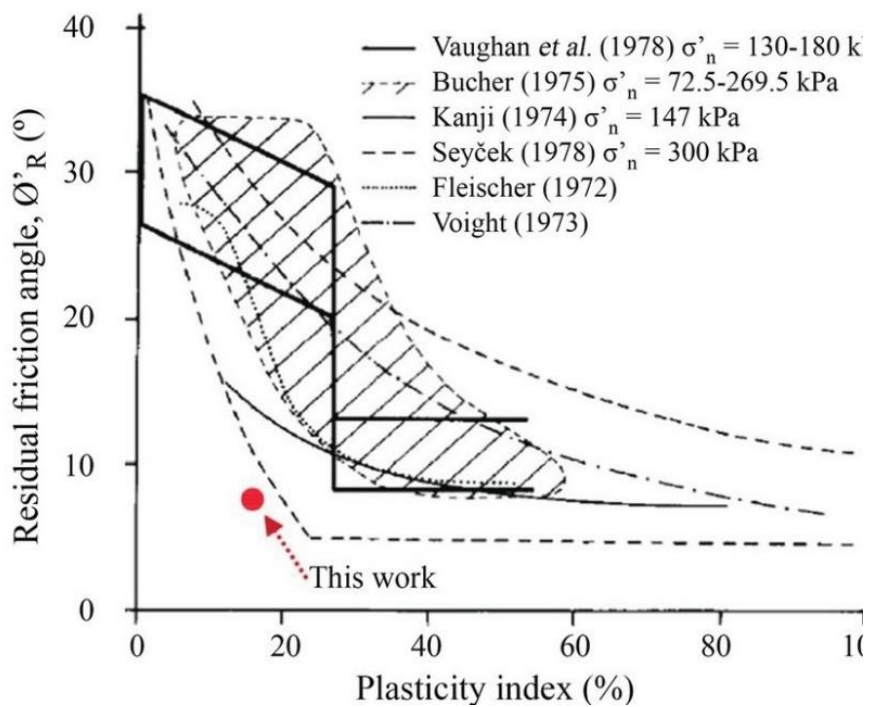
The long-term stability of slopes is based on drainage conditions. In analyzing natural-permanent slopes and the soil (residual) formed on-site, it is necessary to use effective stress analysis, taking into account the highest groundwater level in periods of excessive precipitation.

Residual strength parameters:

- From the cutting box experiment or ring cutting box experiment or,

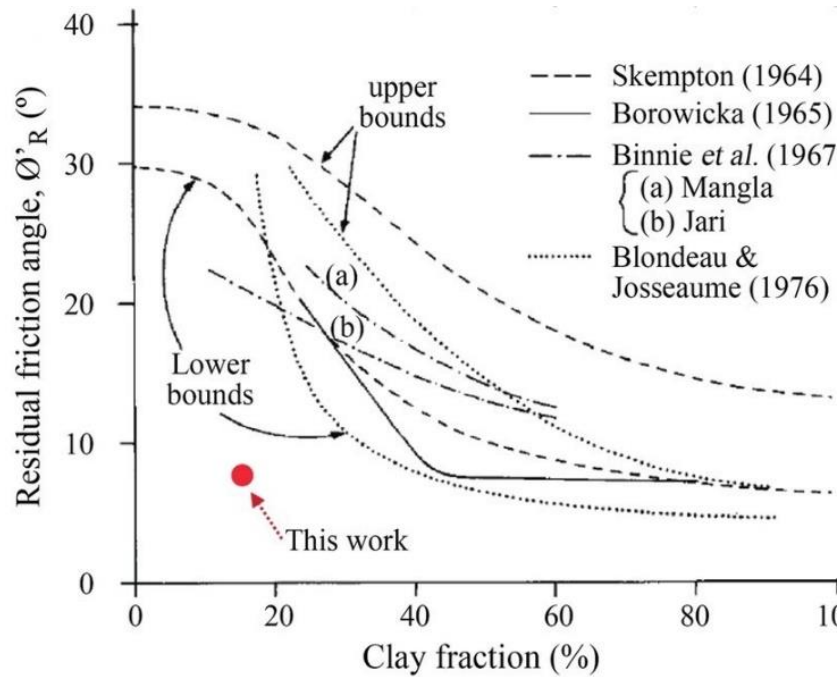
- It is obtained from the graphs that give the value ranges that clay can take according to its plasticity.

The residual strength can be independent of the previous strength of the soil. Therefore, grain size and shape  $\mu$  inter-particle shear angle are affected by mobilized residual strength (Lupini et al., 1981; Skempton, 1964). Microfibersel effects are valid for soil (with no 200 passing), thanks to Atterberg limits, as seen from Figure 2.16. Looking at the experimental results (Bishop et al., 1971; Skempton, 1964; Stark & Eid, 1994),  $PI \geq 40\%$  or  $CF \geq 40\%$  for clays with high plasticity, the shear angle is  $10^\circ$  lower. In particular, Lupini et al. report that for natural clay soils,  $\phi_r'$  is  $5^\circ$  to  $20^\circ$  as seen from Figure 2.17.



**Figure 2.16 :** Plasticity index

Source: (Lupini et al., 1981).



**Figure 2.17 : Liquid limit**

Source: (Stark et al., 2005).

Back-analysis of residual strength parameters of a sliding slope can be obtained with. Since the balance of overturning forces and protecting forces is analyzed in slope stability analysis, the ratio between the forces that overthrew and protect a slope with a crash is 1.0. For this reason, the calculation is made for the slip circle, which is suitable for the geometry of the slip in the land and gives  $FS = 1.0$ .

## 2.8 Factors Affecting Slope Stability Analysis

It is known that many factors are affecting slope stability analysis. The collapse plane geometry that affects the slope stability analysis is as follows, and there are essential factors such as inhomogeneity of soil layers, stress cracks, dynamic effects or earthquakes, and seepage flows (Tolon, 2007).

### 2.8.1 Failure plane geometry

It is known that the plane of failure is circular or non-circular. Explanatory acceptances of the methods used in Table 2.5 are given.

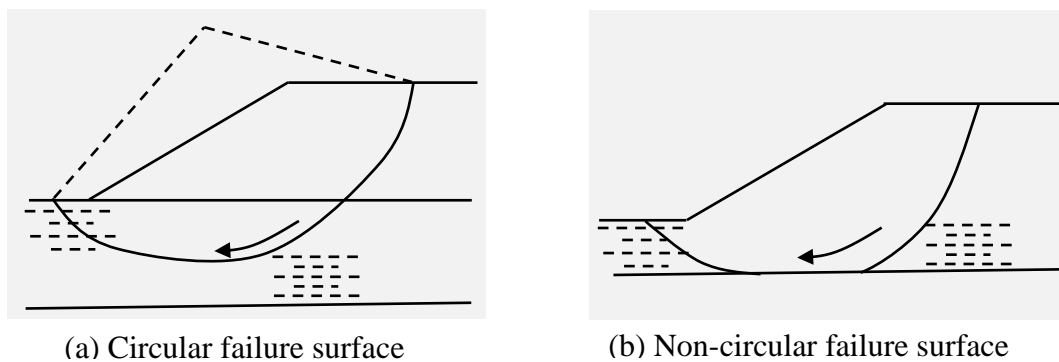
**Table 2.5 : Methods of stability analysis.**

Method	Failure surface	Comments
Bishop (1955)	Circular	<ul style="list-style-type: none"> <li>• There is a balance of force and moment for each slice.</li> <li>• Simplified method. Vertical forces in slices are assumed to be zero.</li> </ul>
Janbu (1972)	Non-circular	<ul style="list-style-type: none"> <li>• There is a balance of force and moment for each slice.</li> <li>• Assumptions should be made in the forces between sections. The vertical force between slices is neglected in the simplified method.</li> <li>• Force and moment are taken into account for each slice.</li> </ul>
Morgenstem & Price (1965)	Non-circular	<ul style="list-style-type: none"> <li>• It is more accurate than the Janbu method.</li> <li>• Similar to Janbu generalized method.</li> <li>• More accurate than the Janbu solution. No simplified method.</li> </ul>
Sarma (1979)	Non-circular	<ul style="list-style-type: none"> <li>• Reduction iterations from Morgenstem &amp; Price.</li> <li>• Reducing time success without loss of accuracy.</li> </ul>

**Source:** (Adaptation from the Geotechnical Control Office, 1984).

Spencer and Chen have argued about the Failure surface. Ultimately, Spencer (1969) argued that circular failure is more critical than non-circular. Chen (1970) concludes that failure geometry is not critical.

However, today computer software has shown that non-circular is more critical; in some failure cases. Circular and non-circular views of the fault plane are given in Figure 2.18. Figure a 'circular failure is shown, and figure b shows non-circular failure (Kasim et al., 2012).



**Figure 2.18 : Circular and non-circular failure surfaces**

**Source:** (Kasim et al., 2012).

### 2.8.2 Non-homogeneity of soil layers

Assuming the soil is homogeneous in geotechnical engineering, the safety factor is calculated. Lo (1965) found that small for un-isotropic steep slopes for steep slopes. Lo developed a general stability analysis method. He suggested in the case of un-isotropic critical for straight slopes. Discontinuity methods can be applied in case of failure due to a failure in split layer soils. High memory is required in computer technology for numerical analysis (Stead et al., 2006). It is also suitable for the complex slope and variable discontinuity geometries with the hybrid modeling technique. The most complex geometries can be solved by numerical methods, but discontinuity characteristic data are required (Hack, 2002).

### 2.8.3 Tension crack

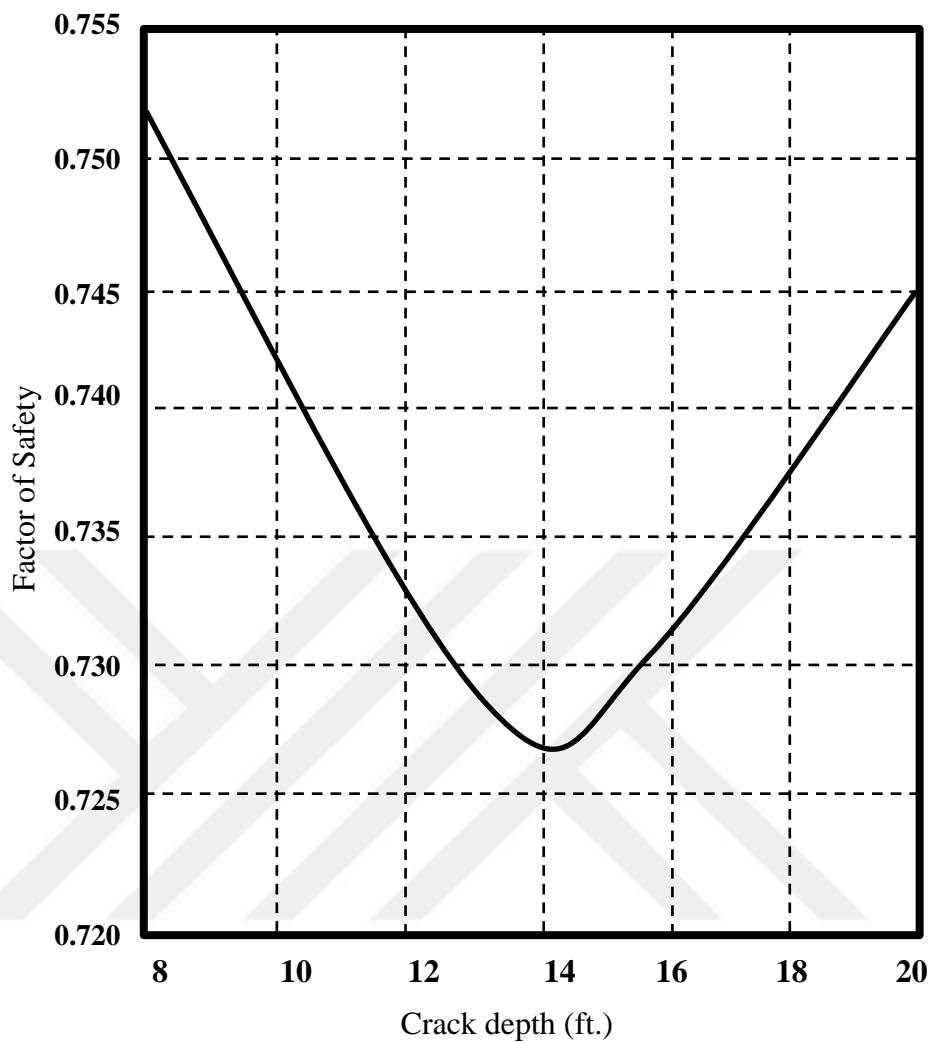
It can occur at the peak of the slope. This is called "Tension Crack". At the top, it points away from the normal slice at the base of the first slice, indicating the presence of tension rather than compression. Especially in cohesive soils, ( $c'$ ) decreases, and this part fails. Therefore, the safety factor change according to the tension crack. Figure 2.19 shows the effect of crack depth on the safety factor. The crack depth has little effect on the safety factor, but the instability increases as the water in the crack rises.

According to Bromhead (1986), If the strength of the soil adheres, as in clay soils that are not completely dyed, the tensile crack's depth varies from 2 to 4 times ( $c / \phi'$ ). The formula is given below. The depth of the tension crack can be determined.

$$Z_0 = \frac{2c'}{\gamma} \tan(45 + \phi'/2) \quad (2.2)$$

$Z_0$  tension crack can be deep. Therefore, sometimes water can penetrate the top (Tolon 2007).





**Figure 2.19 :** The minimum FOS variation with the stress crack depth for the fixed  $c'$  &  $\phi'$   
**Source:** (Feng, 1991).

#### 2.8.4 Dynamic loading

The dynamic load caused by the earthquake should be added to the slope. Seed and Gogman (1967) studied earthquake accelerations and searched on slope stability. Finn (1966) studied the earthquake effect of cohesive soils. It is respectively, earthquake-related studies for slope; Sherard (1967), Seed (1966, 1967) and Majundar (1971). Based on laboratory tests, Ellis and Hartman (1967) reported that soil's dynamic strength might be less or more than the soil strength under static loads; that is, it will give a different result (Tolon 2007). The dynamic analysis will be examined in more detail in Chapter 3.

## 2.9 Limit Equilibrium Analysis

This method is widely used in geotechnical engineering. The slip is calculated by dividing it into a sliding mass or slices in this method, assuming it is along a particular surface. Stresses on the shear surface are compensated by shear strength. There are three main static equilibrium conditions, which are Mohr-Coulomb stress criteria (Hammouri et al., 2008). The proof of the reliability of the limit equilibrium analysis was performed by Singh et al. (2008). The limit equilibrium method gives reliable results, but since the shear strength is assumed to be mobile, the factor safety is low (Yu et al., 1998).

When the FOS value is greater than "1", it shows a stable slope; if less than "1" is unstable, and if the FOS is equal to "1", the slope is in a critical equilibrium state (Hossain, 2011). FOS will be affected by various factors such as; failure plane properties, slope geometry, water forces, and external trigger factors. FOS has a value inversely proportional to the height of the slope. Increasing the height (h) of the slope increases the shear stresses, and therefore the FOS value will decrease (Raghuvanshi et al., 2014; Anbalagan, 1992; Hoek & Bray, 1981; Hack, 2002; Raghuvanshi & Solomon, 2005). As the angle of inclination becomes steeper, the FOS is directly affected.

The main driving force acting on the slope is the gravitational force, which is directly proportional to the slope (Hamza & Raghuvanshi, 2017; Raghuvanshi et al., 2014). Similarly, an increase in the upper slope increases the FOS value (Sharma et al., 1995). The shear strength parameters in the potential failure plane are as follows; cohesion (c) and friction angle ( $\phi$ ). The higher the shear strength, the higher the FOS value.

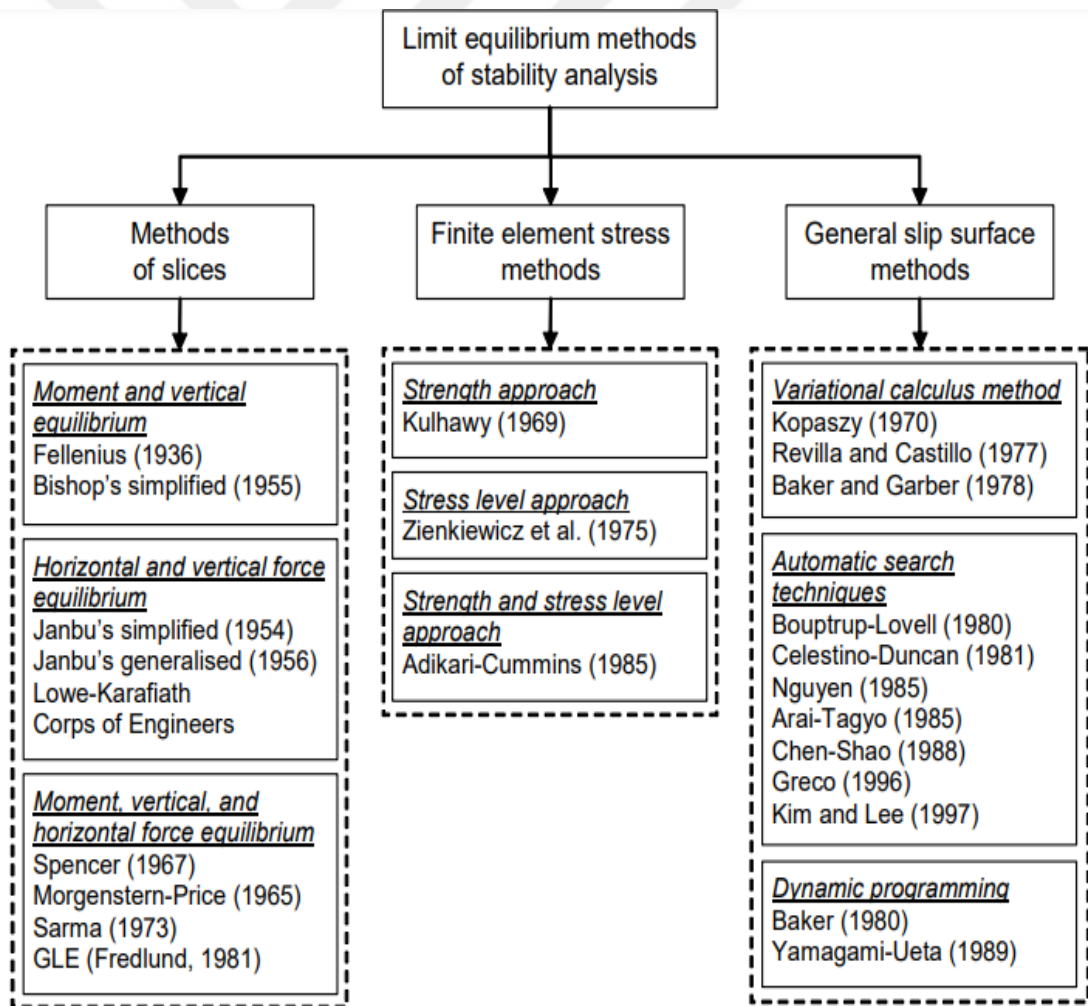
In Figure 2.20, the approaches related to the methods used in calculating the slip factor of safety are grouped. The majority of these methods relate to the division of the shear circle into slices. Some methods use both finite element and slice method together. For example, Kulhawy (1969) calculates the slice base's stresses from the finite element analysis while securing the slip circle according to the slice method (Gitirana, 2005).

Furthermore, the differences between the analysis methods are given in Table 2.6.

**Table 2.6 :** Comparison of existing analysis methods.

	Force Equation		Moment Equation	Shape of Surface	Effect Of slice	Calculation	
	X	Y				Manuel	PC
Fellenius Method	No	No	Yes	Circular	Base Circular	Yes	Yes
Simplified Bishop Method	Yes	No	Yes	Circular	Horizontal	Yes	Yes
Simplified Janbu Method	Yes	Yes	No	All	Hor. Correct Factor	Yes	Yes
Spencer Method	Yes	Yes	Yes	All	Fix Slope	No	Yes
Morgenstern Price Method	Yes	Yes	Yes	All	$X/E=\lambda F(X)(F(X)$ (variable)	No	Yes

Source: (Avşar, 2004)

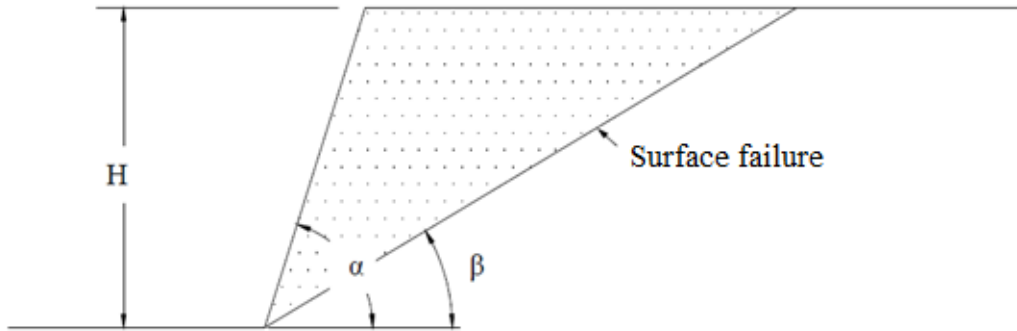


**Figure 2.20 :** Slope stability analysis methods

Source: (Gitirana, 2005).

### 2.9.1 Cullman method

According to Cullman, slip occurs along a plane surface (Figure 2.21). The critical shear angle along the shear surface and the maximum excavation height are calculated (Das, 2006).



**Figure 2.21 : Cullman surface failure**

Source: (Das, 2006).

Critical shear angle,  $\beta_K$ ;

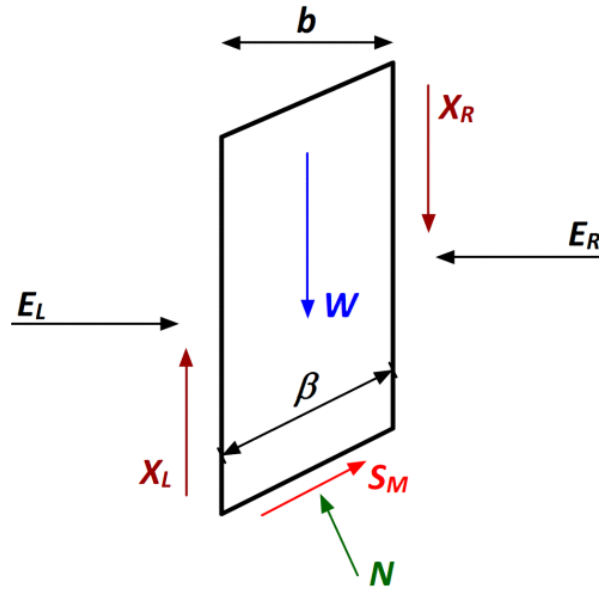
$$\beta_K = \frac{1}{2} \cdot (\alpha + \phi_G) \quad (2.3)$$

Maximum excavation height,  $H_K$ ;

$$H_K = \frac{4c}{\gamma} \left[ \frac{\sin\alpha \cdot \cos\alpha}{1 - \cos(\alpha - \phi)} \right] \quad (2.4)$$

### 2.9.2 Fellenius method (Swedish slice method)

In this method, the circular sliding surface is divided into slices. The slice method is known as the method in which it was first applied. The forces acting on each slice are taken into account. Since the calculation method is simple and has one unknown, it can be calculated manually. The assumption here is; The combination of forces between slices is parallel to the base. The factor of safety is the ratio formed on the sliding surface, shear strength to mobilized shear stress (Krahn, 2004). The E (horizontal) and X (vertical) forces on the slice shown in Figure 2.22 are not taken into account.



**Figure 2.22 :** Forces acting on a slice and force polygon in the Swiss slice method

Source: (Önalp ve Arel, 2004).

$$FOS = \frac{[c\beta + N \tan \phi]}{\sum W \sin \alpha} = \frac{\sum S_{maximum}}{\sum S_{mobilize}} \quad (2.5)$$

$c$  : cohesion

$\beta$  : slice base length

$N$  : base normal force =  $W \cos \alpha$

$\phi$  : internal friction angle

$W$  : slice weight

$\alpha$  : slope base slope

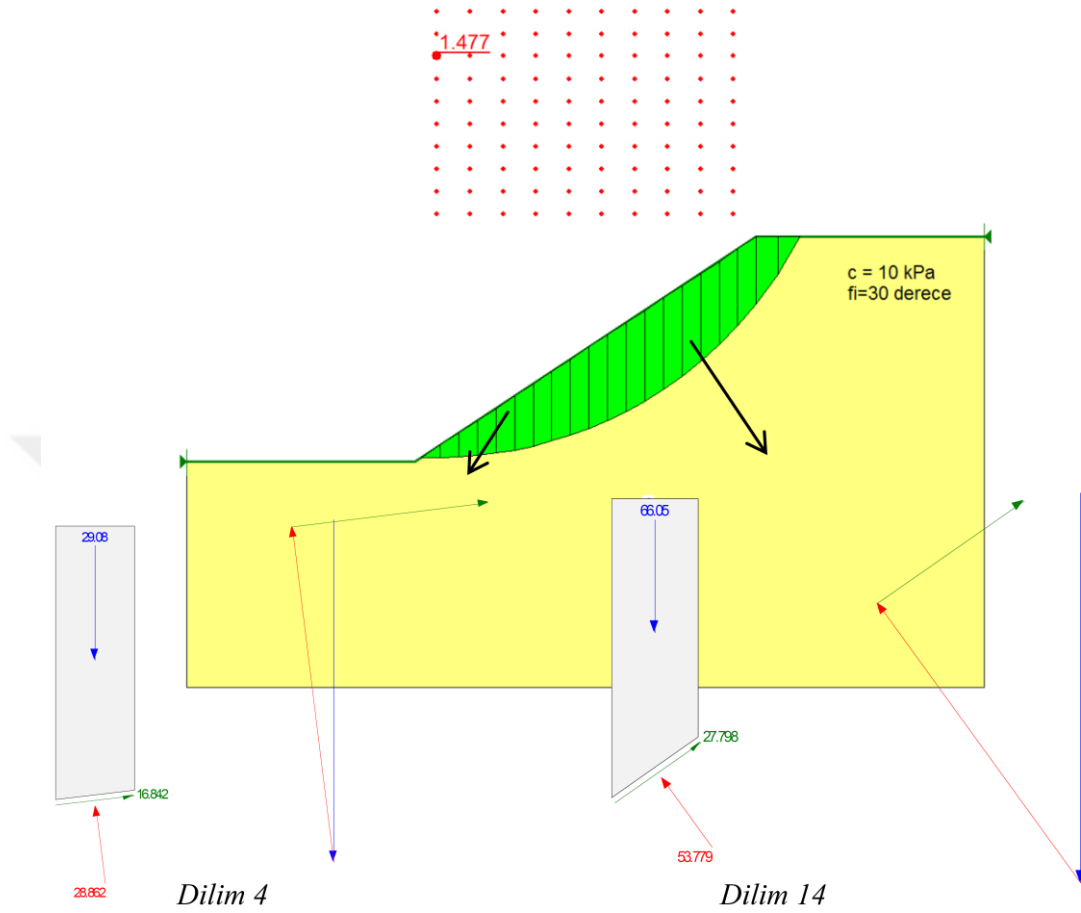
The effect of pore water pressure acting along the bottom of the slice; can be calculated by multiplying the pore water pressure and the slice base length.

$$GS = \frac{[c\beta + (N - u\beta) \tan \phi]}{\sum W \sin \alpha} \quad (2.6)$$

In this method, errors arise due to assumptions. It can be said that if the pore water pressures in the environment are high, and the slope is too low, it increases significantly (Önalp and Arel, 2004).

In this method, inter-slice reaction forces are neglected. For this reason, a force balance cannot be achieved in the free diagram. Vector balance is not provided. Since

there is no other force to balance the slip and normal force at the base of the slice, the force indicator does not close, especially in the horizontal position of the slice base. Therefore, it gives distant results (Krahn, 2004).

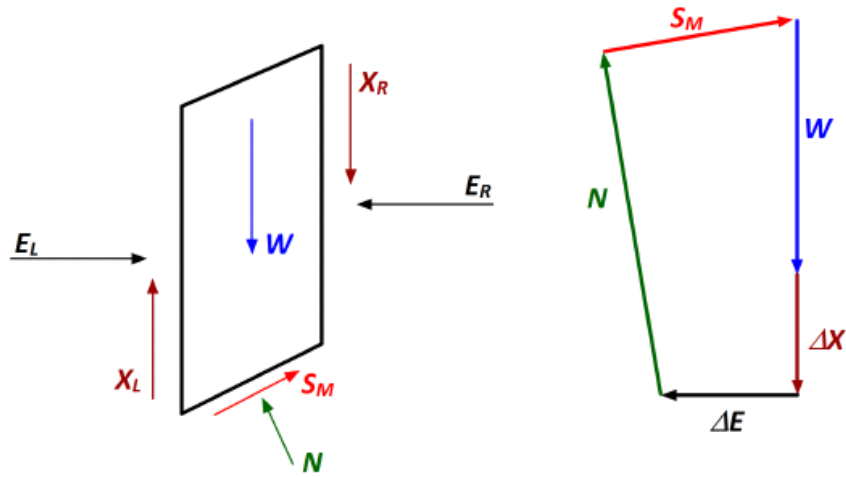


**Figure 2.23 :** Force polygons that are belonging to slices according to the Fellenius method  
**Source:** (GEO-SLOPE, 2012).

### 2.9.3 Bishop and simplified bishop method

Bishop (1950), Fellenius (1927, 1936) first mentioned the shortcomings of the methods. Both moment and force balance conditions are provided on the surface of the circular sliding plane. Due to the calculation obtained in long ways, this method has not found widespread application. The simplified Bishop Method has been used instead of this method (Önalp ve Arel, 2004). With the formula given in Equation 2.7, the normal force N is obtained. In this way,  $\Delta E$  is not taken into account.

$$N' = \frac{W + \Delta X - \beta [u \cos \alpha + c' \sin \alpha / F]}{\cos \alpha + (\tan \phi' / F) \sin \alpha} \quad (2.7)$$



**Figure 2.24 : Forces acting on the slice**

Source: (Bishop, 1955).

$$F = \frac{\sum \{c' b + (W - ub + \Delta X) \tan \phi'\} \frac{\sec \alpha}{1 + \tan \alpha \tan \phi' / F}}{\sum W \sin \alpha} \quad (2.8)$$

The factor of security on both sides of the equation is found by iteration. Bishop sought ways to simplify this situation. It used the force polygon to reassess the X forces. These additional solutions; Solutions where  $\sum \Delta X = 0$  and  $\sum \Delta E = 0$  are zero. Bishop has tried different safety factors considering X and E forces. The effect of the E force of the moment balance is calculated at 1/3 of the slice height. However, the solution difficulty increased in this case, and the results were changed by 1% (Bromhead, 1985). Therefore (2.8), the formula has been published in the literature as a simplified Bishop.

b: slice width,

W : slice total weight,

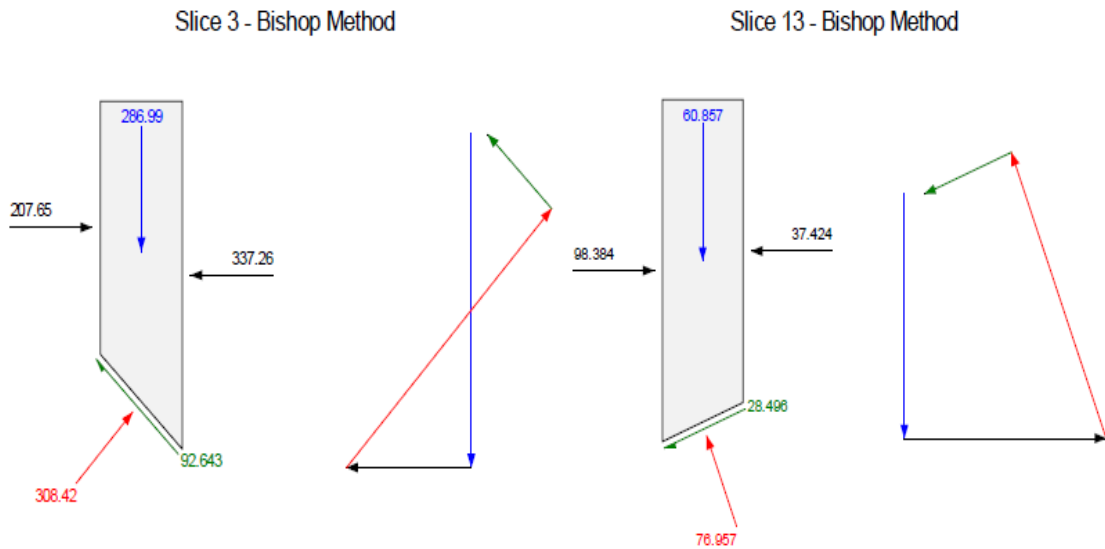
c' : cohesion,

$\phi'$ : internal friction angle,

u: pore water pressure at the base of the slice,

$\alpha$  : the angle between the horizontal and the base of the slice.

As seen in Figure 2.25, there is a difference when looking at the polygons between slices compared to the OMS method. The most significant effect in closing force polygons is the addition of normal forces between slices. As Bishop assumed, the inter-slice shear force was neglected, but the normal force was included.



**Figure 2.25 :** Free and force polygon of the object for Bishop's Simplified method

**Source:** (GEO-SLOPE, 2012).

The slide between sections is not included in the calculations by selecting zero. Moment safety factor ( $f_m$ ) is insensitive to intersection shear forces. The reason is the negligence of the cutting force between slices. The simplified Bishop takes into account the moment balance but not horizontal force balance, as seen in Figure 2.25.

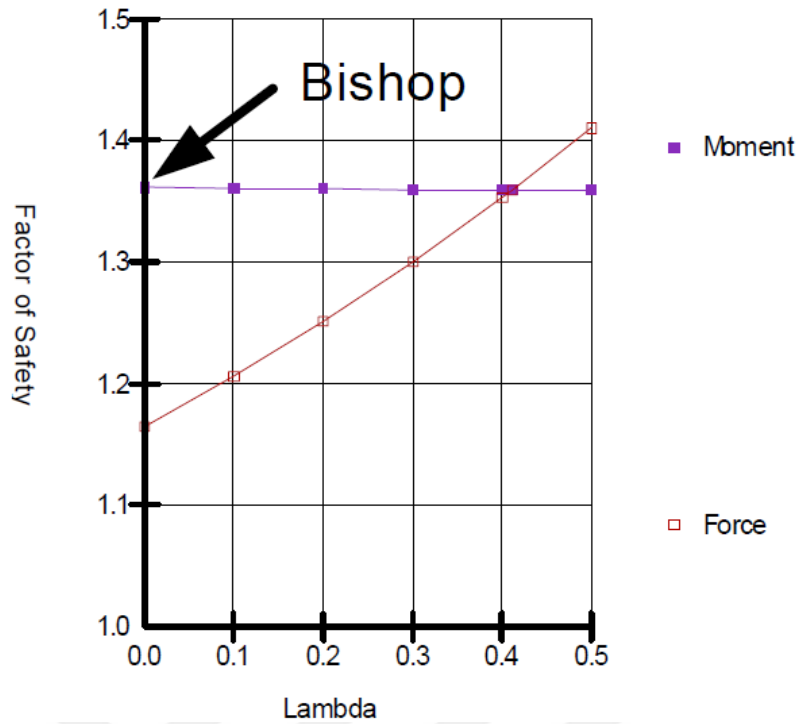
### 2.9.4 Jambu method

Jambu first developed a solution for force balance conditions that could be applied to any sliding surface in 1956. In 1968, three equations with three unknowns were reviewed and named as amb Jambu general method. Later, it was called the "Simplified jambu method" with various simplifications (Önalp ve Arel, 2004).

On the assumption that Jambu X forces are zero, he found the security formula;

$$F_0 = \frac{\sum\{[c' b + ((W \cdot ub) \tan \phi')] \sec \alpha \cdot k_\alpha\}}{W \tan \alpha} \quad (2.9)$$

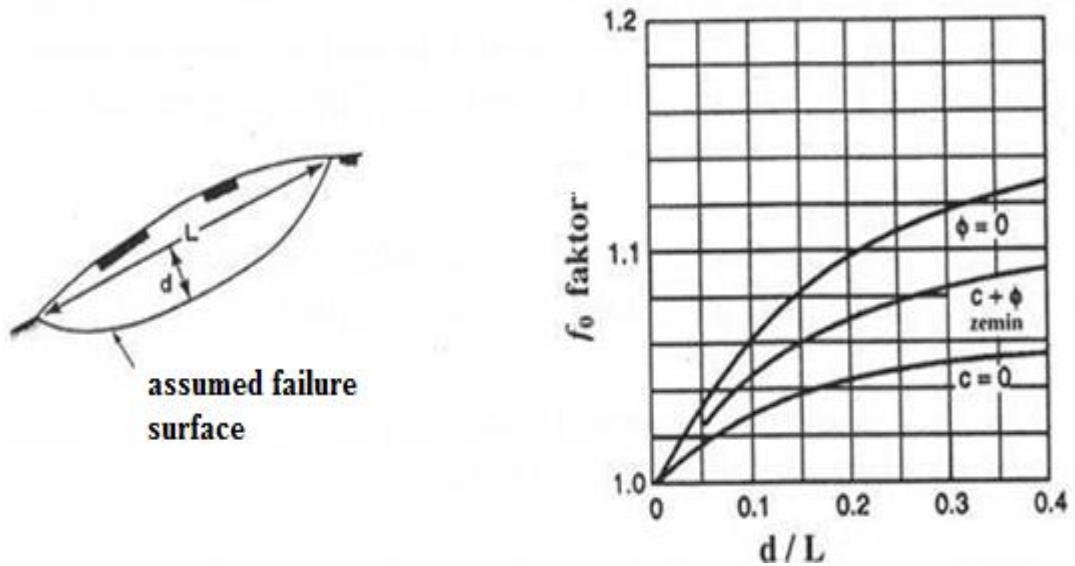




**Figure 2.26 :** Bishop's simplified factor of safety

Source: (GEO-SLOPE, 2012).

A correction coefficient, according to the geometric properties and type of soil, is proposed by Jambu. This coefficient is found in  $f = f_0 (d / L, \text{soil type})$  in relation to the slope's length. This graph shown in Figure 2.27 is for granular and cohesive soils.



**Figure 2.27 :** Jambu factor

Source: (Gökcan, 2014).

Depending on the slip depth  $f_0$  is calculated by the following 2.10 and 2.11 equations (Önalp ve Arel, 2004).

$$f_0 = 1 + b \left[ \frac{d}{L} - 1.4 \left( \frac{d}{L} \right) \right] \quad (2.10)$$

$$Fos = f_0 \cdot F_0 \quad (2.11)$$

As a result, the corrected safety factor of jamb is found by equation (2.11) in equation (2.10); where,

b : slice width,

W : slice total weight,

c : cohesion,

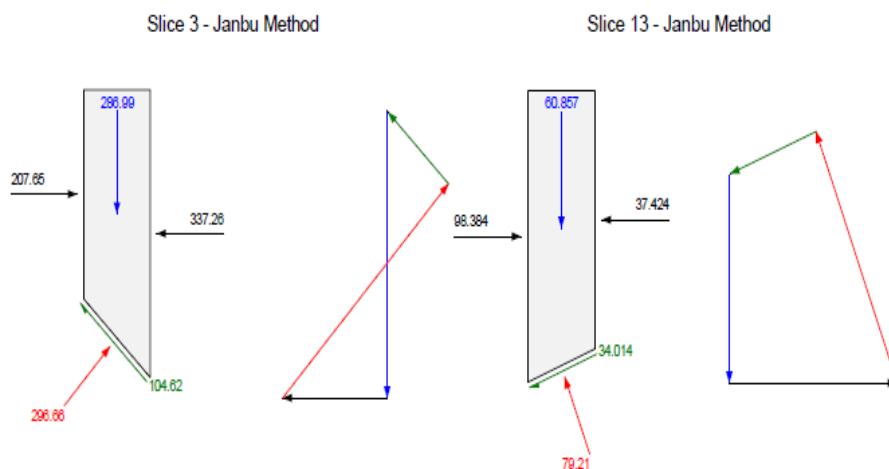
$\phi$  : internal friction angle,

u : pore water pressure at the base of the slice,

$\alpha$  : slope angle of slice base

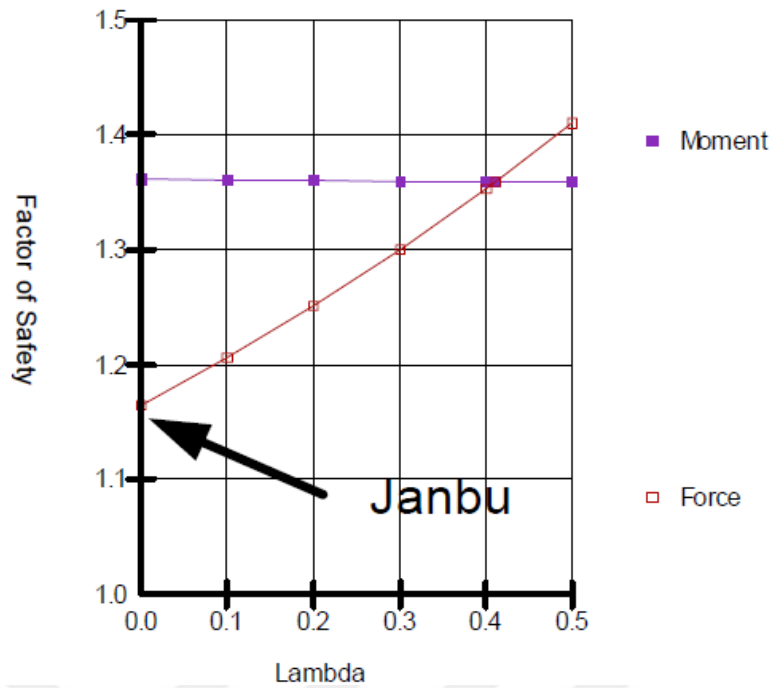
Krahn (2004) proved that there is a difference between Bishop and Janbu methods. Janbu method gave a lower safety factor than the Bishop method. In the study conducted by Kharn, the safety factor found to be 1.36 in the Bishop method was calculated as 1.16 with Janbu.

In the slope analysis given in Figure 2.29, the safety factor calculated as 1.47 with the Fellenius method was calculated as 1.56 with Bishop and 1.45 with the Janbu method. Figure 2.28 shows free body diagrams and force polygons. Closing the range is better than the Simplified Bishop. Although the force polygon closes better in the rim's simplified method, the safety factor is very low because it is only a force balance. As in Figure 2.29, the lambda between slices is considered zero, so that the shear force is neglected.



**Figure 2.28** : Free and force polygon of the object for Janbu's method

Source: (GEO-SLOPE, 2012).



**Figure 2.29** : Janbu's simplified factor of safety

Source: (GEO-SLOPE, 2012).

### 2.9.5 Spencer method

This method was introduced by Spencer in 1967; it can be used for all sliding surfaces. In the method, the relationship between normal and inter-slice shear forces between slices; A flat ratio is accepted. Moment and horizontal force balance is calculated as two separate equations so that the ratio of shear and normal force is obtained. An essential criterion in determining this ratio must meet both equilibrium conditions. The ratio between shear force between slices ( $X$ ) and normal force between slices ( $E$ ) (Krahn, 2004);

$$X = E\lambda f(x) \quad (2.12)$$

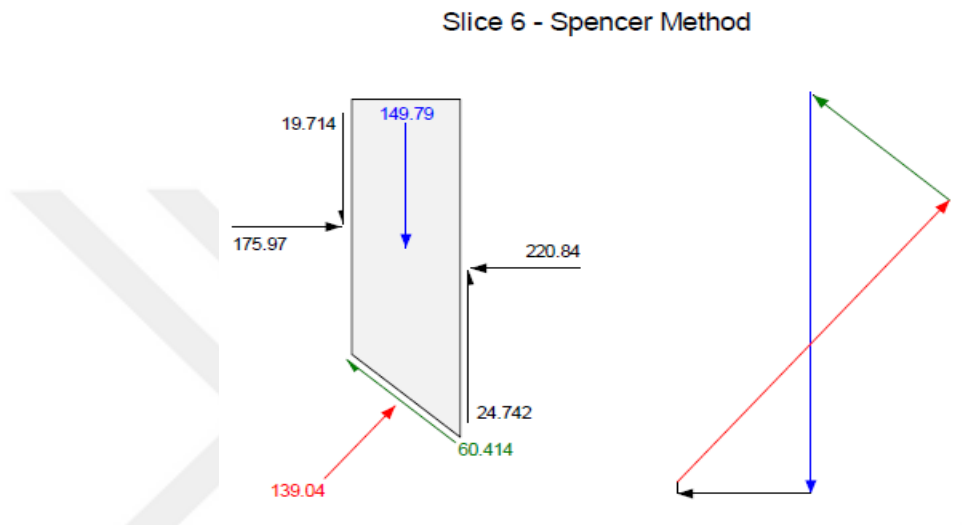
This equation, defined by  $\lambda$  shows the ratio of both forces. According to Spencer,  $\lambda$  is fixed at each slice and is taken as  $f(x) = 1.0$ . Moment and horizontal equilibrium force by Spencer are calculated separately for each  $\lambda$  of equilibrium equations and obtaining the equilibrium value of both equilibrium conditions.

Spencer (1967) proposed method summary is as follows;

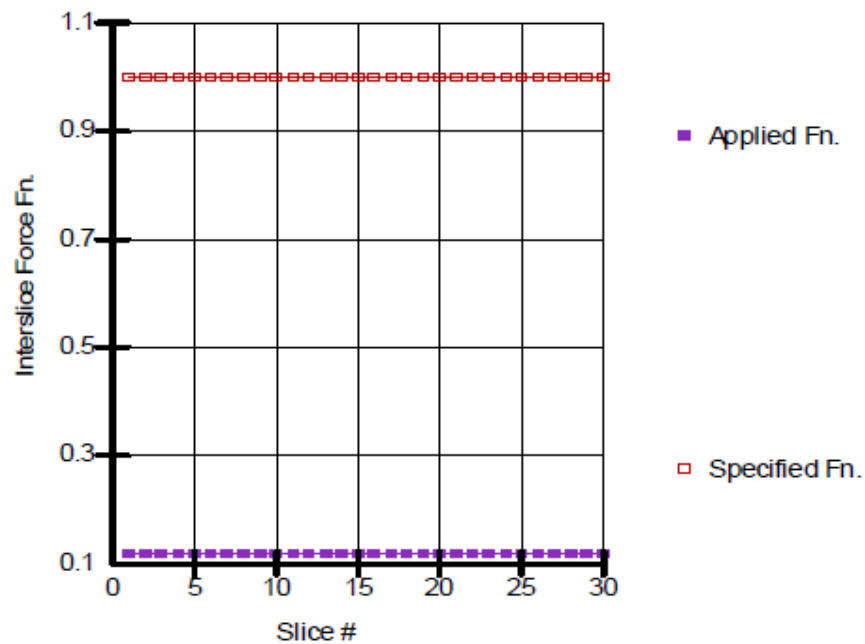
- The normal and shear force between slices is taken into account,
- It takes into account both moment and horizontal force balance, and

- It accepts the constant force ratio ( $X / E$ ) between slices.

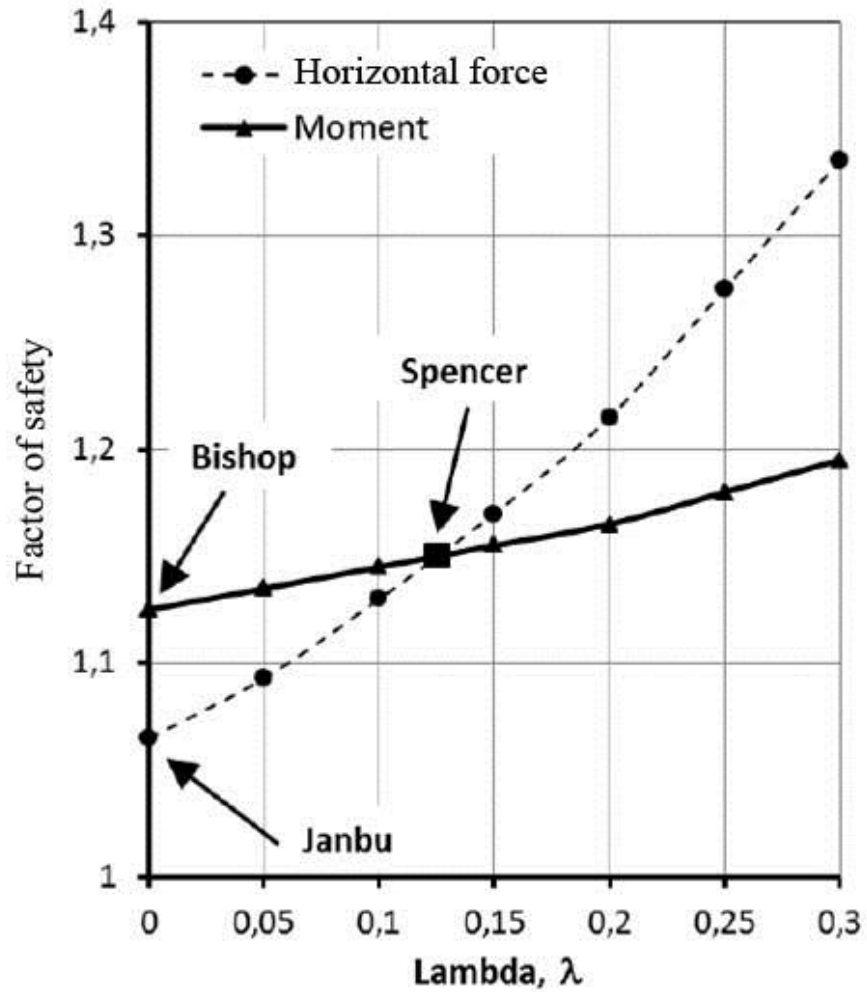
For the given slope,  $c$ ,  $\gamma$ ,  $H$ ,  $b$ ,  $\phi$ ,  $r_u$  values are determined. A typical cross-section diagram can be seen in Figure 2.30. The shear and normal force between slices are closer to more straight. As seen in Figure 2.31, the Spencer safety factor is the point where moment balance and shear force balance intersect. The function  $f(x)$  for the Spencer method is 1.0. The graph of the function is given in Figure 2.32. Note here that every segment has the same value of function  $f(x)$ .



**Figure 2.30 :** Free and force polygon of the object for Spencer's method  
 Source: (GEO-SLOPE, 2012).



**Figure 2.31 :** Spencer factor of safety  
 Source: (GEO-SLOPE, 2012).

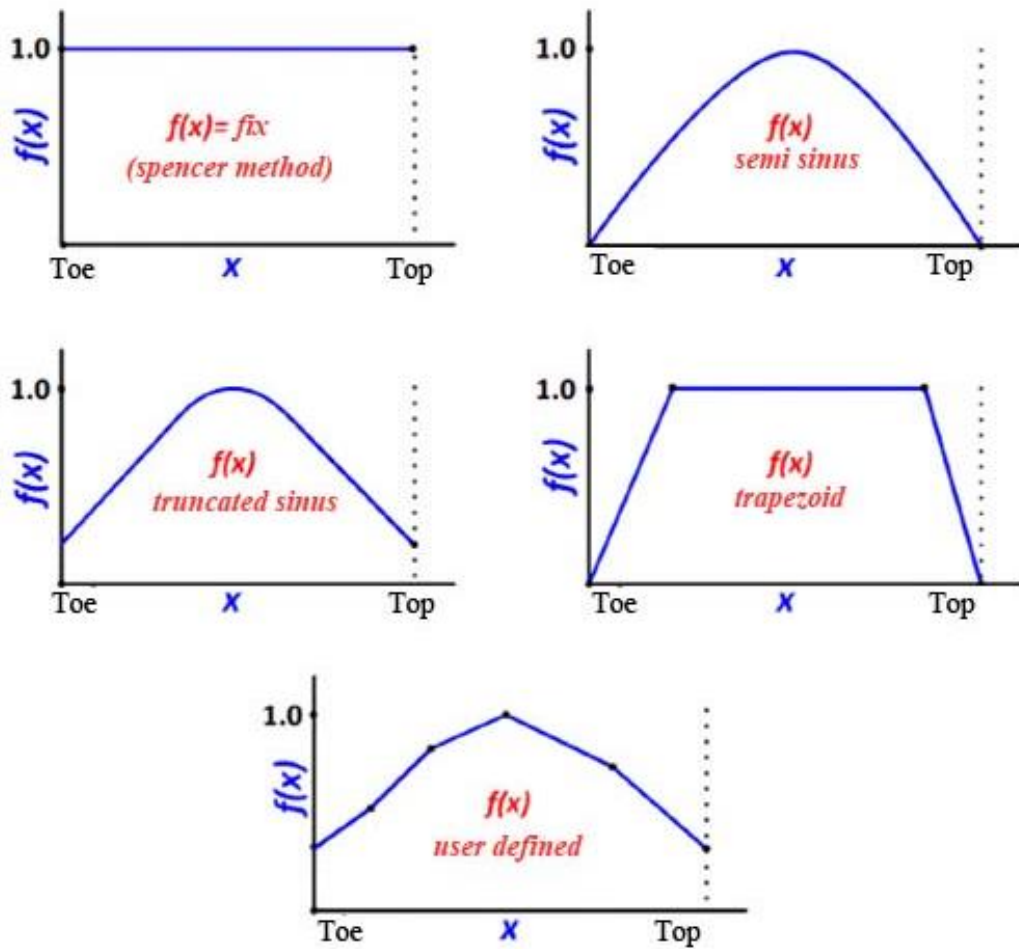


**Figure 2.32** : Calculation of the security number provides both equilibrium equations in the Spencer method using different  $\lambda$  values

Source: (Krahn, 2004).

### 2.9.6 Morgenstern-Price method

Morgenstern-Price (1965) developed a hypothetical method in which sprinter-like inter-slice forces are constant. The only difference between normal and shear forces between slices is defined by different force functions. Functions that are accepted as fixed in the Spencer method; In this method, fixed, half sine, truncated sine, trapezoid, and user-defined functions are defined (Kelesoglu, 2016).



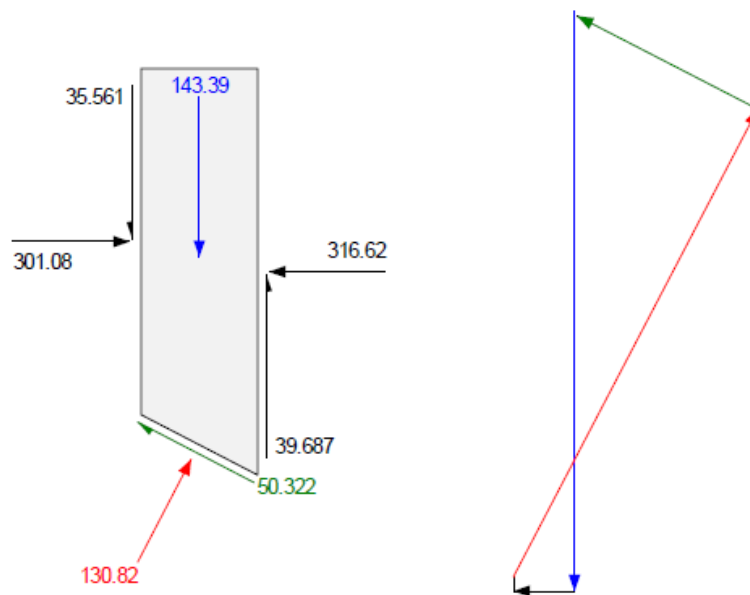
**Figure 2.33 :** Morgenstern-Price method, according to the force function types between slices.

**Source:** (Morgenstern Price 1965).

Comparison of Bishop and M-P methods by Krahn (2004) according to Figure 2.36 due to the assumptions in Figure 2.33 shows the necessity of analysis of a slope where all equations are provided, accordingly the results obtained from Bishop M-P give more remarkable results. This is due to the inverse slope of the moment equilibrium curve. The Bishop method is not correct to mention that the shear force between blocks is always neglected since it is always on the safe side.

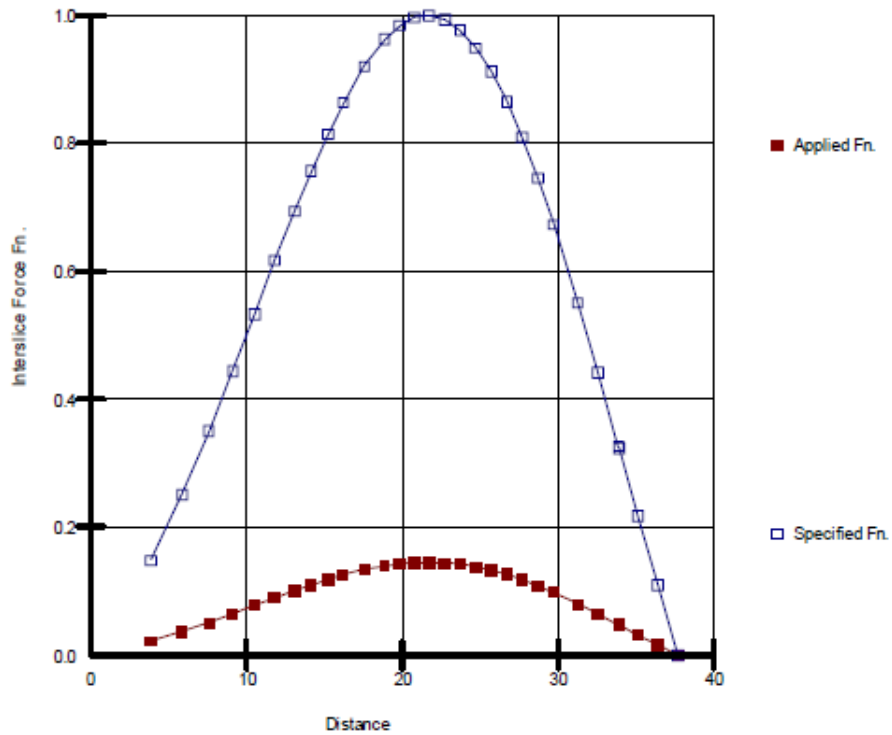
Besides, it is seen that M-P gives more accurate results considering both inter-slice shear and normal force between slices.

Slice 10 - Morgenstern-Price Method



**Figure 2.34 :** Free and force polygon of the object for M&P's method  
 Source: (GEO-SLOPE, 2012).

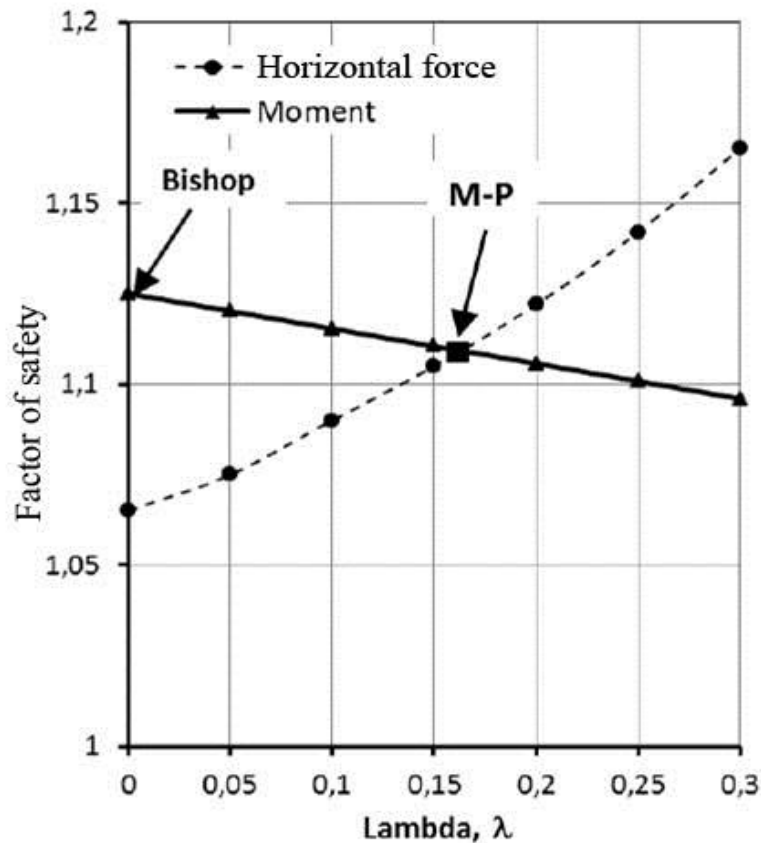
Interslice Force Fn. vs. Distance



**Figure 2.35 :** Alpha interslice force vs. distance for the M-P method  
 Source: (GEO-SLOPE, 2012).

Figure 2.34 shows a typical cross-section diagram. Cutting between slices and normal force are more successful than spencer. As seen in Figure 2.36, the M&P

safety factor is the point where moment balance and shear force balance intersect. For the M&P method, the function  $f(x)$  is different from 1.0, unlike spencer. So the user is optional. The graph of the function is given in Figure 2.35. It should be noted here that each slice has a different lambda value.



**Figure 2.36 :** Comparison of Bishop and M-P methods

Source: (Krahn, 2004).

## 2.10 Finite Element Aided Stress Method

The Soil is divided into a network. Every network is interrelated and interacting with each other. As the amount of mesh increases, the solution becomes more precise. However, the solution time is prolonged. It is, therefore, necessary to approach the optimum mesh width. Although it is impossible to talk about deformation in limit equilibrium methods, the FEA method gives the deformations in detail. Thanks to this approach, more realistic results are obtained. The most significant advantage over the LEM method is that no assumption is made for the critical slip circle. The advantage is that pore water pressures, settlements, and underground water leaks are included in the calculations. The software used in this method; can also control



stability analysis using time-dependent consolidation analysis and strength reduction method (Hammouri et al., 2008). According to Duncan 1996, the deformations in the calculations are more than the real ones. Kim et al. (2002) proved that the rupture circle in finite elements is close to that in limit equilibrium. The shear strength parameters are reduced in finite elements until the system collapses, thanks to software such as Plaxis.

### 2.10.1 Numerical method and shear strength reduction (SSR) technique

It is a powerful method to solve the problem of numerical data. They became popular with the development of computer software. In this method, the shear strength determines a safety factor by reducing the soil's shear strength until collapse occurs. The maximum knot force vector is expressed as an unbalanced or balanced force. This force never reaches zero in numerical analysis. However, it is considered to be in equilibrium when it is close to zero. Here, when the unbalanced force approaches zero and takes a constant value, the malfunction and plastic behavior begins. When SSR is used in finite element or finite difference technique, there is plastic-elastic behavior. The fracture surface is found by comparison with the LEM method (Dawson et al., 1999).

SSR technique gives reliable results. By determining the fault situation, the location of the support elements such as anchors and geosynthetics can be determined (Griffith and Lane, 1999; Dawson et al., 1999; Hammah et al., 2004). The changes in this technique from Mohr-Coulomb power parameters are as follows (Hammah, 2005);

$$c'_{trial} = \frac{1}{FS_{trial}} c_{measured} \quad (2.13)$$

$$\phi'_{trial} = \tan^{-1} \left( \frac{1}{FS_{trial}} \tan \phi \right) \quad (2.14)$$

$$\tau_{max} = c'_{trial} + \sigma_n \tan \phi'_{trial} \quad \text{for the } i^{th} \text{ material} \quad (2.15)$$

When looking at these formulas, "strength reduction factor" (SSR) is used separately for all materials in stability problems (Diederichs et al., 2007).

SSR advantages can be listed as follows;

- (i) The critical sliding surface is found to be more sensitive due to the application of gravitational loads and shear stress in shear force reduction
- (ii) Calculations are made on the complex soil group,
- (iii) Requires no guesswork in shear force distribution in cross-sections, and
- (iv). Unlike LEM, stresses, displacements, and pore pressures can be calculated (Cheng & Lau, 2008). The disadvantage of SSR, on the other hand, is the poor capture of localized slip band formation.

## **2.11 Software Used For Slope Stability**

With the development of computer technology, mathematics has also developed in software. First, limit equilibrium software was produced. Later, the software was developed that can perform feat analysis. It is accepted that the FEA analysis software provides more accurate results than the limit equilibrium method, but the FEA analysis calculation time takes much time.

Therefore, users prefer to solve the conditions determined by the limit equilibrium method in FEA analysis. Some slope stability analysis software that is still used today are given in the Table 2.7. 32 software were analyzed and some criteria were compared. These criteria are; The methods they used were considered as interface and market values. Market demands and academic achievements were also examined. Research has been made about the use of software in academic publications. The user-friendly and secure results of the spelling also affect the market value. How the interfaces work in demo versions was examined. Efforts were made to simplify the parts that force the user in the analyzed Demo versions. These researches had a positive effect on the Matlab code to be written. In general, a package program was created without tiring the user and with little information entry. The developed software was developed by investigating the advantages and disadvantages of 32 different software. Comparative characteristics of the software in the market are given in Table 2.7.

**Table 2.7 : Software used in slope stability analysis.**

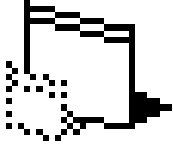

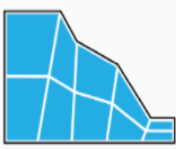


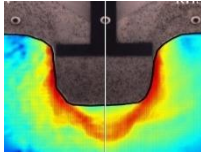
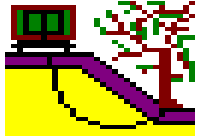

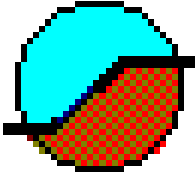


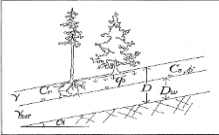



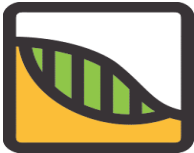

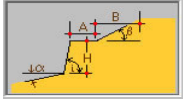


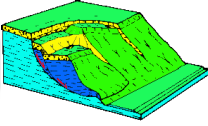


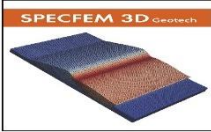

No	Software Name	Logo	Details	Method	Price
1	CLARA-W (Slope Stability Analysis, 2020)		CLARA-W is three-dimensional slope stability software as a Windows version. Although it is similar in concept to its DOS predecessor, which has been used for over a decade, this is an entirely new program with a range of powerful capabilities for both 3D and 2D analysis. Despite its advanced features, the software is very easy to use and learn.	LEM 2D and FEA 2D	FREE
2	CRISP (CRISP Geotechnical Finite Element Analysis Software, 2020)		CRISP engine is written in standard FORTRAN90. The consortium aims to provide an infrastructure for further training, research, and development for CRISP users and developers. The consortium uses the proceeds from the sale of CRISP to invest in further research in the field of geotechnical engineering and to develop the capabilities of the CRISP program further. Using the finite element method has increased the appeal of the software.	FEA 2D	Unknown
3	FLAC/Slope Version 8.1 2020 (Explicit Continuum Factor -fo-Safety Analysis of Slope Stability in 2D)		It can make the two-dimensional calculation of the safety factor (FoS) of FLAC / Slope soil and rock slopes. FLAC / Slope stability can provide solutions under a wide variety of slope conditions with different slope geometries, multiple layers, pore pressure, surface loading, and structural strengthening modules.	FEA 2D	Unknown
4	GALENA (GALENA - Slope Stability Analysis, 2020)		Geotechnical engineers design GALENA to solve geotechnical problems quickly and easily. It can analyze slope stability with a powerful, comprehensive, and easy interface developed for geotechnical, mining, and civil engineers.	LEM 2D	1885 \$
5	GEO5 (Geotechnical Software GEO5   Fine, 2020)		This software uses analytical techniques and FEM to evaluate slope stability, which helps users design structures efficiently. There are many software packages under Geo5. These can be purchased and used gradually.	LEM 2D and FEA 2D	9900 \$
6	GeoPIV (GeoPIV-RG, 2020)		GeoPIV-RG is a software developed for geotechnical and structural engineering applications. There is a MATLAB based image analysis module. It can provide sub-pixel measurement resolution for problems involving large displacements and deformations. The software was written by White (2002) and Take (2002) during Ph.D. research.	FEA 2D	Unknown
7	GGU-STABILITY (GGU-STABILITY - Slope failure calculations and soil nailing, 2020)		This software is only for circular slip surfaces; Bishop can analyze using the general wedge or vertical slice method after Janbu. (Geosysta, 2015). It can analyze the slope and according to DIN 4084 and EC7.	FEA 2D	1078,8 €






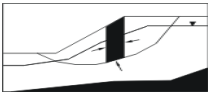

Table 2.7 : Continuation.

8	GSLOPE (Mitre Software Corporation, 2020)		GSLOPE performs the limit equilibrium and slope stability analysis of natural slopes, non-reinforced man-made slopes, or soil reinforced slopes. The software can calculate according to Bishop's Modified method and Janbu's Simplified method. It allows the application of both methods to circular, composite, and non-circular surfaces.	LEM 2D	895 \$
9	GSTABL7 (GSTABL7 with STEDwin Gregory Geotechnical, 2020)		Developed by Gregory Geotechnical Software (in 2001), this software was introduced as an advanced version of STABL designed at Purdue University (1988). This software uses the 2D limit equilibrium analysis slice method to calculate the factor of safety using four procedures, including modified Bishop, simplified Janbu, Spencer, and Morgenstern-Price methods. Fracture surfaces can be used for circular, random, or sliding block failure surfaces.	LEM 2D	Unknown
10	MacSlope (Slope Stability Analysis For The Mac OS, 2020)		The software can calculate with LEM. There are structural strengthening extensions in the package. It detects the failure surfaces by making many iterations in a short time.	LEM 2D	695 \$
11	midas GTS (midas GTS NX   Geotechnical Analysis New Experience, 2020)		This program can perform both 2D and 3D slope stability analysis. It has been developed for geotechnical engineering applications using new generation finite element analysis. It is the software of Korean origin.	LEM 2D and FEA 2D	10000 \$
12	LISA (Level I Stability Analysis) (Soil and Water Engineering - Modeling Software, 2015).		This uses the infinite slope equation to estimate the probability of slope failure for relative stability analyses using Monte Carlo simulation of natural slopes.	2D	Unknown
13	LimitState:Geo (LimitState:GEO - Geotechnical Analysis Software   LimitState, 2020)		This is a slope stability analysis computer program that determines the failure mechanism, rate of fall, and failure states.	3D	2410 £
14	PCStabl (STABL -Slope Stability Analysis Software, 2019)		STABL can handle anchor loading, geosynthetically reinforced soil layers, and Spencer's analysis method.	LEM 2D	Unknown
15	Plaxis (PLAXIS - Essential for geotechnical professionals, 2020)		This program can perform both 2D and 3D slope stability analysis. It was developed for geotechnical engineering applications using finite element analysis. It is used in many literature and academic studies.	LEM 2D and FEA 2D	€ 3,650 - € 6,150
16	QUAKE/W (Dynamic Earthquake Analysis with QUAKE/W - GEO-SLOPE International Ltd., 2020)		QUAKE / W is a finite element software product for modeling earthquake liquefaction and dynamic effects. QUAKE / W can calculate movement and excess pore water pressures caused by earthquake shaking, explosions, or sudden impact loads.	2D	4495 \$

**Table 2.7 : Continuation.**

17	ReActiv (Geocentrix ReActiv - overview, 2020)		ReActiv is computer software for retrofitting with ground nails for a wide variety of floor types.	LEM 2D	1,750 £
18	ReSSA (ReSSA (3.0), 2020)		ReSSA calculates the stability of reinforced and unreinforced slopes and embankments by calculating circular (Bishop method) and two or three-piece wedge failure surfaces (Spencer method).	LEM 2D	1500 \$
19	Slide2 (Slide2, 2020)		Slide2 is a 2D slope stability analysis software using the limit balance method. Slide2 can be used in earth and rock slopes, earth dams, and retaining walls. Slide2 includes finite element groundwater seepage analysis, probabilities, multiple scenario modeling, and plug-in design.	LEM 2D and FEA 2D	1750 \$
D20	Slide3 (Slide3, 2020)		Slide3 is a powerful, user-friendly, 3D slope stability analysis program using the finite element method. Slide3 calculates displacement in hepatic in slope stability analysis. Can compute different layered slope analysis. A high-spec computer is required for complex calculations.	FEA 3D	5295 \$
21	Slope Stability Analysis Program (SSAP2010 (rel. 5 - 2020), 2020)		SSAP2010 is a free software to verify the stability or reinforcement of natural and artificial slopes. The software has modules that contain reinforcement elements to increase the number of security.	LEM 2D	FREE
22	Slope (Oasys Software, 2015)		The program offers several built-in methods for calculating inter-slice forces. Choose between Fellenius or Swedish shear circle analysis, Bishop horizontal method, or constant slope method. For non-circular sliding surfaces, the software provides equivalent Janbu methods.	LEM 2D	1,559 £
23	SLOPE/W (Slope Stability Analysis with SLOPE/W, 2020)		GEO-SLOPE International Ltd., manufactured in Alberta-Canada, in its country. It was developed by the Company. SLOPE / W is slope stability software for slopes in soil and rock types. SLOPE / W can calculate problems under various surface failures, pore water pressures, soil properties, and loading conditions. In addition to the LEM method, there are FEA analysis modules.	LEM 2D and FEA 2D	4495 \$
24	SPECFEM3D GEOTECH (Computational Infrastructure for Geodynamics: Software, 2020)		SPECFEM3D_GEOTECH is an open-source (based on the spectral element method), command-based software for 3D slope stability analysis and advanced excavation simulation.	FEA 3D	Unknown
25	StrataSlope (StrataSlope System - Geogrid, 2020)		This interactive computer program uses Bishop's (1955) method for geogrid reinforced slope stability analysis.	LEM 2D	Unknown

**Table 2.7 : Continuation.**

26	SVSlope® (SoilVision Systems - Geotechnical Finite Element Software - SVSLOPE®, 2020)		SVSlope; More than fifteen different analysis methods can be applied, including the classical slice method and stress-based methods such as Bishop, Janbu, Spencer, Morgenstern-Price, GLE. Calculates tension fields from SVSOLID in 2D and 3D (performs hybrid Kulhawy analysis by importing).	LEM 2D-3D	Unknown
27	TALREN V5 (Software capabilities-terrasol- setec. 2020)		Talren V5; Can calculate classical moment equilibrium (Bishop or Fellenius) or global (force and moment) equilibrium methods for circular or noncircular failure. It also includes yield design calculation methods (with logarithmic spiral fracture surfaces). This enables new applications for the program (gabion stability, soil pressure calculations, additional shear mechanisms, etc.).	LEM 2D	4,500 €
28	TSLOPE (Geotechnical Software - 3D Slope Stability – Geotechnical Software for a 3D World, 2020)		TSLOPE models provide valuable information regarding slope behavior. 2D and 3D Modeling is possible.	LEM 2D-3D	Unknown
29	VERSAT-2D (Wu, 2013)		VERSAT-D2D is a software package consisting of three modules, including VERSAT-2D and VERSAT-S2D. VERSAT-2D software creates input data for VERSAT-S2D and VERSAT-D2D. The program uses FEM to perform slope stability analysis.	FEA 2D	1250 \$
30	XSLOPE (Slope stability - XSLOPE - Civil Engineering - The University of Sydney, 2020)		XSLOPE calculates a simplified world slope stability using the Bishop (1955) method for the analysis of cyclic error surfaces or Morgenstern and Price (1965, 1967) for non-cyclic error surfaces. This program is an improved version of the first DOS version released in 1982.	LEM 2D	FREE
31	XSTABL (XSTABL home page, 2020)		This software, developed at Purdue University, is an integrated software for slope stability analysis.	LEM 2D	450 \$
32	ZSoil (Zace Services Ltd ZSoilPC software for geotechnics and geomechanics, 2020)		Zace Services Ltd. Company. The software analyzes underground and aboveground structures, excavation conditions, soil-structure interaction, and dynamic conditions. The ZSoil software is written for the MS-Windows environment and performs slope stability analysis based on the finite element method.	FEA 2D	11340 \$

**Source:** (Url-1 and Url-2).

When the table below is examined, the following results have emerged for 32 slope software. The software works with 25% FEA infrastructure. 47% of the software

works with LEM infrastructure. 19% of the software works with FEA and LEM infrastructure. The software works with 9% other method infrastructure .

**Table 2.8 :** Software used in the market.

Method	% Used
FEA-FEM	25%
LEM	47%
FEM And LEM	19%
Other Method	9%
Total	100%

If we evaluate the table; The availability of LEM based software available on the market is observed. When the price and performance criteria are met, the software to be written with Matlab code will be attractive. It is also aimed to be used in international articles.

### **2.11.1 Matlab software**

MATLAB (matrix lab) is a numerical computing software (multi-paradigm) and a fourth-generation programming language. Fourth-generation programming language: Less code writing instructions, simple to use, ready-to-use templates, and wizards to develop specialized practical solutions for specific needs.

MATLAB is developed by MathWorks. MATLAB allows the user to work with programs written in other languages such as C, C ++ and Java, matrix operations, function and data drawing, algorithm development, and user interface creation. Researchers and developers first accepted MATLAB in control engineering.

Also, linear algebra is a popular language for teaching numerical analysis and image processing. With MATLAB, you can call functions in the C programming language or Fortran and write subprograms. MATLAB, Linear algebra, statistics, optimization, numerical analysis, optimization, Fourier analysis, such as mathematical calculations, can be done effectively and quickly. The MATLAB programming language is also used for 2D and 3D graphics drawing. With MATLAB, even very complex mathematical calculations are completed in a short time. Two and three-dimensional graphs of basic mathematical functions can be drawn with MATLAB.

You can easily draw any kind of two and three-dimensional mathematical graph MATLAB, especially polynomials, parabols, sine, cosine waves (Url-3).

### **2.11.2 Slope stability analyses with matlab**

The main purpose of this thesis is to prepare a slope stability software using the MATLAB script. It was aimed to find the defects in the breaking surface of the slope. Normal and tangential stress components will be created. There will be a safety factor for stress failures on the X and Y surfaces. The accepted terms for the MATLAB script are:

- The slope is assumed to break circularly.
- The slope is optionally offered as an ellipse.
- The break point range must be entered by the user.
- The precision in an iteration of the account to be made depends on the user.
- Increasing the number of slices increases the sensitivity, but the processing time increases.
- While creating the geometry, some warnings appear to warn the user, and these are to facilitate the operations.
- Many soils with different properties can be selected, but parameters can be changed by the user. However, at least two soil types must be selected.
- The properties of soil parameters to be used are excluded from responsibility.
- In the thesis, the calculations made in the MATLAB script have been verified by other software.
- In the thesis, the developed MATLAB code name has been determined as "SlopeME". It is aimed to develop and update the MATLAB code.



### 3. DEVELOPED MODEL

In this study, it is aimed to find the most critical failure surface of the slope. Slope stability is investigated according to the test results obtained from the laboratory. Many arrangements are made for LEM accounts. These regulations make the calculations difficult but increase the security of the safety factor.

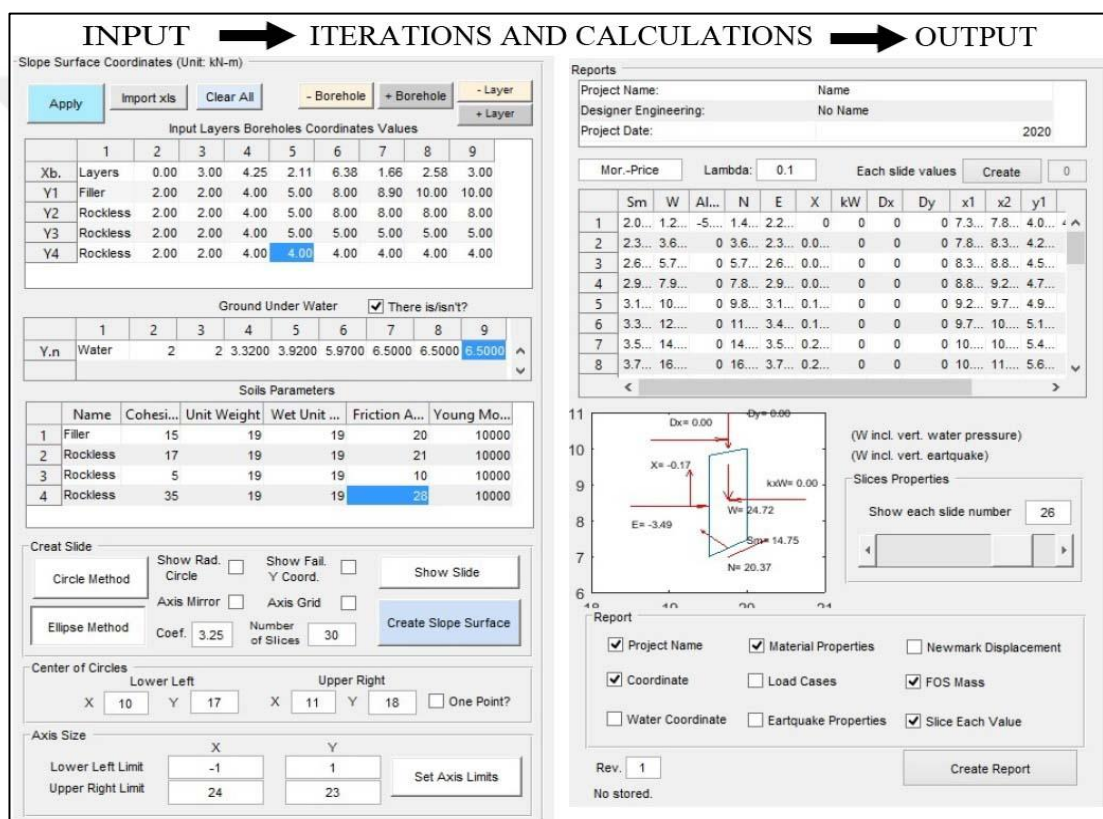
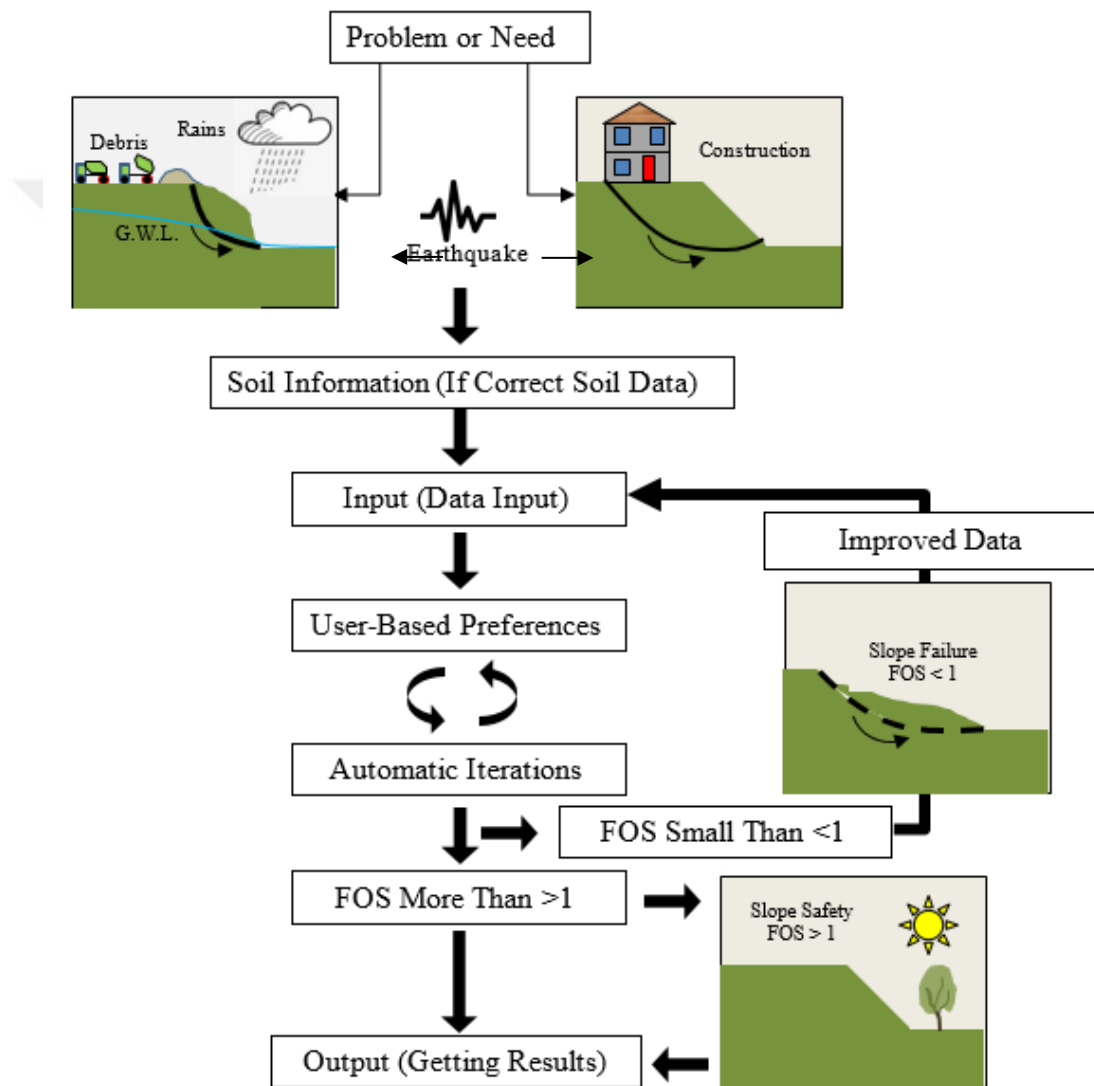


Figure 3.1 : Input and Output in developed model.

The model to be developed consists of two main parts. These are input and output interfaces in Figure 3.1. Although these have different functionality, they are actually a whole. Input is the part where data is entered, and geometry is defined. Here the user is asked to make some choices. The reason for this is related to LEM account acceptance. The software is aimed to make maximum iterations in optimum time. Thus, more precise and realistic solutions are achieved.

The output is the conclusion part of the entered data and assumptions. Calculated details and Calculated reporting section can be accessed here. The user selects the sections he wants to appear in the report. The parts that will appear in the account report are available in the relevant earthquake regulation. However, the administration to be submitted may require some changes. Another purpose of the software is to have the skills and abilities to be used in scientific research. Detailed explanations about the input and output are given below in subheadings.



**Figure 3.2 :** Calculation algorithm in the developed model.

The algorithm of the software developed above is given. If the FOS is greater than 1, the reporting part is passed. If FOS is less than 1, improved ground data are re-entered. For example, lowering the groundwater level. The important thing here is

that the software is user-friendly. The academic meaning of the software depends on the efficiency of the comparisons. It is aimed at the comparisons to be examined under the next heading to give results as close as possible.

### **3.1 Input of Data**

To solve a slope problem, the terrain must be well known. Knowing the land well will reduce the complexity of the problem. Converting the land to a digital database directly affects the solution quality of the problem.

#### **3.1.1 Geometry created with the developed model**

One borehole is assumed for every Y coordinate change in the geometry. A minimum of 4 points is required to create a geometry. Data entry is made with Matlab gui table interface. You can enter as many points as the gui table allows (thought to be more than 100). It is necessary to enter the bedrock layer at the bottom. + Borehole increases the default drill count. -Borehole decreases the default drill count. + Layer increases the number of layers in the soil. - Layer reduces the number of layers in the soil.

Apply: It ensures that the geometry changes are transferred to the graphics section in an updated manner. Import xls: It is used to import data from Excel files directly. It is currently not working during the development phase. Clear All: Deletes all data in the geometry. -Borehole: Deletes drilling log. + Borehole: Adds drilling log. + Layer: Adds a soil layer. -Layer: Erases the soil layer. Y coordinates of the groundwater level can also be entered here. This is entirely at the user's discretion. It is sufficient to know three parameters in limit equilibrium analysis. Soil plastic analysis parameters (with drainage). These are internal friction angle ( $\phi'$ ), unit volume weight ( $\gamma$ ), and cohesion ( $c'$ ). When these parameters are known, analysis can be made for any Limit equilibrium method.

Also, the user decides whether the fracture surface is circular or elliptical. In addition, the user decides on the selection of "Number of Slices". Since this affects the resolution time, the user decides.

Slope Surface Coordinates (Unit: kN-m)

Apply Import xls Clear All - Borehole + Borehole - Layer + Layer

Input Layers Boreholes Coordinates Values

	1	2	3	4	5	6	7	8	9
Xb. Layers	8.00	4.00	4.00	5.40	2.30	3.30	1.00	1.00	
Y1 Filler	15.00	15.00	10.30	10.30	5.80	5.80	2.00	2.00	
Y2 Rockless	1.00	1.00	1.00	1.00	1.00	1.00	1.00	1.00	
Y3									
Y4									

Ground Under Water  There is/isn't?

	1	2	3	4	5	6	7	8	9
Y.n Water	13	10	6.3000	5.5000	3	2.8000	1.5000	1	

Soils Parameters

	Name	Cohesi...	Unit Weight	Wet Unit ...	Friction A...	Young Mo...
1	Filler	2	19	19	24	10000
2	Rockless	5	20	20	32	100000

Crear Slide

Circle Method  Show Rad. Circle  Show Fail. Y Coord.  Show Slide

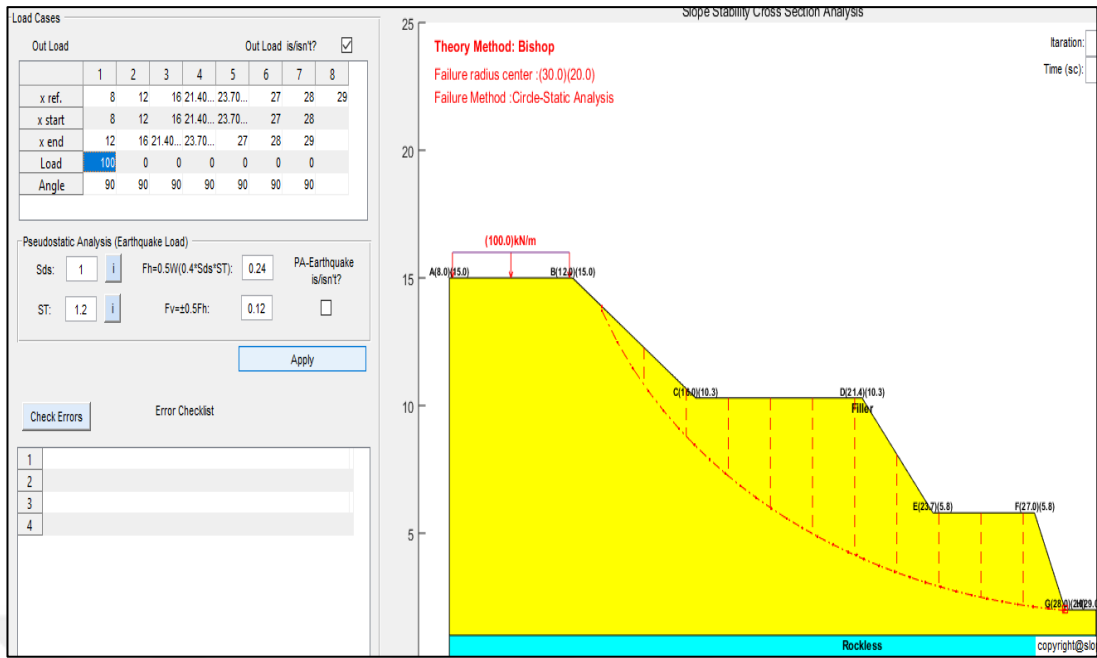
Ellipse Method  Axis Mirror  Axis Grid  Create Slope Surface

Coef. 1 Number of Slices 10

**Figure 3.3 :** Input geometry in developed model.

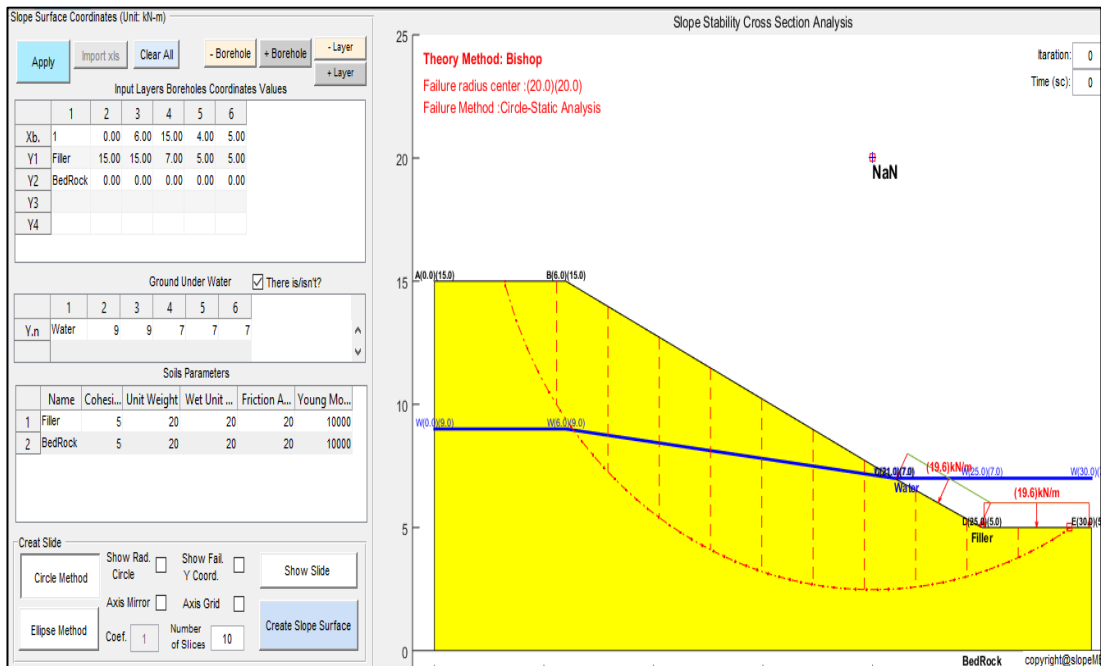
### 3.1.2 Loading with developed model

Surcharge loads can be added on the slope in this section. These loads act as a distributed load. However, loads can be added to a point if desired. Surcharge loads can be, for example, the load of a building. Overloads should not always be considered negative. For example, in a lake, distributed loads at the heel point positively affect the safety factor.



**Figure 3.4 :** Loading in developed model.

For example, the surge that will occur on the heel in a pond can make the distributed load stabilize the system. In this case, the safety factor increases the safety with the surge load reverse torque effect. In the slope stability calculation, surcharge loads at the heel increase the safety charge, while the surge loads at the Top decrease the safety factor.



**Figure 3.5 :** Water loading in developed model.

### 3.1.3 Check error list in developed model

Various checks must be made on the created model. This is a must for almost any software. It is an interface developed for the user to reach the solution more easily. It is a suspension that will prevent the results from being meaningless. Ugun is confirmed with a plus (+). If there is an incompatibility, it warns the user by giving an old (-) yellow warning.

## 3.2 Dynamic Loading

### 3.2.1 Pseudo-static analysis

Seismic investigation of soil stability started in the 1920s. It is calculated by the effect of earthquake effects with a fixed horizontal and vertical coefficient. The pseudo-static analysis was first applied by terzaghi in the 1950s.

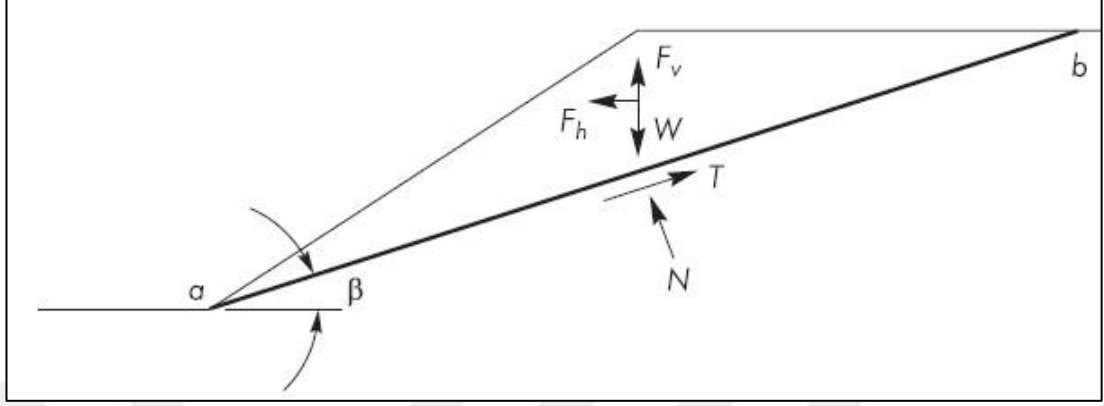
Check Errors		Error Checklist	
1	Drawing of layers is suitable for calculation.(+)		
2	The cohesion value of the materials is within acceptable limits.(+)		
3	The unit value of the materials is within acceptable limits.(+)		
4	The friction angle value of the materials is within acceptable limits.(+)		
5	Load starting point is correct.(+)		
6	Load ending point is correct.(+)		
7	Failure starting point B is correct.(+)		
8	Failure ending point C is correct.(+)		
9	You should calculate OMS after each geometry change.		
10	For ellipse method, re-determine initial coef. after each geometry change.		

**Figure 3.6 :** Check error list in developed model.

In pseudo-static analyzes, the effects of earthquake shaking are represented by pseudo-static forces that generate inertia.  $F_h$  and  $F_v$  are the horizontal and vertical inertia force. These inertial forces  $F_h$  and  $F_v$  pass through the center of gravity of the mass under the calculation. It is as follows:

$$Fh = \frac{a_h W}{g} = k_h W \quad (3.16)$$

$$Fv = \frac{a_v W}{g} = k_v W \quad (3.17)$$



**Figure 3.7 :** The loads acting on the triangular fracture surface in pseudo-static loading

Source: (Kramer 2003).

Where  $a_v$  and  $a_h$  are vertical and horizontal accelerations,  $k_v$  and  $k_h$  are dimensionless coefficients.  $W$  is the weight of the fractured mass. The earthquake regulations should be based on the selection of these coefficients.

$$FS = \frac{\text{holding forces}}{\text{failure forces}} = \frac{cl_{ab} + [(W - Fv) \cos \beta - Fh \sin \beta] \tan \phi}{(W - Fv) \sin \beta + Fh \cos \beta} \quad (3.18)$$

Where  $c$  and  $\phi$  mohr-coulomb strength parameters are  $l_{ab}$ : length of failure recovery. Pseudo-static forces reduce the safety factor as seen. The pseudo-static approach can be easily applied to planar, circular, and non-circular fracture surfaces. Most commercial software written on limit equilibrium slope static stability has a pseudo-static analysis option (Kramer 2003).

In TBDY 16.13.9, in the equivalent static analysis, the soil mass will be influenced as follows in addition to the loads present on the slope.

$$Fh = 0.5W(0.4S_{DS}S_T) \quad (3.19)$$

$$Fv = 0.5Fh \quad (3.20)$$

$W$ : weight of the sliding mass.

$S_{DS}$ : short-period design spectral acceleration coefficient.

$S_T$ : short-period design spectral acceleration coefficient.

### 3.2.2 Pseudo-static coefficient chosen

The most influencing factor on the results of pseudo-static analysis depends on the  $k_h$  seismic coefficient value. Choosing this coefficient in the pseudo-static analysis is the most difficult issue. Because the material is not rigid and peak accelerations in an earthquake are effective in a short time. Pseudo-static coefficients used in practice generally correspond to a value far below  $a_{max}$ . The first studies on this subject were carried out by Terzaghi (1950). Terzaghi suggested taking  $k_h = 0.10$  for large earthquakes,  $k_h = 0.2$  for catastrophic earthquakes and  $k_h = 0.5$  for catastrophic earthquakes.

Many pseudo-static assumptions have been developed for use on the dam from 1966 to 1986. Seed (1979) extracted the pseudo-static criteria for 14 dams in 10 earthquake zones. He stated that the pseudo-static safety coefficient is 1.15 for the dams built using ductile soils (soils that do not contain high pore water pressure or lose 15% of the strength under repeated loads), at crest accelerations lower than 0.75g. It states that when  $k_h = 0.1$  and ( $M = 6.5$ )  $k_h = 0.15$  ( $M = 8.25$ ) the deformations remain within acceptable limits. Hynes-Griffin and Franklin (1984), in their groaning on more than 350 Newmark sliding blocks, concluded that if the safety coefficient in your pseudo-static field is taken above 1.0, the deformations do not change to a "dangerous extent". Although engineering judgment is required in almost all cases, Hynes-Griffin and Franklin (1984) criteria are suitable for most slopes (Kramer 2003).

**Table 3.1 :** Pseudo-static results of slope failure effect of an earthquake

Barrage	$k_h$	FOS	Earthquake Effect
Sheffied Barrage	0,10	1,2	completely failure
Down San Fernando Barrage	0,15	1,3	upstream surface failure
Top San Fernando Barrage	0,15	2-2,5	downstream face shifted 6ft including crest
Mine Waste Barrage	0,20	1,3	Barrage failure

Source: (Sees, 1979).



### 3.2.3 Pseudo-static load in developed model

The coefficient selection in the pseudo-static analysis is complex, but it was specified in TBDY 2018-16.13.10 how to take these coefficients. Matlab code is compatible with TBDY 2018. After the slope is divided into slices, the center of gravity of each slice is calculated automatically. Increasing the number of slices does not affect finding the center of gravity of the slices. Matlab code is able to calculate the horizontal and kv vertical forces kh selected to the center of gravity of each slice.

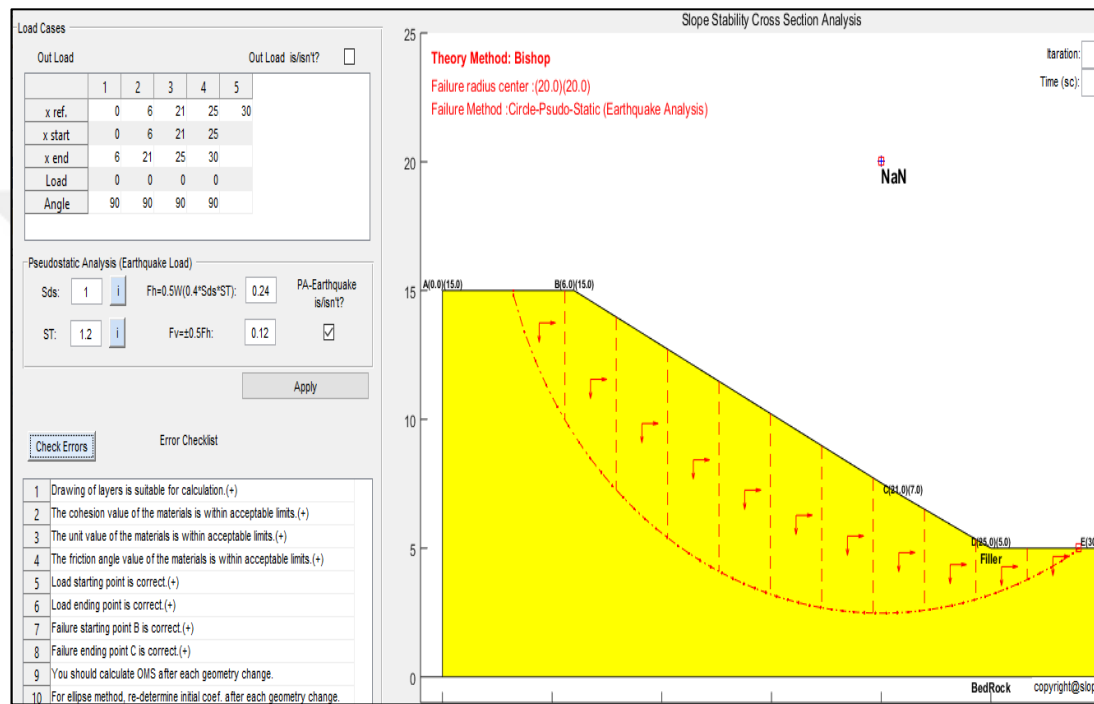
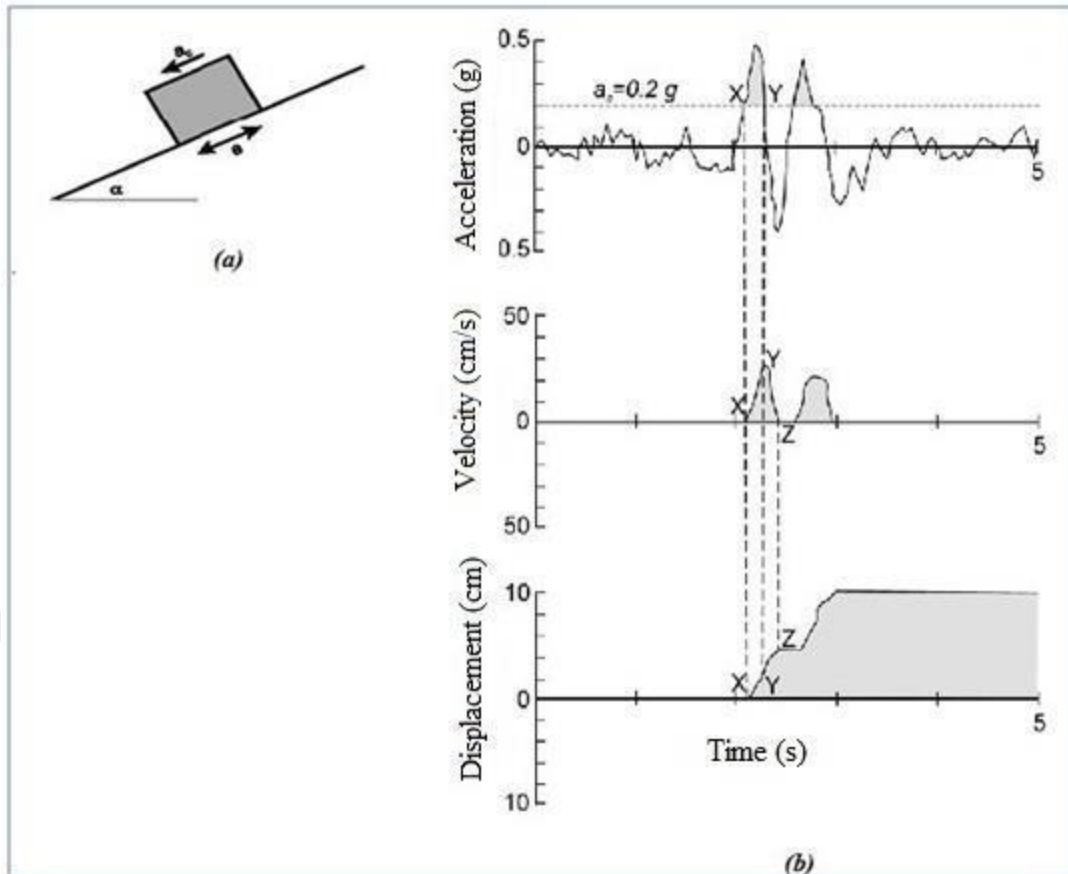


Figure 3.8 : Pseudo-static loading in developed model.

## 3.3 Displacement Calculation

### 3.3.1 Newmark sliding block analysis

It was proposed by Newmark to calculate or predict earthquake-induced ground motions. Newmark derived the logarithmic formula by comparing the soil to a sliding block. In this method, the soil slides as a block. Dynamic and static loads are distributed homogeneously. Pore water pressure is not considered. Critical acceleration is considered constant throughout the analysis. The sliding block cannot move in the opposite direction. As a disadvantage, it does not give meaningful results as there will be no block movement in cohesionless soils. Increasing pore water pressures and liquefaction are also not considered.



**Figure 3.9 :** a) Sliding block b)Newmark analysis algorithm

Source: (Kramer, 2003).

Here the acceleration vs. time record is at the left of the X point below the ac record of the acceleration record if  $a_c = 0.2g$ . To the left of point X, above the ac record, is the velocity-time graph with the time-dependent integration of the acceleration. The velocity peaks at the Y point. The motion continues despite the acceleration force falling below  $a_c$  after Y point because the trigger inertia is provided.

On the other hand, the Z point stops thanks to the friction and resistance forces. Subsequently, if the  $a_c$  critical acceleration is exceeded, the block continues to slide, and eventually, the soil displacement is calculated. The name of this movement is Newmark sliding block analysis.

The threshold value ( $a_c$ ) that will trigger a block to start motion is the critical acceleration value. The block is assumed to be at rest before the critical acceleration value is reached. Therefore it is extremely important. Finding the critical acceleration value in different sources has been given. However, the most important ones are given by the formulas below.

$$ac = g(FS - 1) \sin \alpha \quad (3.21)$$

Finding another critical acceleration value is the horizontal coefficient  $k_h$  that makes  $FS = 1$ . It is necessary to iterate by increasing  $k_h$  until the safety factor is 1. It is a laborious method, but most software that performs slope analysis has this feature.

A lot of work has been done based on the Newmark method. The most used of these are listed below.

The following regression is given by Ambraseys and Menu (1988) to calculate Newmark displacement using 50 data from 11 earthquakes. Critical acceleration ( $a_c$ ) and maximum acceleration ( $a_{max}$ ) must be known.

$\delta$ : Refers to the total displacement on the slope.

$a_c$ : critical acceleration.

$$\log \delta = 0.90 + \log \left[ \left( 1 - \frac{a_c}{a_{max}} \right)^{2.53} \left( \frac{a_c}{a_{max}} \right)^{-1.09} \right] \pm 0.30 \quad (3.22)$$

Yigit et al. (2017) have occurred in Turkey between the years 1976-2013 by the  $M_w \geq 5.5$  earthquake data (AFAD, 2013) and  $a_c = 0.02g; 0.05g; 0.1g; 0.2g; 0.3g$ ; Using  $0.4g$  values, 29 earthquake record data gave the following equation as  $R^2 = 0.67$  and standard deviation  $\sigma = 0.55$ .

$$\log \delta = 0.07 + \log \left[ \left( 1 - \frac{a_c}{a_{max}} \right)^{1.461} \left( \frac{a_c}{a_{max}} \right)^{-1.506} \right] \quad (3.23)$$

Jibson (1993); Newmark has developed a formula that contains the arias index ( $I_a$ ) and the maximum acceleration ( $a_{max}$ ) value to calculate the displacement.  $a_c = 0.02g; 0.05g; 0.1g; 0.2g; 0.3g$ ; Jibson (1993) developed the form with 11 displacement motion records for  $0.4g$ . In determining the equality,  $R^2 = 0.87$ .

$$\log \delta = 1.460 \log I_a - 6.642 a_c + 1.546 \pm 0.409 \quad (3.24)$$

Yigit et al. (2017) gave the following equation as  $R^2 = 0.79$  and standard deviation  $\sigma = 0.442$ .

$$\log \delta = 1.34 \log I_a - 8.202 a_c + 1.71 \quad (3.25)$$

Displacement (cm),  $a_c$ ; critical acceleration is arias index  $I_a$  (m / s). Awarded by the Arias index (Arias 1970).

$$I_a = \frac{\pi}{2g} \int_0^{T_d} [a(t)]^2 dt \quad (3.26)$$

Using the previous equation, Jibson (1998) proposed the following equation by taking  $R^2 = 0.83$  over 13 earthquake records with 555 data.

$$\log \delta = 1.521 \log I_a - 1.993 \log a_c - 1.546 \pm 0.375 \quad (3.27)$$

Yiğit et al. (2017) gave the following equation as  $R^2 = 0.855$  and standard deviation  $\sigma = 0.365$ .

$$\log \delta = 1.492 \log I_a - 2.021 \log a_c - 1.5125 \quad (3.28)$$

Hsieh et al. (2011) proposed the following equation, including displacement and critical acceleration relations with the index of displacement and arias. In determining the equality,  $R^2 = 0.89$ .

$$\log \delta = 0.847 \log I_a - 10.62 a_c + 6.587 a_c \log I_a + 1.84 \pm 0.295 \quad (3.29)$$

Yiğit et al. (2017) gave the following equation as  $R^2 = 0.855$  and standard deviation  $\sigma = 0.365$ .

$$\log \delta = 1.158 \log I_a - 9.4776 a_c + 5.62 a_c \log I_a + 1.7158 \quad (3.30)$$

Jibson (2007/1) worked on the Ambraseys formula and found the following equation by modifying it. In determining the equality,  $R^2 = 0.87$ .

$$\log \delta = -2.71 + \log \left[ \left( 1 - \frac{a_c}{a_{max}} \right)^{2.335} \left( 1 - \frac{a_c}{a_{max}} \right)^{-1.438} \right] + 0.424M \pm 0.454 \quad (3.31)$$

Yiğit et al. (2017) gave the following equation as  $R^2 = 0.78$  and standard deviation  $\sigma = 0.45$ .

$$\log \delta = -2.785 + \log \left[ \left( 1 - \frac{a_c}{a_{max}} \right)^{1.793} \left( 1 - \frac{a_c}{a_{max}} \right)^{-1.313} \right] + 0.459M \quad (3.32)$$

Jibson (2007/2) gave the following equation by developing the critical acceleration and arias index. In determining the equality,  $R^2 = 0.75$ .

$$\log \delta = 0.561 \log I_a - 3.8331 \log \left( \frac{a_c}{a_{max}} \right) - 1.474 \pm 0.616 \quad (3.33)$$

Yiğit et al. (2017) gave the following equation as  $R^2 = 0.77$  and standard deviation  $\sigma = 0.46$ .

$$\log \delta = 0.536 \log I_a - 1.8441 \log \left( \frac{a_c}{a_{max}} \right) - 0.322 \quad (3.34)$$

### 3.3.2 Newmark sliding block analysis in developed model

Newmark displacement module is included in the developed model. Many valid equations are presented here. The important thing here is to access earthquake records. The distance of the earthquake record stations to the location to be analyzed is an important effect on the calculations.

Newmark's Sliding Block - Displacement

Newmark analysis. OK?

FOS Method Properties

Theory Method 1.25

Average slope

$\alpha$ (alpha): 24.1455 Degree

Izmit 1999-Sakarya Bay. 1

Izmit 1999-Sakarya Ba...	
Magnitude:	7.4000
Epicentral Distance(km):	0.4200
Focal Distance(km):	34
Rupture Distance(km):	18
Arias Intensity Ia:	1.7080
PGA(g):	0.4177
PGV(cm/sec):	-
PGD(cm):	-
Main Period(sec):	0.3200

(Critical Acceleration)

$ac=g*(FOS-1)*\sin\alpha$

Before static FOS run! => Theory Method

ac= 0.102264 g Cal.

Calculate completed.

Import .xls Graphic

Earthquake

	Time	(g's)
1		
2		
3		
4		

← Cal.

Displacement Method

Jibson (1998)

Displacement (cm) 7842.98

Jibson (1998)

$\log(Dis)=1.492\log Ia-2.021\log ac-1.5125$

Show in Draw

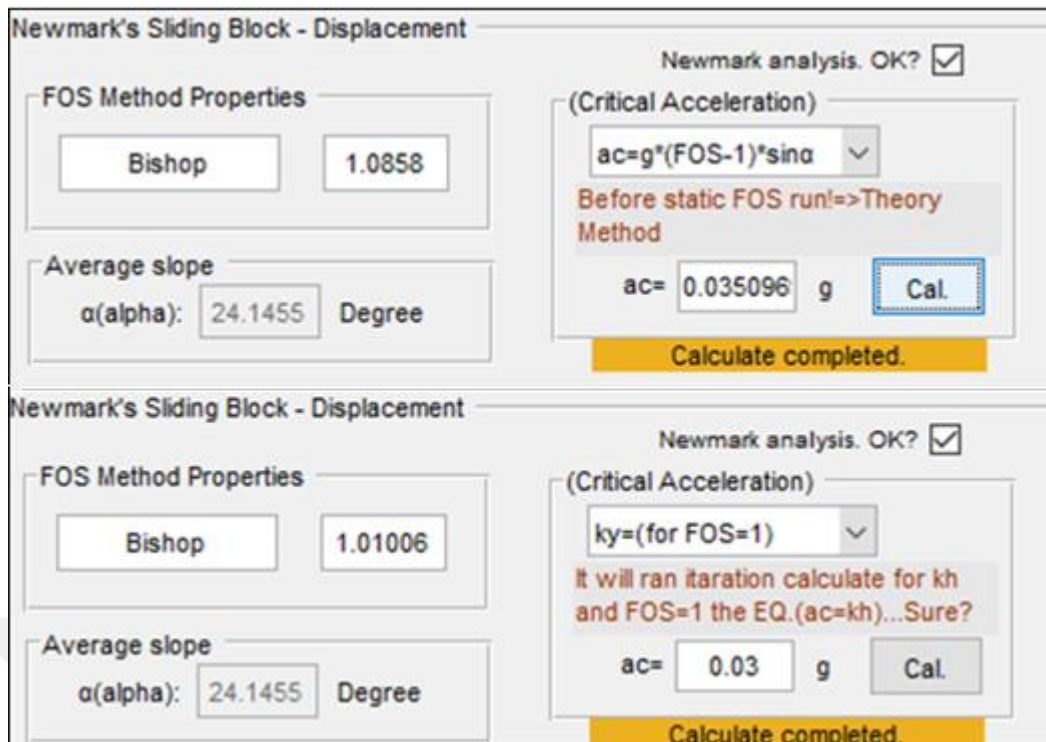
Calculate

**Figure 3.10 :** Newmark analysis algorithm in the developed model.

The choice of critical acceleration is left to the user. The slope average is automatically found by the developed Matlab code. The critical acceleration ( $a_c$ ) based on the slope and the horizontal coefficient ( $k_y$ ) gives the safety factor 1 give results close to each other.

$a_c$ : the critical acceleration.

$k_y$ : the horizontal coefficient.



**Figure 3.11 :** Critical acceleration calculation.

The comparison of critical acceleration is given above. The user has to make this choice that affects the displacement. Developed Matlab code according to TBDY 2018: 16.13.8, Newmark is capable of sliding block analysis and it works fully compatible.

### 3.4 General Limit Equilibrium (GLE)

In Table 3.2, Abramson (1996) compares the limit equilibrium methods. As seen in the table, the force balances used in finding the safety factors are summarized. Fredlund and Krahn (1977) developed a method that covers the methods given in Table 3.2. This method, which covers the key points of other methods in the literature, is called General Limit Equilibrium Theory - GLE. Details are provided by Krahn (2004). The safety factor in slope stability is the concept that reduces the sliding resistance across the sliding surface. Shear strength information is required for calculations.

**Table 3.2 :** Comparison of limit equilibrium analysis in terms of moment and force balance.

Method	Force Balance		Moment Balance
	X Direction	Y Direction	
Fellenius	No	No	Yes
Bishop	Yes	Yes	Yes
Janbu	Yes	Yes	No
Morgenstern-P.	Yes	Yes	Yes
Spencer	Yes	Yes	Yes

**Source:** (Abramson, 1996).

Effective stress analysis is given by the Mohr-Coulomb hypothesis as follows.

$$s = c' + (\sigma_n - u) \tan \phi' \quad (3.35)$$

In this formula;

$s$ : shear strength

$c'$ : effective cohesion

$\sigma_n$ : total stress

$\phi'$ : effective internal friction angle

$u$ : pore water pressure

Pore water pressure is neglected in total stress calculations, and the strength parameters are found by the total stress.

There are two important assumptions that the GLE approach uses:

- The safety numbers of the cohesion and friction components that make up the strength of the floors are the same.
- The number of security is the same for all slices forming the sliding circle examined.

Vertical and horizontal forces are applied to any slice on a circular (in Figure 3.12) and non-circular (in Figure 3.13) sliding circle. These terms exist as (Krahn, 2004):

$N$  = slice base normal force.

$S_m$  = slice base shear force.

$E$  = lateral force in the slice. Subscript given as L indicates the slice's left side, and the subscript given as R indicates the right side of the slice.

$W$  = total weight of a slice (depending on width  $b$  and height  $h$ )

$X$  = vertical force between slices. Subscript given as L indicates the slice's left side, and the subscript given as R indicates the right side of the slice.

$D$  = point load in an external location.

$kW$  = horizontal seismic load acting on the center of gravity of each slice.

$R$  = is the radius of the circle of failure. The moment arm is related to the shear force ( $S_m$ ), mobile shear force in a slice.

$f$  = vertical deviation distance from the center of rotation of the normal force or the center of moments. A positive slope (slope facing left) is considered to be positive at distances  $f$  to the left of the center of rotation and negative to the left of the center of the turn. The sign rule is reversed for positive slopes.

$x$  = the horizontal distance from the center of each slice to the center of the failure circle (horizontal distance to the center of rotation).

$e$  = vertical distance from the center of gravity of each slice to the center of the failure circle.

$d$  = Perpendicular distance from the center of gravity of each segment to the center of the failure circle.

$h$  = the geometric distance between the top and bottom line from the center of each slice.

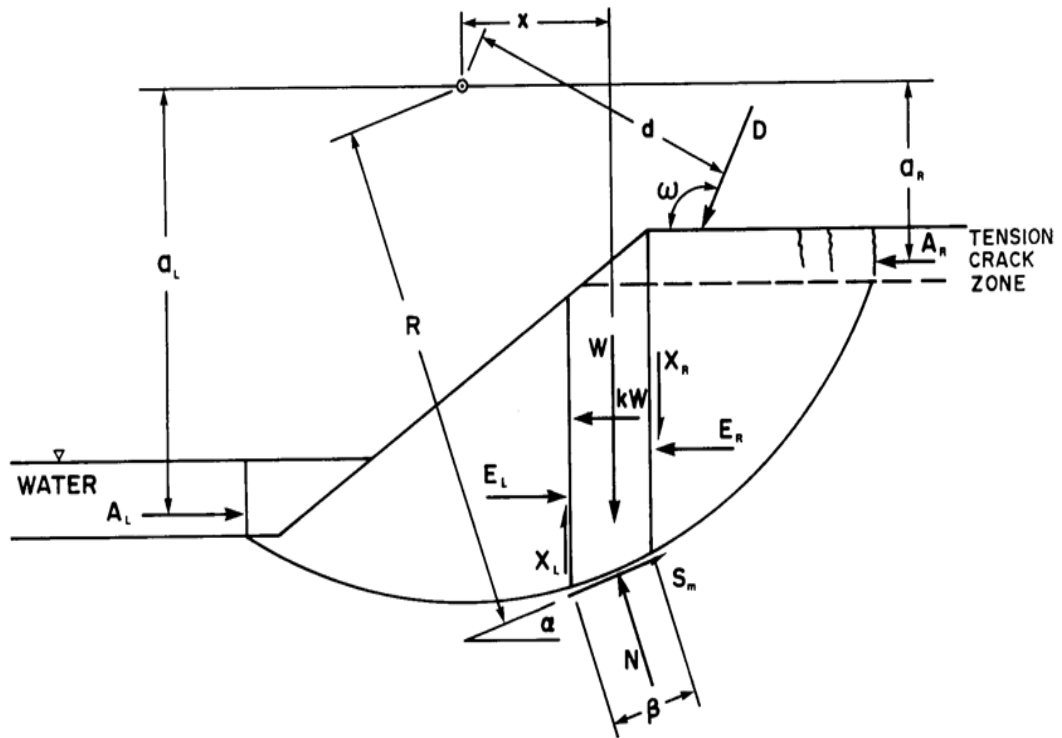
$a$  = vertical distance from the outer water force to the center of rotation (to the center of moments). L and R (lower symbols) indicate the left and right sides of the slope, respectively.

$A$  = vertical distance from outer water force to the center of error circle. L and R (lower symbols) indicate the left and right sides of the slope.

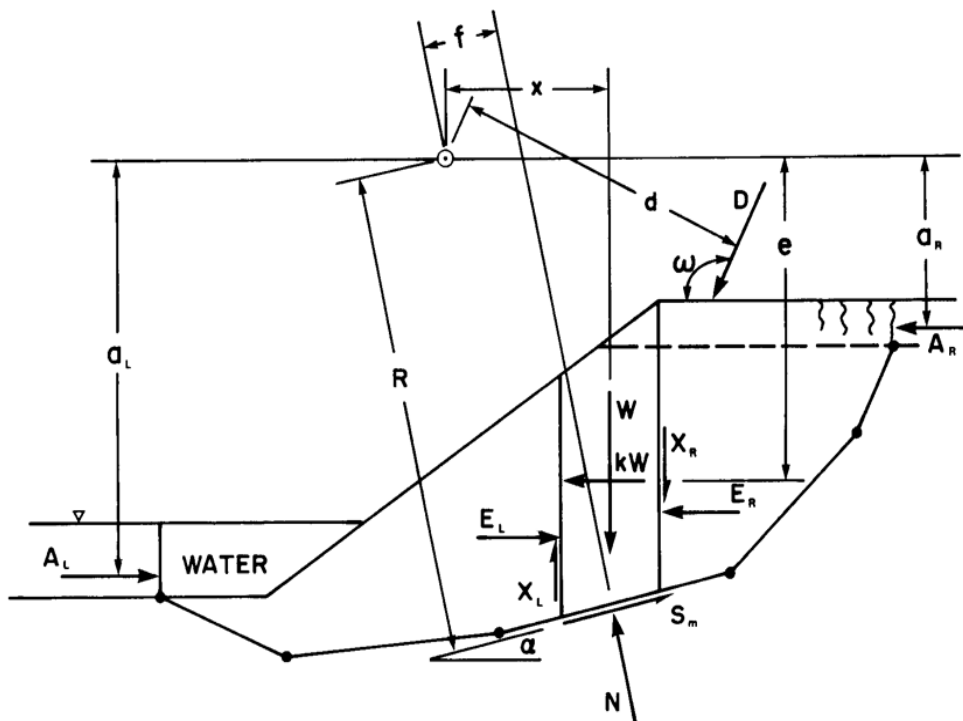
$\omega$  = load angle between horizontal and point. This angle is determined counterclockwise (positive) from the x-axis.

$\alpha$  = It is the angle between the horizontal and the tangent of the base center of each segment. The rule is that the angle is tilted in the same direction.





**Figure 3.12 :** Forces that are acting on a slice in a circular sliding circle  
 Source: (Krahn, 2004).



**Figure 3.13 :** Forces that are acting on a slice in a circular sliding non-circle  
 Source: (Krahn, 2004).

In order to meet the limit equilibrium condition, the shear strength that should be mobilized at the bottom of the slice is found by the formula below. In this formula,  $F$  is the safety factor, and  $\beta$  is the width of the slice base.

$$S_m = \frac{s\beta}{F} = \frac{\beta(c' + (\sigma_n - u) \tan \phi')}{F} \quad (3.36)$$

If the equilibrium given in Equation 3.36 can be solved, the safety factor is obtained. Three known equilibrium equations should be used. Besides, it is necessary to use the Mohr-Coulomb migration hypothesis. After that, four equations are written for each slice on the sliding circle. If the sliding circle has  $n$  slices, the equilibrium equation is written as  $4n$  (Table 3.3).

Nevertheless, the number of the unknowns is higher than the known. (Table 3.4) The list of unknowns is provided. In this case, the system is hyperstatic. An isostatic system is needed for the solution. Because there are three unknowns in the isostatic system. The force acting on the base is admitted as follows. The normal force gives the load to the middle of the base of the slice. Other assumptions are inter-force magnitudes and direction or impact point.

**Table 3.3 :** Parameters with the known solution in safety factor calculation.

Number of Known Quantities	Description
$n$	Summation of forces in the horizontal direction
$n$	Summation of forces in the vertical direction
$n$	Summation of moments
$n$	Material Shear Failure Criterion
<b><math>4n</math></b>	<b>Total number of equations</b>

**Source:** (Krahn, 2004).

**Table 3.4 :** Parameters with an unknown solution in safety factor calculation.

Quantities	Description
Number of Unknown	
n	Normal force acting on the center of the base of the slice, N
n	Point of normal force N acting on the base of the slice
n - 1	Normal force acting on the cross-section, E
n - 1	The shear force acting on the slice, X
n - 1	Application point of forces between sections
n	The shear force acting on the base of each slice, $S_m$
1	The factor of safety, F
1	Value of Lambda, $\lambda$
$6n - 1$	Total number of unknowns

**Source:** (Krahn, 2004).

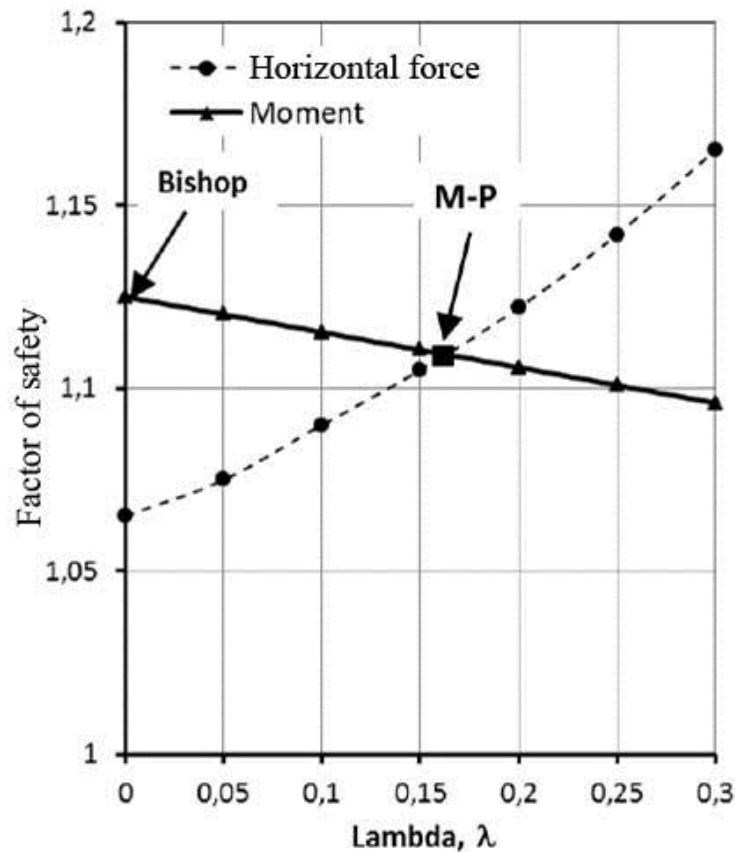
The methods given above are; (i) used in finding the safety factor (vertical, horizontal force or moment) and; (ii) assumptions about inter-slice forces to convert to isostatic. Bishop (1955), (i) takes into account horizontal and vertical force between slices; (ii) neglects sliding force between slices. Spencer (1967), (i) takes care of all three slices between slices, and; A constant ratio between slip and normal force is defined.

GLE method calculates safety factor according to the following assumptions (Krahn, 2004):

- The vertical force sum of each slice is equal to N normal force at the bottom of the slice.
- The sum of the horizontal forces acting on each slice is E. The calculation of E should be made by starting at the crown.
- Moments are collected at a common turning point for all slices. The resulting total gives the number of torque balances  $F_m$ .
- From the sum of the horizontal forces between all slices, the force balance  $F_f$  safety factor is found.

Despite the above assumptions, the system is still hyperstatic. Therefore, it is necessary to accept for the direction of the resultant force between slices. The cross-

slice force function of Morgenstern-Price (1967) should be used. The resultant force direction is decided by the selected force function. With normal force and force function between slices; Using the selected direction together, the shear force between slices is calculated. In the next step, security factors, moment balance  $F_m$ , and horizontal force balance  $F_f$  can be calculated separately. The force gives the percentage of the function  $\lambda$ , and; security factor also varies. As seen in Figure 3.14, depending on  $\lambda$  values,  $F_m$ , and  $F_f$  safety factors vary.  $\lambda$  value giving  $F_f$  and  $F_m$  values equally; is the safety factor. In the M-P method only, the force function can be given as desired by the user. In the M-P method, the user can reach  $\lambda$  values as he wishes. The most important feature of the GLE method is this feature of the M-P method.



**Figure 3.14 :** Comparison of Bishop and M-P methods

Source: (Krahn, 2004).

### 3.4.1 Moment balance safety factor, $F_m$

If the moment balance is written according to the shear circle in Figure 3.12, (3.36) equation is obtained. If the equation (3.37) is written in the equation below, the safety factor  $F_m$  (3.38) is obtained for the Moment balance (Krahn, 2004).

$$\sum Wx + \sum SmR - \sum Nf + \sum kWe \pm \sum Dd \pm \sum Aa = 0 \quad (3.37)$$

$$F_m = \frac{\sum(\beta c' R + (N - u\beta) R \tan \phi')}{\sum Wx - \sum Nf + \sum kWe \pm \sum Dd \pm \sum Aa} \quad (3.38)$$

The N force in the equation is also found because it is a function of the safety factor (3.38).

### 3.4.2 Force balance safety factor, $F_f$

In Figure 3.12, if the horizontal force balance is written according to the sliding circle in each slice, (3.37) equation is obtained. The sum of inter-slice forces in this equation  $\sum(E_L - E_R)$  must be equal to zero (Krahn, 2004).

$$\begin{aligned} \sum(E_L - E_R) - \sum(N \sin \alpha) + \sum(Sm \cos \alpha) - \dots \\ \dots \sum kW + \sum D \cos \omega \pm \sum A = 0 \end{aligned} \quad (3.39)$$

If the equation is written instead of  $Sm$  (3.39), there is a force balance safety factor.

$$F_f = \frac{\sum(\beta c' \cos \alpha + (N - u\beta) \tan \phi' \cos \alpha)}{\sum(N \sin \alpha) + \sum kW - \sum D \cos \omega \pm \sum A} \quad (3.40)$$

### 3.4.3 Normal force on slice base, N

The vertical balance equation for the normal force at the bottom of the slice is as follows (Krahn, 2004).

$$(X_L - X_R) - W + N \cos \alpha + S_m \sin \alpha - D \sin \omega = 0 \quad (3.41)$$

Substituting  $S_m$  in the equation has the following equation (3.42).

$$N = \frac{W + (X_R - X_L) - \frac{c' \beta \sin \alpha + u\beta \sin \alpha \tan \phi'}{F} + D \sin \omega}{\cos \alpha + \frac{\sin \alpha \tan \phi'}{F}} \quad (3.42)$$

However, (3.42) is not linear because it contains the safety factor (F). If calculating for moment balance, F value is F<sub>m</sub>. If calculating for the force balance, the F value is F<sub>f</sub>. In the base normal force equation, sliding force X<sub>L</sub> and X<sub>R</sub> between slices are unknown.

For the safety factor calculation, first of all, the normal forces (E) between slices are ignored. In this case, the normal force (N) in the slice base can be calculated by the following equation (Krahn, 2004).

$$N = W \cos \alpha - kW \sin \alpha + [D \cos \alpha (\omega + \alpha - 90)] = 0 \quad (3.43)$$

A more specific approach is to include normal force between slices in the calculation of the normal force at the bottom of the slice. In this case, the normal force between slices is neglected.

$$N = \frac{W + \frac{c' \beta \sin \alpha + u \beta \sin \alpha \tan \phi'}{F} + D \sin \omega}{\cos \alpha + \frac{\sin \alpha \tan \phi'}{F}} \quad (3.44)$$

In the equation, if F is substituted for the safety factor that gives the moment balance, F<sub>m</sub>, the Bishop safety factor, is found. If F is replaced by the safety factor that gives the force balance, the Janbu safety factor is found.

#### 3.4.4 Inter-slice forces, E, and X

Inter-slice forces are normal force and shear force between two adjacent slices. In a gliding circle trying to slide from left to right; The normal force in each slice is calculated with a calculation starting from the slice on the left. The horizontal force balance for each slice is as follows.

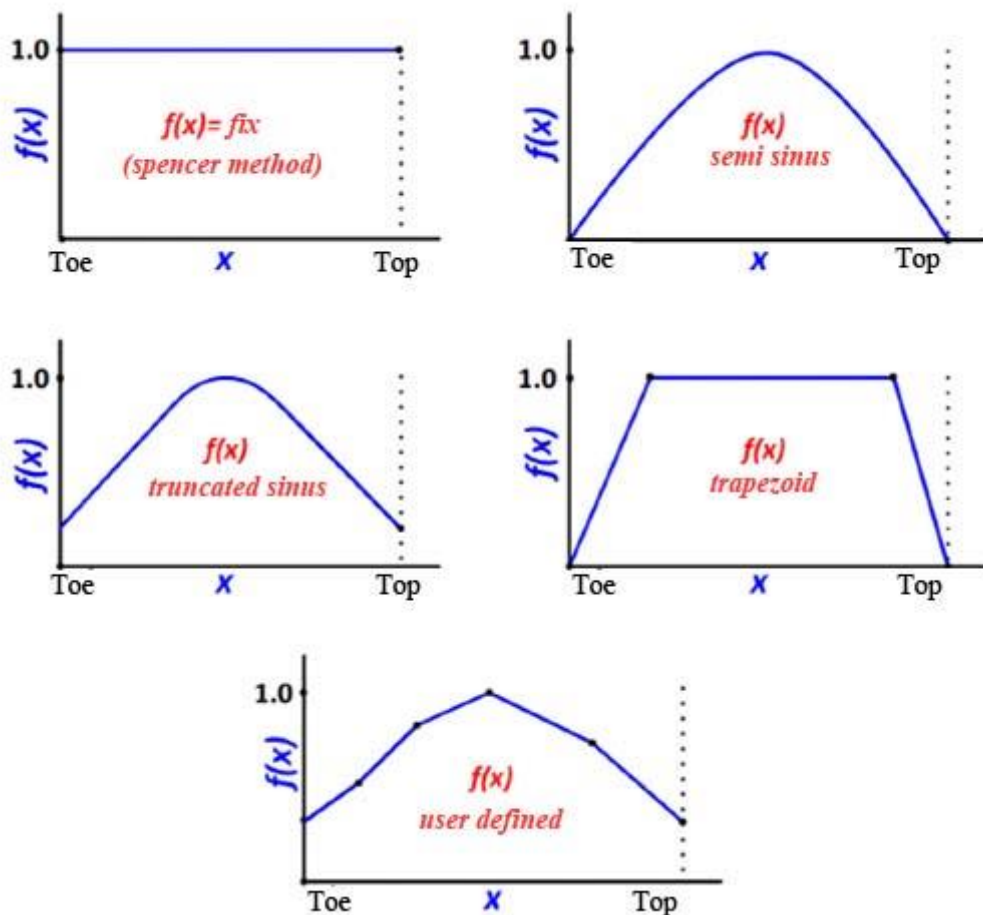
$$(E_L - E_R) + N \sin \alpha + S_m \cos \alpha + kW - D \sin \omega = 0 \quad (3.45)$$

Substituting S<sub>m</sub> in the equation has the following equation (3.46).

$$E_R = E_L + \frac{(c' \beta \sin \alpha + u \beta \tan \phi') \cos \alpha}{F} + N \left( \frac{\tan \phi' \cos \alpha}{F} - \sin \alpha \right) \dots \dots kW - D \sin \omega \quad (3.46)$$

The normal force ( $E = 0$ ) on the first slice is zero. It is calculated starting from the top point. Inter-slice shear force as a ratio of normal force; was proposed by Morgenstern-Price (1965) with the following formula.

$$X = E \lambda f(x) \quad (3.47)$$



**Figure 3.15 :** Morgenstern-Price method, according to the force function types between slices

**Source:** (Morgenstern-Price 1965).

$f(x)$  = Force function between slices

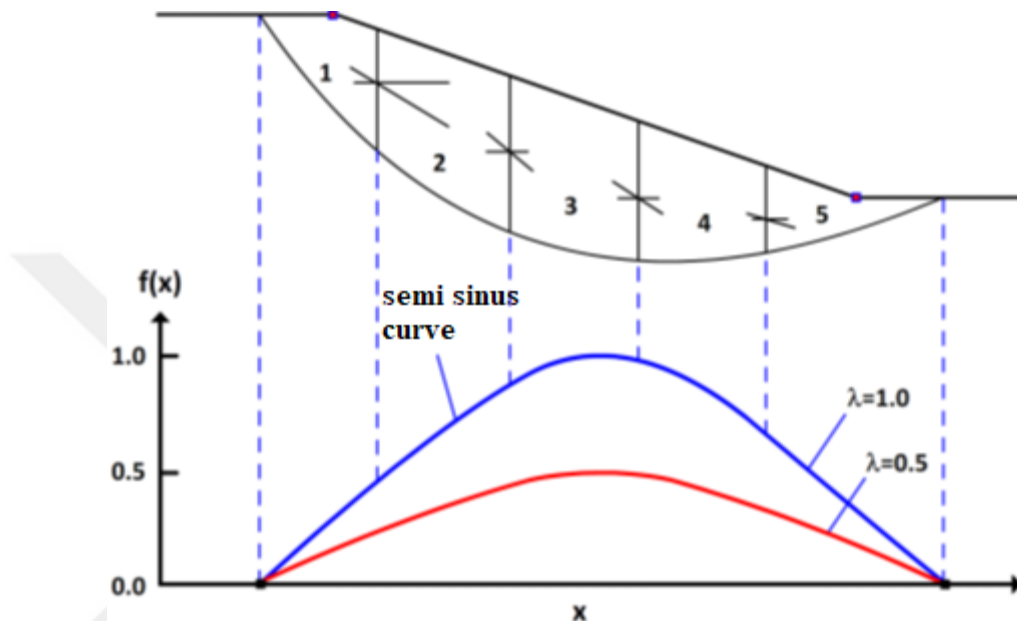
$\lambda$  = The ratio indicates the amount of force used.

Used in Morgenstern-Price's (1965) method and given in Figure 3.15; constant, semi-sine, truncated sine, keystone, and user-defined force functions are also valid GLE. In an example given by Krahn (2004), the functions of force functions and the coefficient of  $\lambda$  are described. In the example given by Krahn (2004); In figure 3.16, the normal force between Sections 1 and 2 is taken as  $E = 100$  kN, and it is assumed

that the half sine force function is used when  $\lambda = 0.5$ . According to the equation (3.47), the value of the half-sine function between Sections 1 and 2 is  $f(x) = 0.45$  and  $\lambda = 0.5$ ;

$$X = 100 * 0.5 * 0.45 = 22,5 \text{ kN}$$

In this example, while the lambda values in the crown and heel part of the slip circle are zero, it reaches its greatest value of 0.5 in the middle of the sliding circle.



**Figure 3.16 :** Using the half sine force function with two different lambda values

Source: (Krahn, 2004)

### 3.4.5 Method chosen in the developed model

The calculation method is fully compatible with GLE. The tolerance amount for the account is left to the user. First, the safety factor must be found with OMS. This should be done after all geometry changes. The user can compare the results of Bishop, Janbu, Spencer, M&P, and Sarma methods simultaneously. The analysis calculation report is prepared only according to the method to be determined (Figure 3.17).



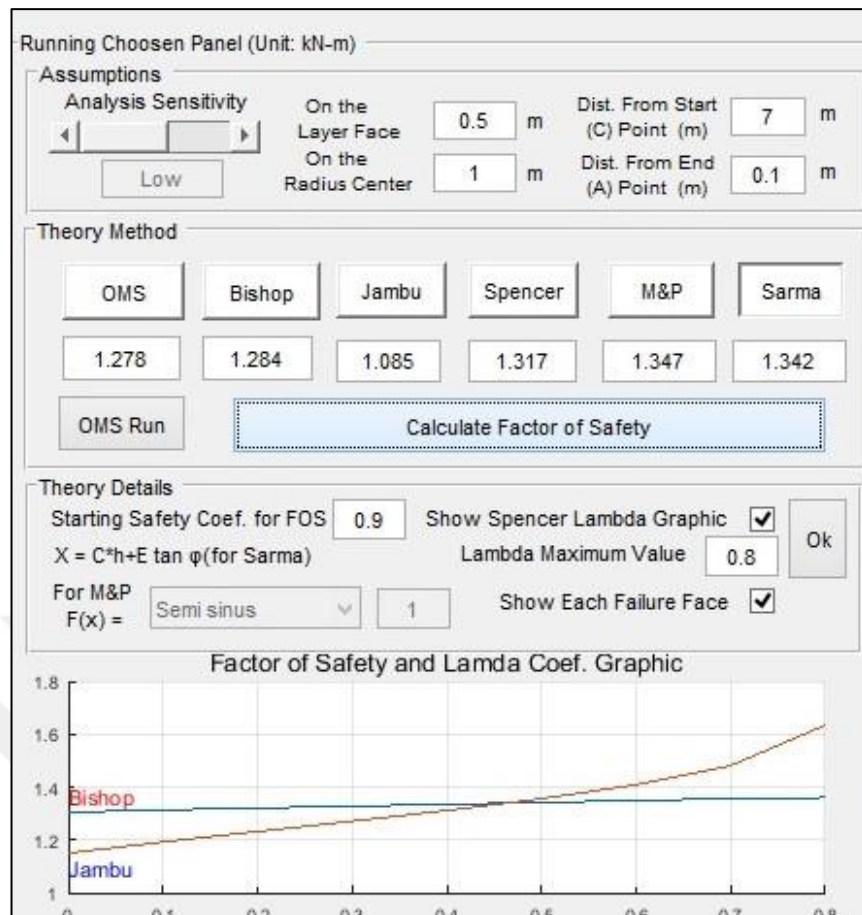
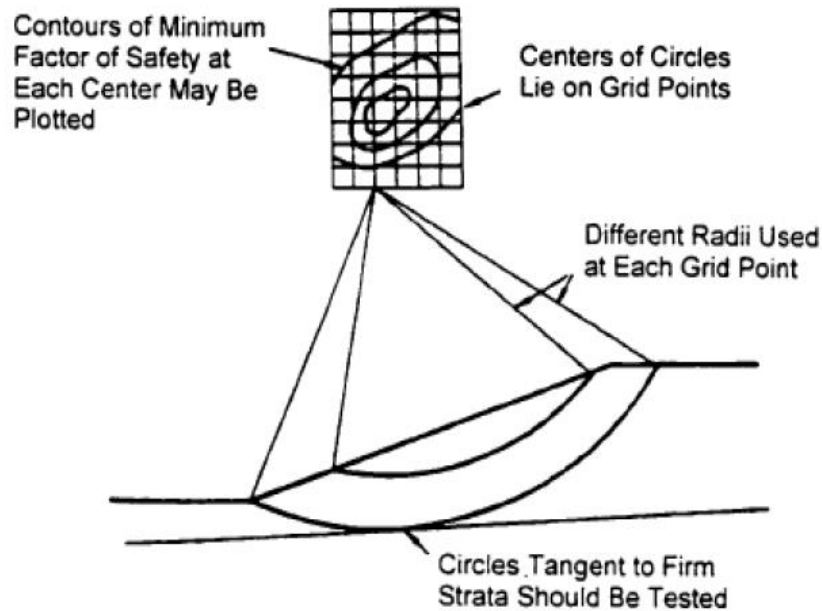


Figure 3.17 : Method chosen in the developed model.

### 3.5 Getting the most critical circle

Barker (1980), in order to obtain the factor of safety, a set of trial rectangles should be selected to obtain the point that gives the lowest factor of safety. He argued that trial and error should be analyzed. Handling these processes is a very laborious process today. Because of the many unknowns and most processes require trial and error, it will be boring, tiring, and troublesome. A grid spacing is defined by computer software. Refraction circles are formed by determining a radius from each point in this grid interval. Here, the most inconvenient of these is the circle, the most critical rupture circle. Doing this with a computer is fast, practical, and more reliable. As seen in Figure 3.18, it creates a FOS series of the most unfavorable grids. There is a rupture circle on the slope due to the radius at each grid point. Transforming them into graphics with computer software; For example, coloring provides convenience to the user.

An automatic finding of circle coordinates and radius for minimum FOS will make things relatively easy. Boutrup and Lovell (1980) proposed the simplex reflection method. The method works as follows, finding the factor of safety for a two-dimensional circular sliding surface is the goal.



**Figure 3.18 :** Grid search pattern

Source: (Mostyn and Small, 1987 ).

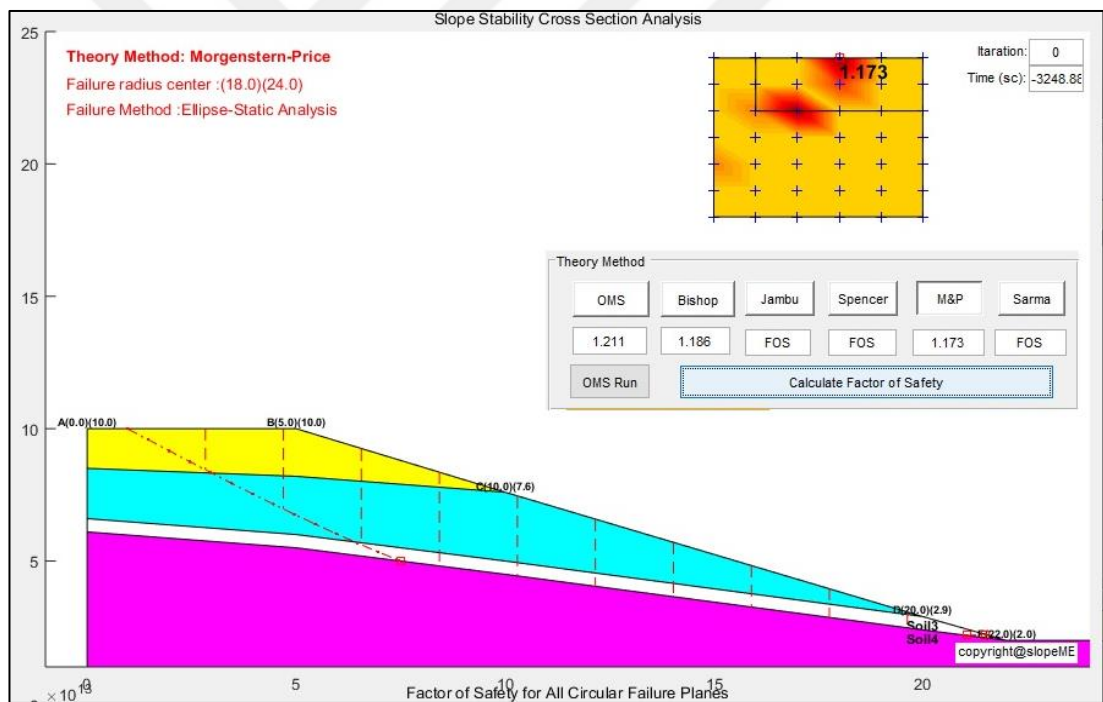
The problem is basically solved like this. For the FOS (factor of safety), the minimizing circle's center coordinates  $a$ ,  $b$ , and  $R$  break diameter is found. It should be done by finding the FOS at the four corners of the rectangle in the defined,  $x$ ,  $y$ ,  $R$  space. The FOS value in each corner decides in which direction it should move for the lower FOS. That is, the rectangle with the highest FOS must be at the vertex. Depending on the specified coordinates and radii, the minimum FOS can be found quickly (Tolon, 2007).

### 3.5.1 Calculating the most critical circle with the developed model

In the developed Matlab code, a circle center will automatically appear first. This point is determined automatically by the code by making various assumptions. The software offers multiple breakout options if the user wishes. If the user wants, can also define the boundary range of circle centers as Rectangular. The sensitivity selection for the specified rectangle belongs to the user. The higher the sensitivity, the higher the actual fracture surface, but it affects the solution time. The circle

centers' locations most susceptible to breaking on the specified rectangle are automatically displayed in red.

Also, as a more precise solution, a smaller rectangle is suggested. As the lowest FOS will be displayed on the specified rectangle, all FOS values can also be displayed if desired. Thus, the user understands where the rectangular borders to be created should be. The software scans the circle centers within this rectangle very quickly to find the most unfavorable situation. It is almost impossible to do this manually. Because in the previous section, it was stated that the method that can be done manually is OMS, and it is quite difficult because the number of the unknown in other methods is more than 1. No matter how complex the geometry is, there will be no difference in the code being developed. The software is capable of solving any kind of geometry. This will be demonstrated in many trials in the next chapter.



**Figure 3.19 :** The rectangle is shown in the developed model.

## 4. CODE VERIFICATION RESULTS AND DISCUSSION

In this chapter, the stability of slopes with different geometries will be analyzed with the developed code. The geometry models selected will be the previously found models in the literature and used in the thesis. In this way, the reliability of the developed code will be revealed. In the models to be compared, fault surface and safety factors will be compared.

### 4.1 Program Test Examples

For Toe in the software, the user must select the iteration range. The most unfavorable situation is always considered in slope design analysis. In other words, FOS in slope analysis expresses the most negative situation. If there is more than one FOS in the software, can make the automatic selection for FOS.

#### 4.1.1 Method chosen with developed model

This chapter will be comparatively done for two different geometries. Soil properties are given in Table 4.1 and Table 4.2.

##### Case 1 (Problem 1):

**Table 4.1 :** Slope height and soil parameters.

	$c'$	$\phi'$	$\gamma$	H
	(kPa)	( $^\circ$ )	(kN/m <sup>3</sup> )	(m)
Case 1	15	38	18	5

Source: (Atarigiya 2012)

##### Case 2 (Problem 2):

**Table 4.2 :** Slope height and soil parameters.

	$c'$	$\phi'$	$\gamma$	H
	(kPa)	( $^\circ$ )	(kN/m <sup>3</sup> )	(m)
Case 2	5	28	16	5

Source: (Atarigiya 2012)

Account steps will be shown, and transactions will be shown on the software developed. Thus, in the software's demo version, users are expected to get the same results when they input the same values.

**Calculation Steps with Developed Software (SlopeME) Inputting for Case 1:**

As described in Chapter 2.4, the parameters that should be known according to the Limit Equilibrium Method (LEM) are specified. For example, in limit equilibrium analysis, it is sufficient to know three parameters. These are the internal friction angle ( $\phi$ ), unit volume weight ( $\gamma$ ), and cohesion ( $c$ ). These parameters and geometric properties are given in Table 4.1. Case 1 "Parameters" will be created with the developed software (SlopeME) as follows.

**Slope Surface Coordinates (Unit: kN-m)**

Buttons: Apply, Import xls, Clear All, - Borehole, + Borehole, - Layer, + Layer

**Input Layers Boreholes Coordinates Values**

	1	2	3	4	5
Xb.	1	0.00	15.00	5.00	5.00
Y1	Soil1	7.00	7.00	2.00	2.00
Y2	Soil2	0.00	0.00	0.00	0.00
Y3					
Y4					

**Ground Under Water**  There is/isn't?

	1	2	3	4	5
Y.n	Water	0	0	0	0

**Soils Parameters**

	Name	Cohesi...	Unit Weight	Wet Unit ...	Friction A...	Young Mo...
1	Soil1	15	18	18	38	10000
2	Soil2	17	19	19	21	10000

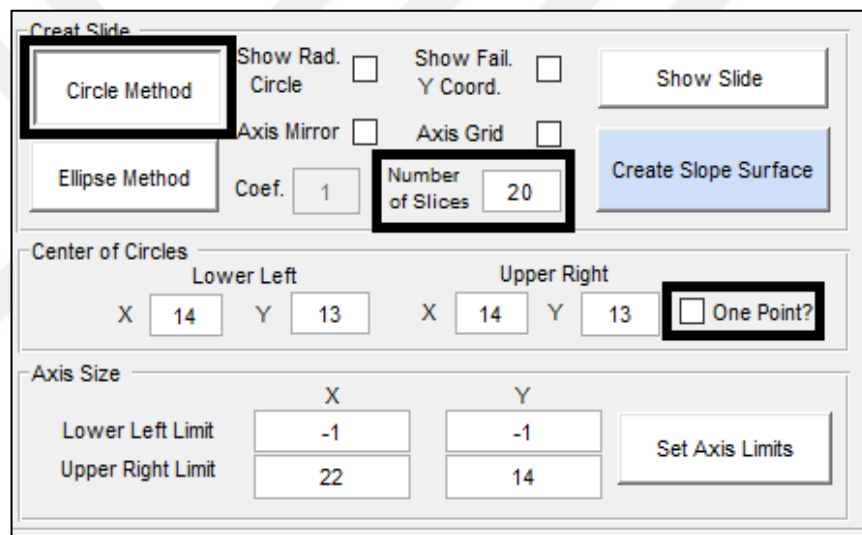
**Figure 4.1 :** SlopeME input of properties: Case 1.

As shown in Figure 4.1; **Layers Boreholes** With "Layers Borehole", the X-dependent change distances of the Y coordinate on the slope are entered. Case 1 has 1 "Layer", but another one has been entered for "Bedrock". However, the coordinates of

"Bedrock" were entered as zero (not to enter soil parameters). It was explained in Chapter 3.1.1, it is necessary to enter at least 2 points for Y (one of them is bedrock) and at least 4 points for X.  There is/isn't? No selection was no due to the lack of groundwater. Soil parameters were entered in accordance with "Case 1".

**Calculation Steps with Developed Software (SlopeME) Creat Slide for Case 1:**

As described in Chapter 2.8.1, circular and non-circular fault surfaces were mentioned. It is stated in Chapter 3.1.1 that the user will ultimately choose the choice of the circular or non-circular fracture surface. Case 1 "Slide" will be created as follows with the developed software (SlopeME).



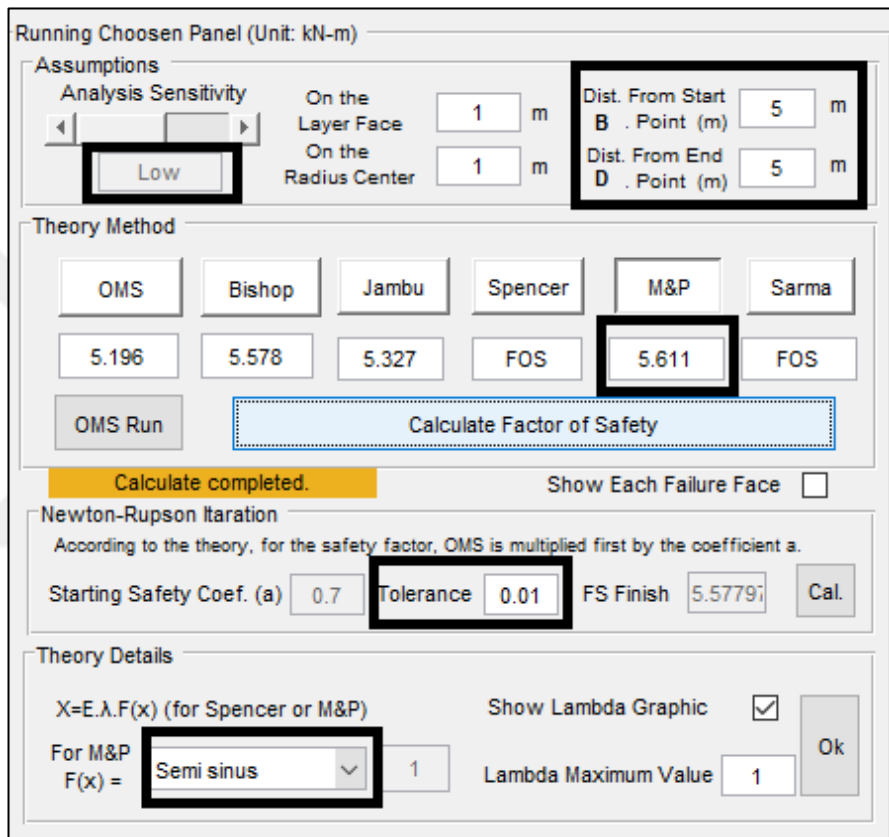
**Figure 4.2 :** SlopeME input of creat slide: Case 1.

It is shown in Figure 4.2. The "Circle Method" was preferred because it was done this way for the Case 1 example. "Number of Slices" 20 were selected. It has been explained in Chapter 3.1.1, if the number of slices increases, the processing time increases because the sensitivity will increase.

**One Point?** The software first determines a random point. When we cancel this option, either a single point must be entered, or a rectangular selection range is required for the center of the FOS refraction circle. X: 14m and Y: 13m were chosen to be the same as the Case 1 example.

**Calculation Steps with Developed Software (SlopeME) Running for Case 1:**

Generalized Methods (GLE) are mentioned in Chapter 3.4. It is explained here that there is no interaction between OMS slices. It is explained that the Bishop method works in Moment balance and that only normal force affects between slices. It is explained that Moment and Force balance is sought in Spencer and M&P methods. It has been explained that there are different acceptances to achieve this balance. Case 1 "Running" will be created as follows with the developed software (SlopeME).



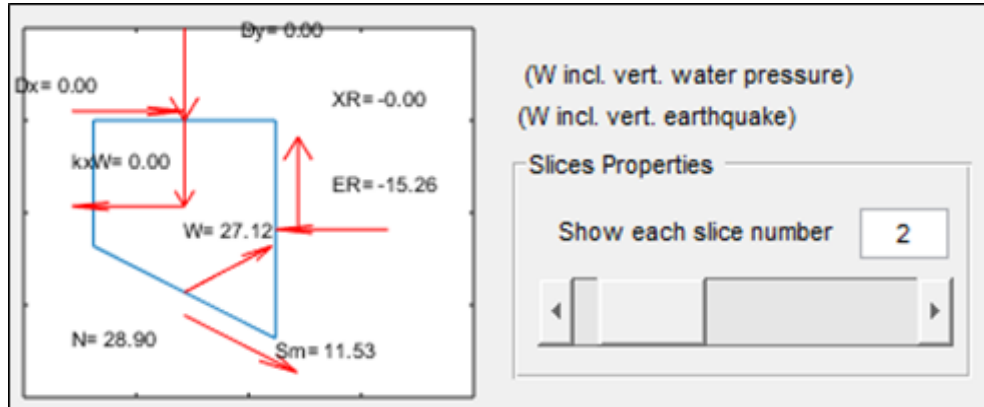
**Figure 4.3 :** SlopeME output of running: Case 1.

As shown in Figure 4.3; Since Case 1 example is "Toe Failure", was want the break to happen here. Therefore, B: 4m and D: 5m were chosen. As it is described in Chapter 3.4.1, how OMS, Bishop, and M&P methods are calculated. The software first determines the most critical fracture surface with OMS.

This fracture surface is accepted if it is critical within the Bishop method. If not, the iterations will continue in any case. Tolerance 0.01 The higher the tolerance, the longer the processing time. Semi sinus It has been chosen as Semi-sinus for M&P. The critical thing here is how the interaction between slices is.

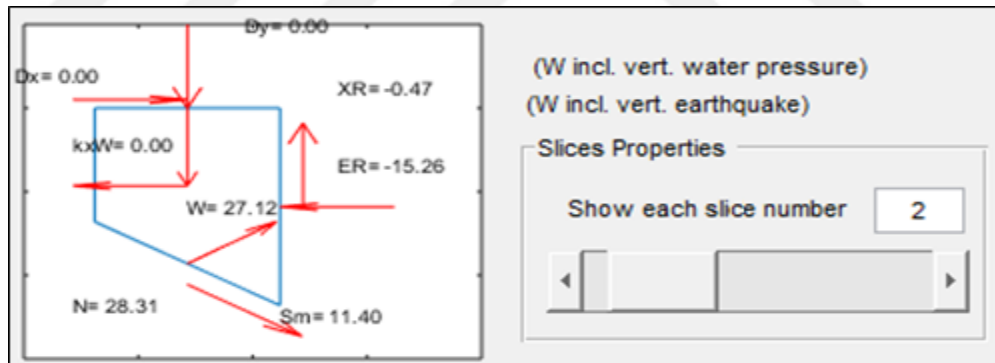
**Calculation Steps with Developed Software (SlopeME) Internal Forces for Case 1:**

Generalized Methods (GLE) are mentioned in Chapter 3.4. With the developed software (SlopeME), Case 1, “Internal Forces” was formed as follows.



**Figure 4.4 :** SlopeME output of internal forces for slice number 2: Bishop.

Shown in Figure 4.4; In Bishop results, slice weight (W): 27.12 kN, slice base reaction force (N): 28.90 kN, slice base friction force (Sm): 11.53 kN, total lateral force in slice (ER-EL): -15.26 kN and total friction force on the slice edge (XR-XL): calculated as 0 kN.



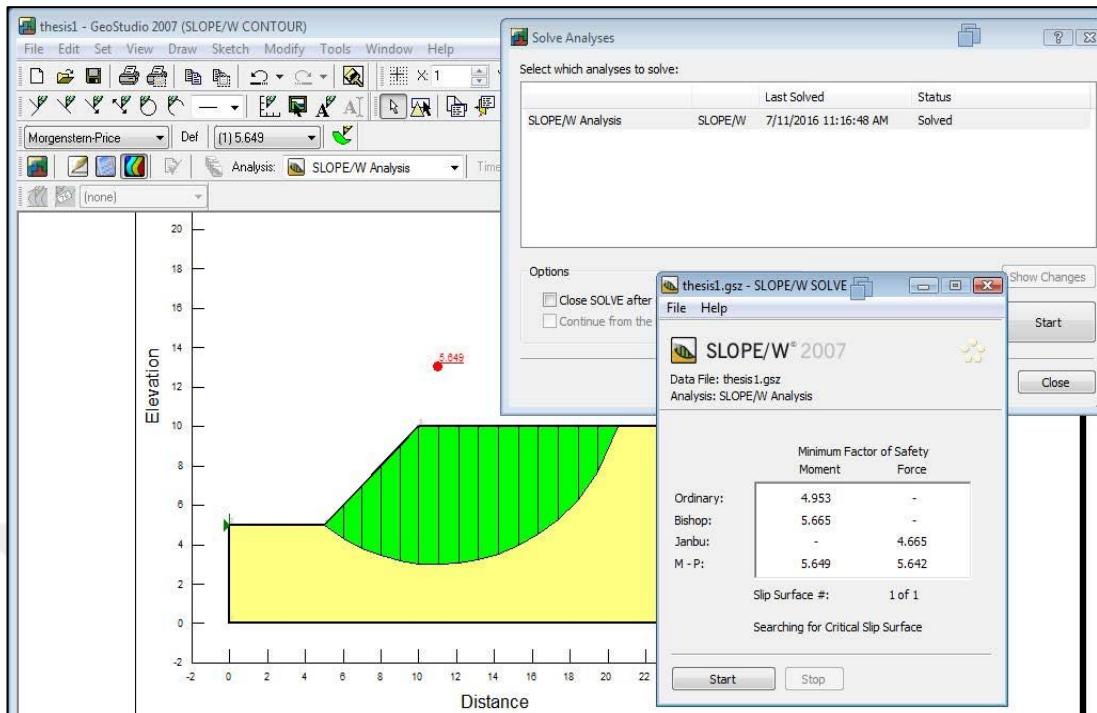
**Figure 4.5 :** SlopeME output of internal forces for slice number 2: M&P.

Shown in Figure 4.5; In M&P results, slice weight (W): 27.12 kN, slice base reaction force (N): 28.31 kN, slice base friction force (Sm): 11.40 kN, total lateral force on slice (ER-EL): -15.26 kN and total friction force (XR-XL) at the slice edge: was calculated as -0.47 kN. The relationship between E and X is described in Chapter 3.4.4. For slice 2, the value of the half-sine function and the X force is calculated as follows;  $f(x) = 0.10$  (function for semi-sinus) and  $\lambda = 0.3$  (from the balance of moment and force);  $X = W * \lambda * f(x)$ .

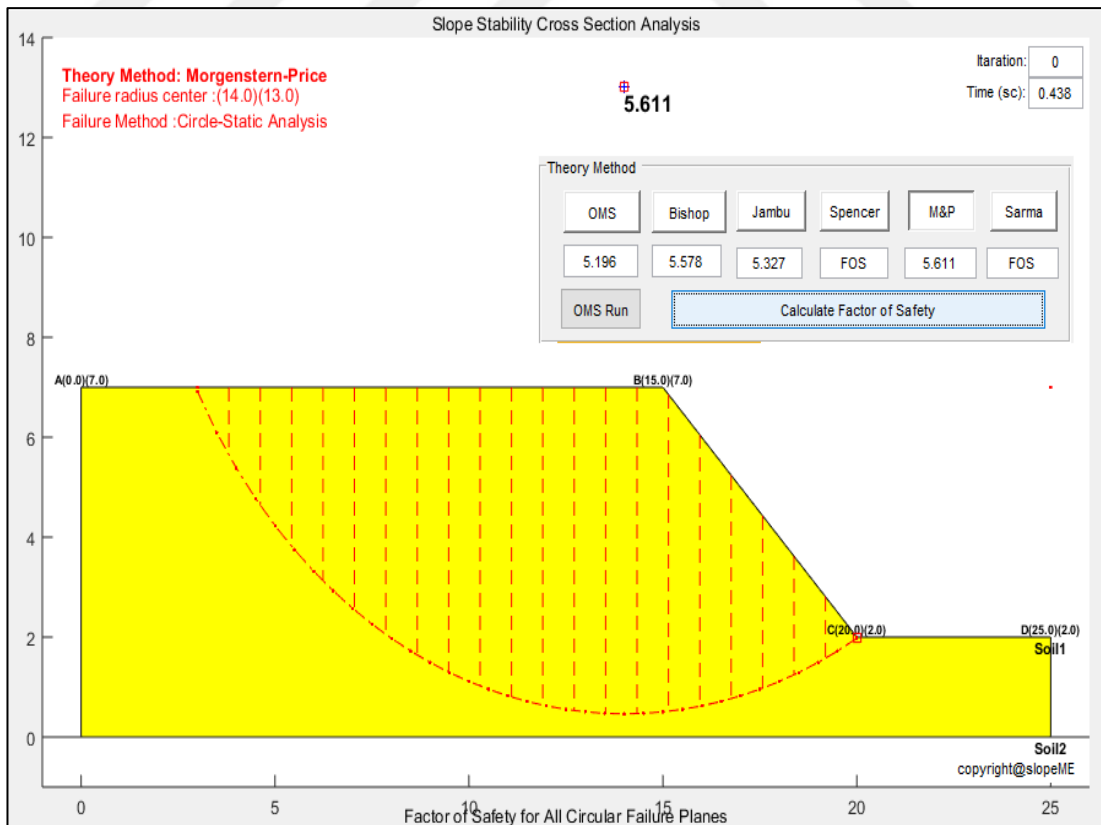
$$X = 15.26 * 0.3 * 0.10 = 0.47 \text{ kN (calculated horizontal forces for a slice)}$$



**Comparison of (SlopeME) and SLOPE / W Results For Case 1:**



**Figure 4.6 :** SLOPE/W output of toe failure: Case 1  
**Source:** (Atarigiya, 2012).



**Figure 4.7 :** SlopeME output of toe failure: Case 1.

**Calculation Steps with Developed Software (SlopeME) Inputting for Case 2:**

As described in Chapter 2.4, the parameters that should be known according to the Limit Equilibrium Method (LEM) are specified. For example, in limit equilibrium analysis, it is sufficient to know three parameters. These are the internal friction angle ( $\phi$ ), unit volume weight ( $\gamma$ ), and cohesion ( $c$ ). These parameters and geometric properties are given in Table 4.2. Case 2 "Parameters" will be created with the developed software (SlopeME) as follows.

As shown in Figure 4.8; **Layers Boreholes** With "Layers Borehole", the X-dependent change distances of the Y coordinate on the slope are entered. Case 2 has 1 "Layer", but another one has been entered for "Bedrock". However, the coordinates of "Bedrock" were entered as zero (not to enter soil parameters). It was explained in Chapter 3.1.1, it is necessary to enter at least 2 points for Y (one of them is bedrock) and at least 4 points for X.  There is/isn't? No selection was no due to the lack of groundwater. Soil parameters were entered in accordance with "Case 2".

Slope Surface Coordinates (Unit: kN-m)

Apply Import xls Clear All - Borehole + Borehole - Layer + Layer

Input Layers Boreholes Coordinates Values

	1	2	3	4	5
Xb.	1	0.00	15.00	5.00	5.00
Y1	Soil1	7.00	7.00	2.00	2.00
Y2	Soil2	0.00	0.00	0.00	0.00
Y3					
Y4					

Ground Under Water  There is/isn't?

	1	2	3	4	5
Y.n	Water	0	0	0	0

Soils Parameters

	Name	Cohesi...	Unit Weight	Wet Unit ...	Friction A...	Young Mo...
1	Soil1	5	16	16	28	10000
2	Soil2	17	19	19	21	10000

**Figure 4.8 :** SlopeME input of properties: Case 2.

**Calculation Steps with Developed Software (SlopeME) Creat Slide for Case 2:**

As described in Chapter 2.8.1, circular and non-circular fault surfaces were mentioned. It is stated in Chapter 3.1.1 that the user will ultimately choose the choice of the circular or non-circular fracture surface. Case 2 "Slide" will be created as follows with the developed software (SlopeME).

It is shown in Figure 4.9. The "Circle Method" was preferred because it was done this way for the Case 2 example. "Number of Slices" 20 were selected. It has been explained in Chapter 3.1.1, if the number of slices increases, the processing time increases because the sensitivity will increase.

**One Point?** The software first determines a random point. When we cancel this option, either a single point must be entered, or a rectangular selection range is required for the center of the FOS refraction circle. X: 14m and Y: 13m were chosen to be the same as the Case 2 example.

The screenshot shows the 'Creat Slide' dialog box in SlopeME. The 'Circle Method' is selected. The 'Number of Slices' is set to 20. The 'One Point?' checkbox is unchecked. The center of circles is set to X: 14, Y: 13. The axis size limits are set to X: -1 to 22 and Y: -1 to 14.

Center of Circles	
Lower Left	
X	14
Y	13
Upper Right	
X	14
Y	13

Axis Size	
Lower Left Limit	
X	-1
Y	-1
Upper Right Limit	
X	22
Y	14

**Figure 4.9 :** SlopeME input of creat slide: Case 2.

**Calculation Steps with Developed Software (SlopeME) Running for Case 2:**

Generalized Methods (GLE) are mentioned in Chapter 3.4. It is explained here that there is no interaction between OMS slices. It is explained that the Bishop method works in Moment balance and that only normal force affects between slices. It is explained that Moment and Force balance is sought in Spencer and M&P methods. It

has been explained that there are different acceptances to achieve this balance. Case 2 "Running" will be created as follows with the developed software (SlopeME). As shown in Figure 4.10; Since Case 2 example is "Toe Failure", was want the break to happen here. Therefore, B: 5m and D: 5m were chosen and described in Chapter 3.4.1, how OMS, Bishop, and M&P methods are calculated. The software first determines the most critical fracture surface with OMS.

This fracture surface is accepted if it is critical within the Bishop method. If not, the iterations will continue in any way. **Tolerance** 0.01 | The higher the tolerance, the longer the processing time. **Semi sinus** It has been chosen as Semi-sinus for M&P. The important thing here is how the interaction between slices is.

Running Chosen Panel (Unit: kN-m)

**Assumptions**

Analysis Sensitivity:  (Low)

On the Layer Face:  m

On the Radius Center:  m

Dist. From Start B . Point (m):  m

Dist. From End D . Point (m):  m

**Theory Method**

OMS	Bishop	Jambu	Spencer	<b>M&amp;P</b>	Sarma
3.167	3.499	FOS	FOS	3.472	FOS

Buttons: OMS Run, Calculate Factor of Safety

Calculate completed. Show Each Failure Face

**Newton-Rupson Iteration**

According to the theory, for the safety factor, OMS is multiplied first by the coefficient a.

Starting Safety Coef. (a):  Tolerance:  FS Finish:  Cal.

**Theory Details**

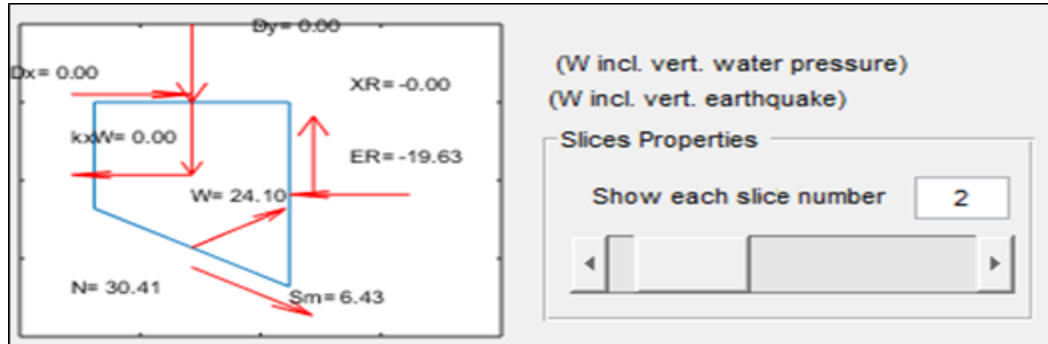
X=E.A.F(x) (for Spencer or M&P) Show Lambda Graphic

For M&P F(x) =  Lambda Maximum Value:  Ok

**Figure 4.10 :** SlopeME input of running: Case 2.

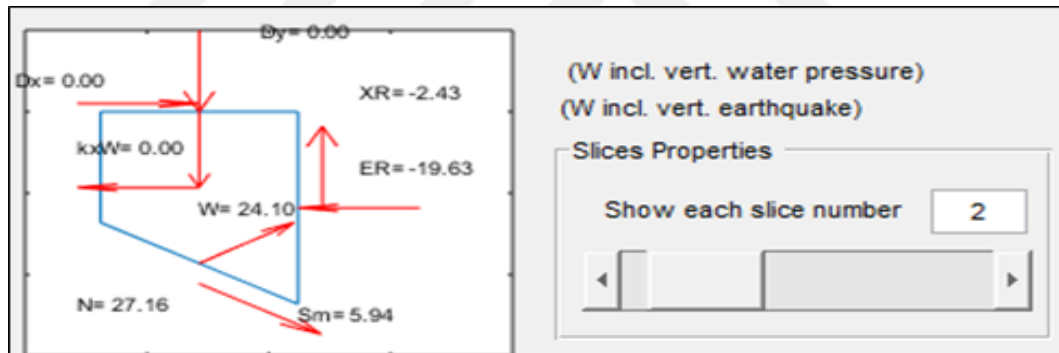
**Calculation Steps with Developed Software (SlopeME) Internal Forces for Case 2:**

Generalized Methods (GLE) are mentioned in Chapter 3.4. With the developed software (SlopeME), Case 2, “Internal Forces” was formed as follows.



**Figure 4.11 :** SlopeME output of internal forces for slice number 2: Bishop

Shown in Figure 4.11; In Bishop results, slice weight (W): 24.10 kN, slice base reaction force (N): 30.41 kN, slice base friction force (Sm): 6.43 kN, total lateral force in slice (ER-EL): -19.63 kN and total friction force on the slice edge (XR-XL): calculated as 0 kN.



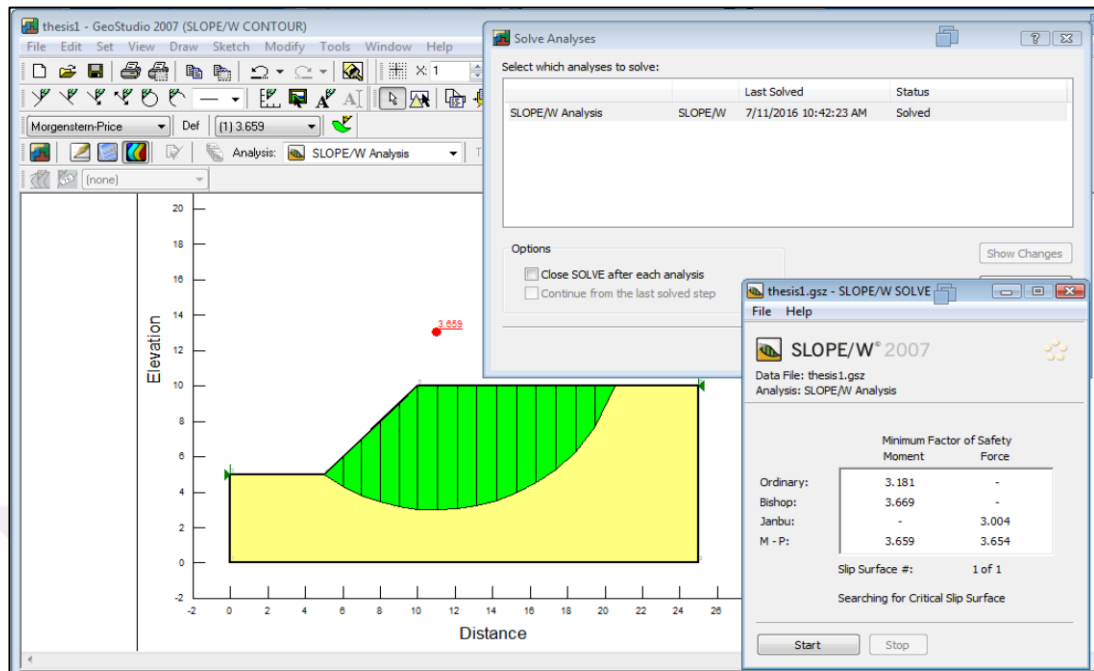
**Figure 4.12 :** SlopeME output of internal forces for slice number 2: M&P

Shown in 4.12 in the figure; In M&P results, slice weight (W): 24.10 kN, slice base reaction force (N): 27.16 kN, slice base friction force (Sm): 5.94 kN, total lateral force on slice (ER-EL): -19.63 kN and total friction force (XR-XL) at the slice edge: was calculated as -2.43 kN.

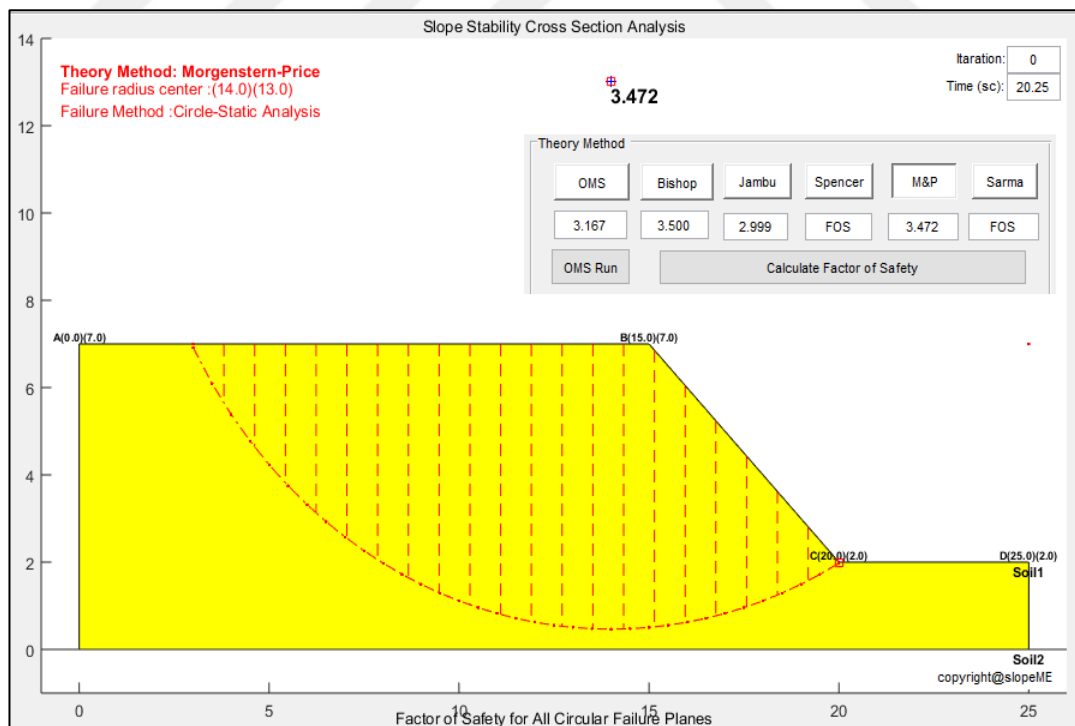
The relationship between E and X is described in Chapter 3.4.4. For slice 2, the value of the half-sine function and the X force is calculated as follows;  $f(x) = 0.355$  (function for semi-sinus) and  $\lambda = 0.35$  (from the balance of moment and force);  $X = W * \lambda * f(x)$ .

$$X = 19.63 * 0.35 * 0.355 = 2.43 \text{ kN (calculated horizontal forces for a slice)}$$

**Comparison of (SlopeME) and SLOPE / W Results For Case 2:**



**Figure 4.13 :** SLOPE/W output of toe failure: Case 2  
**Source:** (Atarigiya 2012).



**Figure 4.14 :** SlopeME output of toe failure: Case 2.

#### 4.1.2 Comparison with cases from literature

This chapter will be comparatively done for two different geometries. Soil properties are given in Table 4.3 and Table 4.4.

##### Case 3 (Problem 3):

**Table 4.3 :** Slope height and soil parameters.

	$c'$	$\phi'$	$\gamma$	H
	(kPa)	( $^\circ$ )	(kN/m <sup>3</sup> )	(m)
Case 3	5	20	20	10

Source: (GEO-SLOPE 2012).

##### Case 4 (Problem 4):

**Table 4.4 :** Slope height and soil parameters.

	$c'$	$\phi'$	$\gamma$	H
	(kPa)	( $^\circ$ )	(kN/m <sup>3</sup> )	(m)
Soil1	19	19	19	1,80
Soil2	17	19	21	1,00
Soil3	5	19	10	0,50
Soil4	35	19	28	-

Source: (bSLOPE 2012).

Account steps will be shown, and transactions will be shown on the software developed. Thus, in the software's demo version, users are expected to get the same results when they input the same values. The solution of the slopes in the literature is important in terms of software reliability.

##### Calculation Steps with Developed Software (SlopeME) Inputting for Case 3:

As described in Chapter 2.4, the parameters that should be known according to the Limit Equilibrium Method (LEM) are specified. For example, in limit equilibrium analysis, it is sufficient to know three parameters. These are the internal friction angle ( $\phi'$ ), unit volume weight ( $\gamma$ ), and cohesion ( $c'$ ). These parameters and geometric properties are given in Table 4.3. Case 3 "Parameters" will be created with the developed software (SlopeME) as follows.

Slope Surface Coordinates (Unit: kN-m)

Apply Import.xls Clear All - Borehole + Borehole - Layer + Layer

Input Layers Boreholes Coordinates Values

	1	2	3	4	5	6
Xb.	1	0.00	6.00	15.00	4.00	5.00
Y1	Filler	15.00	15.00	7.00	5.00	5.00
Y2	BedRock	0.00	0.00	0.00	0.00	0.00
Y3						
Y4						

Ground Under Water  There is/isn't?

	1	2	3	4	5	6
Y.n	Water	9	9	7	7	7

Soils Parameters

	Name	Cohesi...	Unit Weight	Wet Unit...	Friction A...	Young Mo...
1	Filler	5	20	20	20	10000
2	BedRock	5	20	20	20	10000

**Figure 4.15 :** SlopeME input of properties: Case 3.

As shown in Figure 4.15; **Layers Boreholes** With "Layers Borehole", the X-dependent change distances of the Y coordinate on the slope are entered. Case 3 has 1 "Layer", but another one has been entered for "Bedrock".

However, the coordinates of "Bedrock" were entered as zero (not to enter soil parameters). It was explained in Chapter 3.1.1, it is necessary to enter at least 2 points for Y (one of them is bedrock) and at least 4 points for X.  **There is/isn't?** Election was made due to groundwater. Soil parameters were entered in accordance with "Case 3".

**Calculation Steps with Developed Software (SlopeME) Creat Slide for Case 3:**

As described in Chapter 2.8.1, circular and non-circular fault surfaces were mentioned. It is stated in Chapter 3.1.1 that the user will completely choose the choice of the circular or non-circular fracture surface. Case 3 "Slide" will be created as follows with the developed software (SlopeME).



The screenshot shows the 'Creat Slide' dialog box in SlopeME. It is divided into three sections:

- Method Selection:** 'Circle Method' is selected. Other options include 'Ellipse Method'. Checkboxes for 'Show Rad. Circle', 'Show Fail. Y Coord.', 'Axis Mirror', and 'Axis Grid' are present.
- Center of Circles:** 'Lower Left' and 'Upper Right' coordinates are both set to X: 20, Y: 20. The 'One Point?' checkbox is checked.
- Axis Size:** 'Lower Left Limit' is X: -1, Y: -1. 'Upper Right Limit' is X: 31, Y: 25. A 'Set Axis Limits' button is available.

Additional controls include 'Coef.' set to 1, 'Number of Slices' set to 30, and buttons for 'Show Slide' and 'Create Slope Surface'.

**Figure 4.16 :** SlopeME input of creat slide: Case 3.

It is shown in Figure 4.16. The "Circle Method" was preferred because it was done this way for the Case 3 example. "Number of Slices" 30 were selected. It has been explained in Chapter 3.1.1, if the number of slices increases, the processing time increases because the sensitivity will increase.  One Point? The software first determines a random point. When we cancel this option, either a single point must be entered, or a rectangular selection range is required for the center of the FOS refraction circle. X: 20m and Y: 20m were chosen to be the same as Case 3 example.

**Calculation Steps with Developed Software (SlopeME) Running for Case 3:**

Generalized Methods (GLE) are mentioned in Chapter 3.4. It is explained here that there is no interaction between OMS slices. It is explained that the Bishop method works in Moment balance and that only normal force affects between slices. It is explained that Moment and Force balance is sought in Spencer and M&P methods. It has been explained that there are different acceptances to achieve this balance. Case 3 "Running" will be created as follows with the developed software (SlopeME).

As shown in Figure 4.17, B: 2m and D: 1m were automatically chosen and described in Chapter 3.4.1, how OMS, Bishop, and M&P methods are calculated. The software first determines the most critical fracture surface with OMS. This fracture surface is accepted if it is critical within the Bishop method. If not, the iterations will continue in any way. Tolerance 0.01 | The higher the tolerance, the longer the processing

time.  Semi sinus  It has been chosen as Semi-sinus for M&P. The important thing here is how the interaction between slices is.

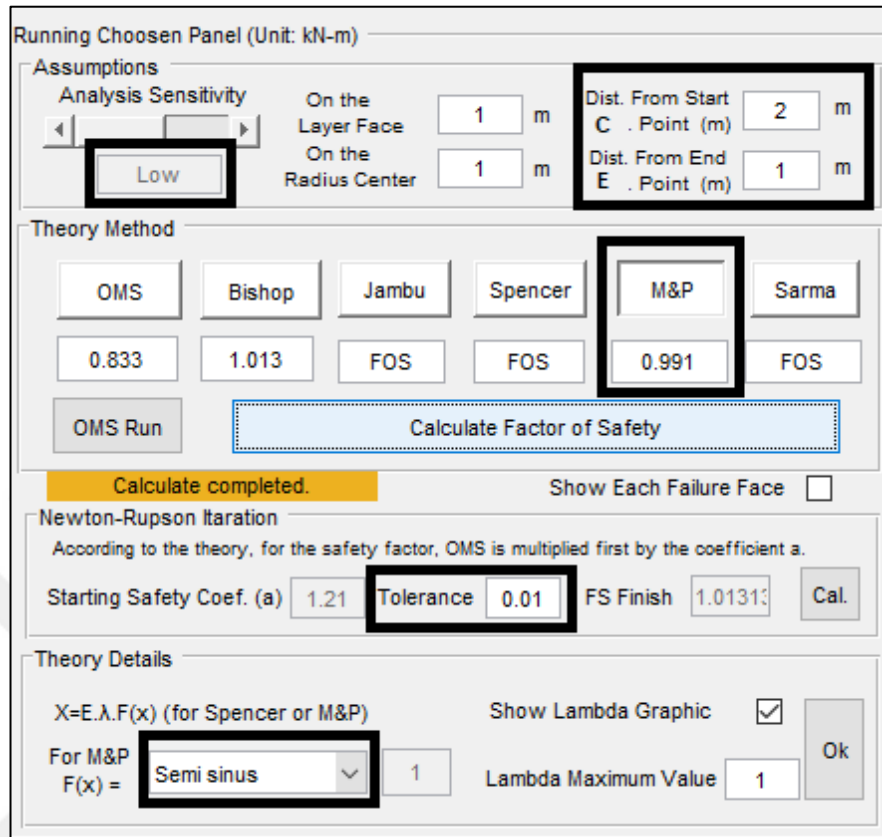


Figure 4.17 : SlopeME input of running: Case 3.

**Calculation Steps with Developed Software (SlopeME) Internal Forces for Case 3:**

Generalized Methods (GLE) are mentioned in Chapter 3.4. With the developed software (SlopeME), Case 3 “Internal Forces” was formed as follows.

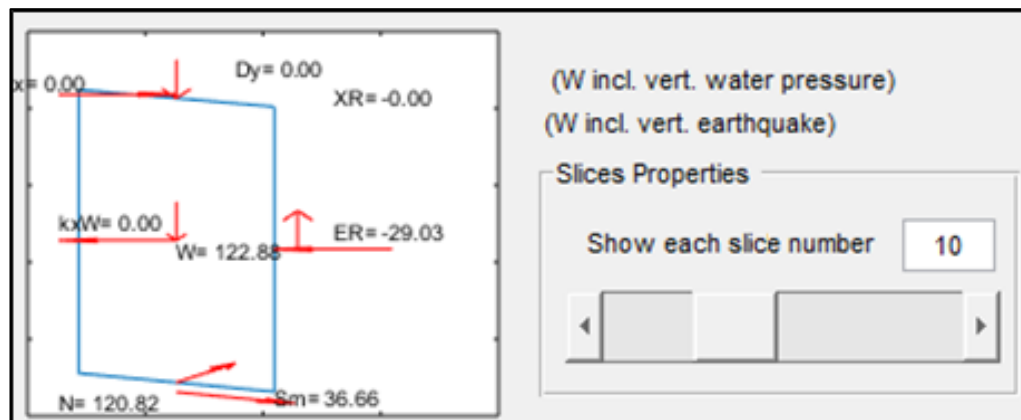
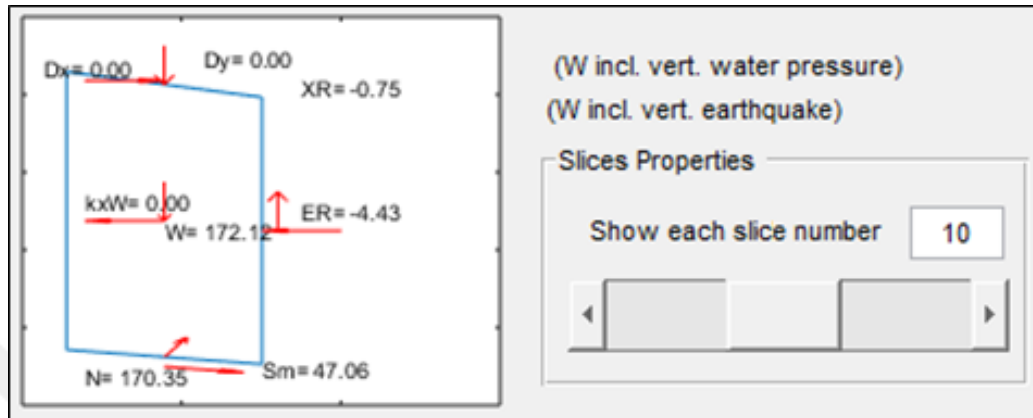


Figure 4.18 : SlopeME output of internal forces for slice number 10: Bishop

As shown in Figure 4.18; In Bishop results, slice weight (W): 122.88 kN, slice base reaction force (N): 120.82 kN, slice base friction force (Sm): 36.66 kN, total lateral force in slice (ER-EL): -29.03 kN and total friction force on the slice edge (XR-XL): calculated as 0 kN.



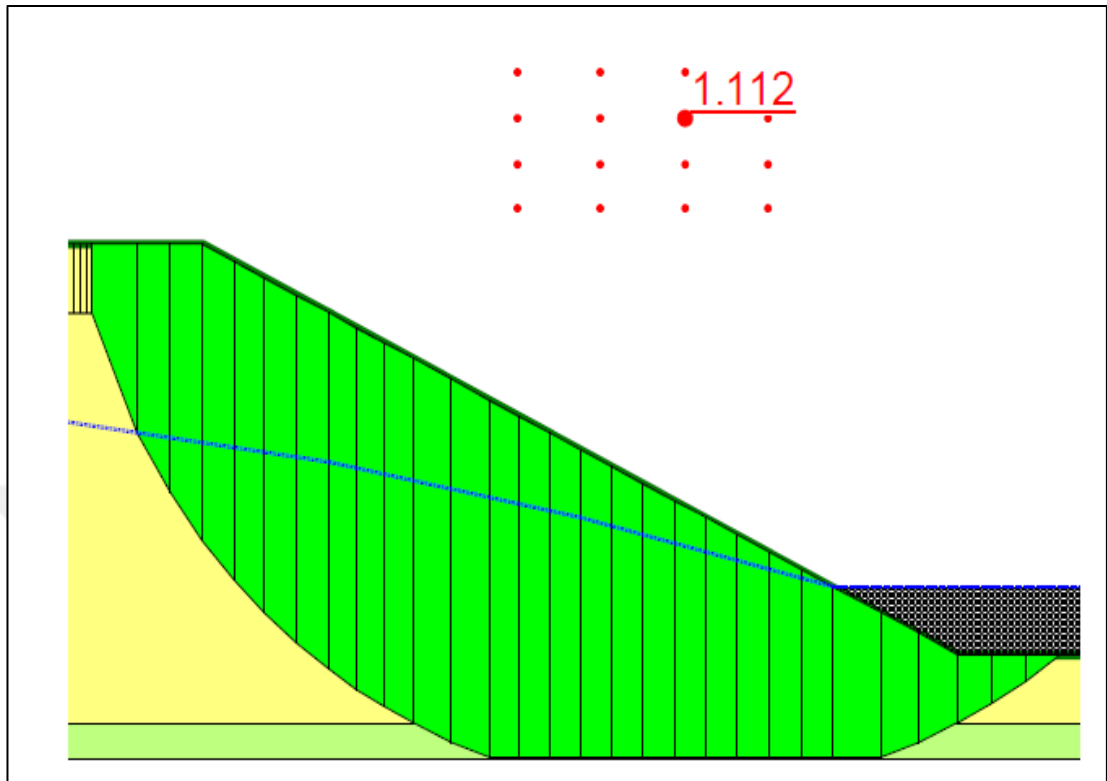
**Figure 4.19 :** SlopeME output of internal forces for slice number 10: M&P

Shown in 4.19 in the figure; In M&P results, slice weight (W): 172.10 kN, slice base reaction force (N): 170.35 kN, slice base friction force (Sm): 47.06 kN, total lateral force on slice (ER-EL): -4.43 kN and total friction force (XR-XL) at the slice edge: was calculated as -0.75 kN.

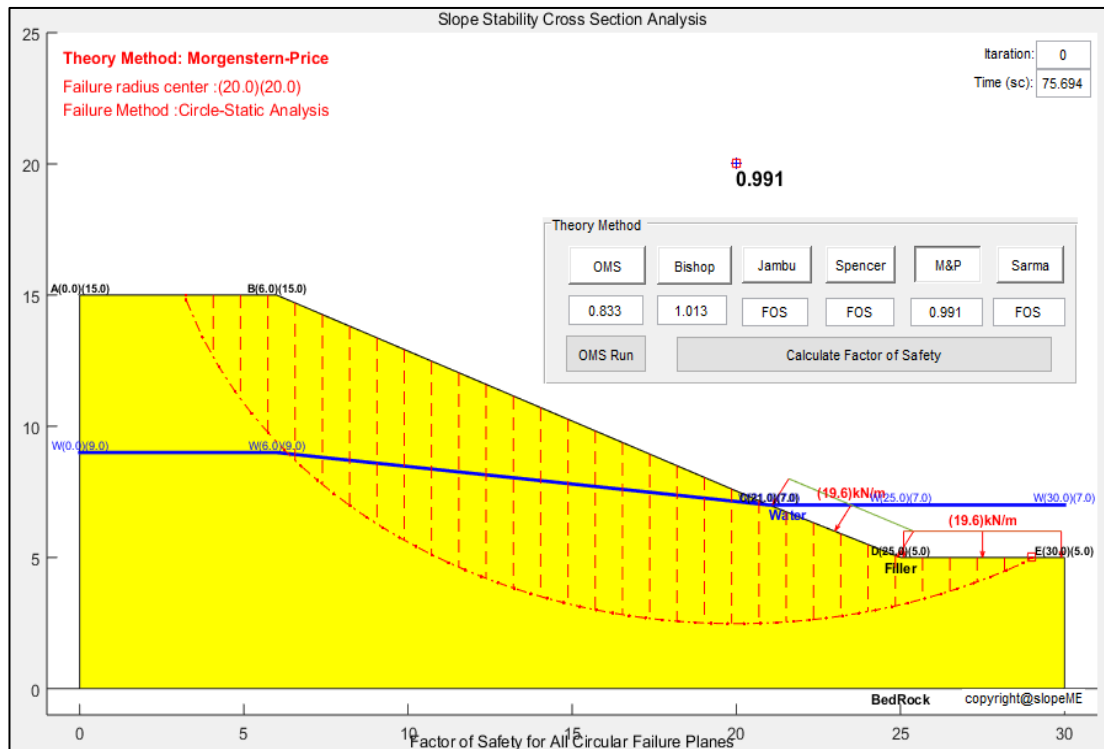
The relationship between E and X is described in Chapter 3.4.4. For slice 10, the value of the half-sine function and the X force is calculated as follows;  $f(x) = 0.34$  (function for semi-sinus) and  $\lambda = 0.5$  (from the balance of moment and force);  $X = W * \lambda * f(x)$ .

$$X = 4.43 * 0.5 * 0.34 = 0.75 \text{ kN (calculated horizontal forces for a slice)}$$

**Comparison of (SlopeME) and SLOPE / W Results For Case 3:**



**Figure 4.20 :** SLOPE/W output of FOS: Case 3  
 Source: (GEO-SLOPE, 2012).



**Figure 4.21 :** SlopeME output of FOS: Case 3.

**Calculation Steps with Developed Software (SlopeME) Inputting for Case 4:**

As described in Chapter 2.4, the parameters that should be known according to the Limit Equilibrium Method (LEM) are specified. For example, in limit equilibrium analysis, it is sufficient to know three parameters. These are the internal friction angle ( $\phi$ ), unit volume weight ( $\gamma$ ), and cohesion ( $c$ ). These parameters and geometric properties are given in Table 4.4. Case 4 "Parameters" will be created with the developed software (SlopeME) as follows.

As shown in Figure 4.22; **Layers Boreholes** With "Layers Borehole", the X-dependent change distances of the y coordinate on the slope are entered. In Case 4, there are 3 "Layers", but another layer has been entered for "Bedrock". However, the coordinates of "Bedrock" were entered as zero (not to enter soil parameters). It was explained in Chapter 3.1.1, it is necessary to enter at least 2 points for Y (one of them is bedrock) and at least 4 points for X.  There is/isn't? No selection was no due to the lack of groundwater. Soil parameters were entered in accordance with "Case 4".

**Slope Surface Coordinates (Unit: kN-m)**

Buttons: Apply, Import xls, Clear All, - Borehole, + Borehole, - Layer, + Layer

	1	2	3	4	5	6	7
Xb.	1	0.00	3.00	5.00	10.00	2.00	3.00
Y1	Soil1	10.00	10.00	7.60	2.90	2.00	2.00
Y2	Soil2	8.50	8.20	7.60	2.90	2.00	2.00
Y3	Soil3	6.60	6.00	5.00	2.90	2.00	2.00
Y4	Soil4	6.10	5.50	4.50	2.40	2.00	2.00

Ground Under Water  There is/isn't?

	1	2	3	4	5	6	7
Y.n	Water	8	7	6	2.9000	2	2

	Name	Cohesi...	Unit Weight	Wet Unit ...	Friction A...	Young Mo...
1	Soil1	19	19	19	20	10000
2	Soil2	17	19	19	21	10000
3	Soil3	5	19	19	10	10000
4	Soil4	35	19	19	28	10000

**Figure 4.22 :** SlopeME input of properties: Case 4.

**Calculation Steps with Developed Software (SlopeME) Creat Slide for Case 4:**

As described in Chapter 2.8.1, circular and non-circular fault surfaces were mentioned. It is stated in Chapter 3.1.1 that the user will completely choose the choice of the circular or non-circular fracture surface. Case 4 "Slide" will be created as follows with the developed software (SlopeME).

The screenshot shows the 'Creat Slide' dialog box in SlopeME. It has three main sections: 'Method Selection', 'Center of Circles', and 'Axis Size'. In the 'Method Selection' section, 'Ellipse Method' is selected with a thick black border. Other options include 'Circle Method', 'Show Rad. Circle', 'Show Fail. Y Coord.', 'Axis Mirror', and 'Axis Grid'. The 'Number of Slices' is set to 30, also with a thick black border. The 'Center of Circles' section has 'Lower Left' (X: 16, Y: 22) and 'Upper Right' (X: 20, Y: 26) coordinates. There is an unchecked 'One Point?' checkbox. The 'Axis Size' section has 'Lower Left Limit' (X: -1, Y: 1) and 'Upper Right Limit' (X: 30, Y: 30). Buttons include 'Show Slide', 'Create Slope Surface', and 'Set Axis Limits'.

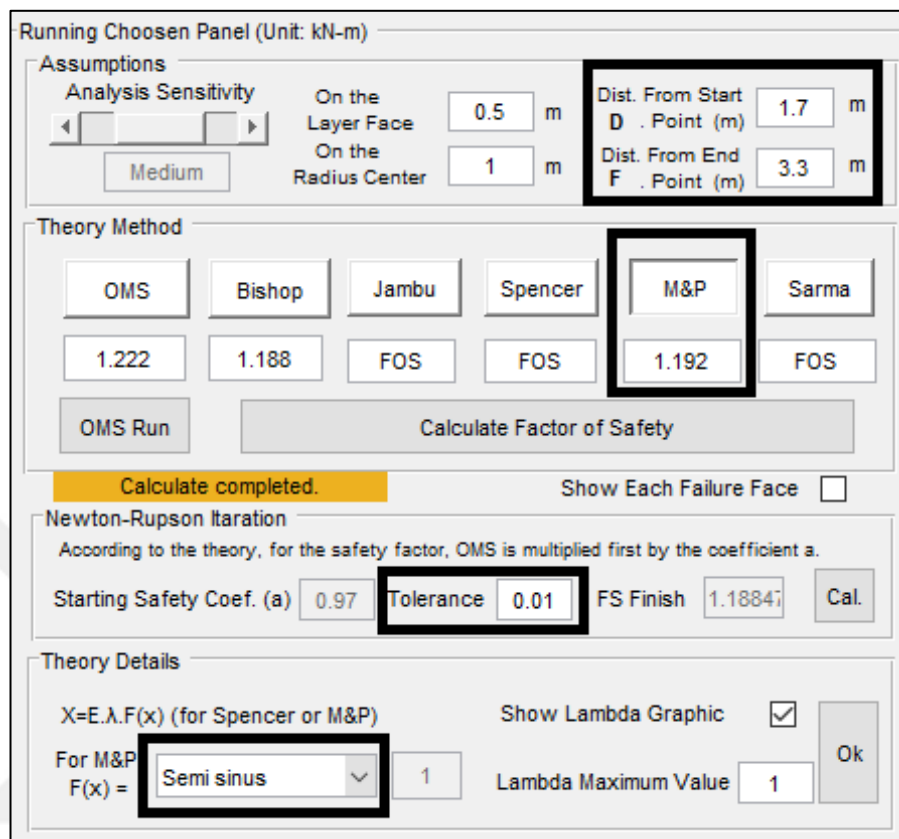
**Figure 4.23 :** SlopeME input of creat slide: Case 4.

It is shown in Figure 4.23. "Ellipse Method" was preferred because it was done this way for the Case 4 example. "Number of Slices" 30 were selected. It has been explained in Chapter 3.1.1, if the number of slices increases, the processing time increases because the sensitivity will increase.  One Point? The software first determines a random point. When we cancel this option, either a single point must be entered, or a rectangular selection range is required for the center of the FOS refraction circle. X: 16-20m and Y: 22-26m were chosen to be the same as the Case 4 example.

**Calculation Steps with Developed Software (SlopeME) Running for Case 4:**

Generalized Methods (GLE) are mentioned in Chapter 3.4. It is explained here that there is no interaction between OMS slices. It is explained that the Bishop method works in Moment balance and that only normal force affects between slices. It is explained that Moment and Force balance is sought in Spencer and M&P methods. It

has been explained that there are different acceptances to achieve this balance. Case 4 "Running" will be created as follows with the developed software (SlopeME).

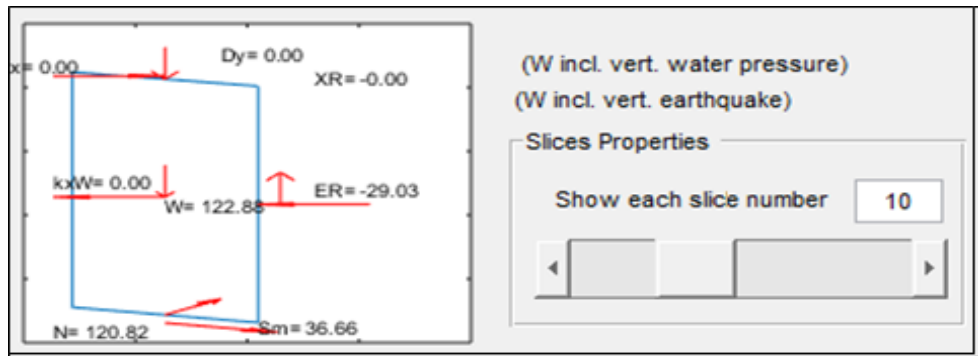


**Figure 4.24 :** SlopeME input of running: Case 4.

As shown in Figure 4.24, B: 1.7m and D: 3.3m were chosen and described in Chapter 3.4.1, how OMS, Bishop, and M&P methods are calculated. The software first determines the most critical fracture surface with OMS. This fracture surface is accepted if it is critical within the Bishop method. If not, the iterations will continue in any way. **Tolerance** 0.01 | The higher the tolerance, the longer the processing time. **Semi sinus** | It has been chosen as Semi-sinus for M&P. The important thing here is how the interaction between slices is.

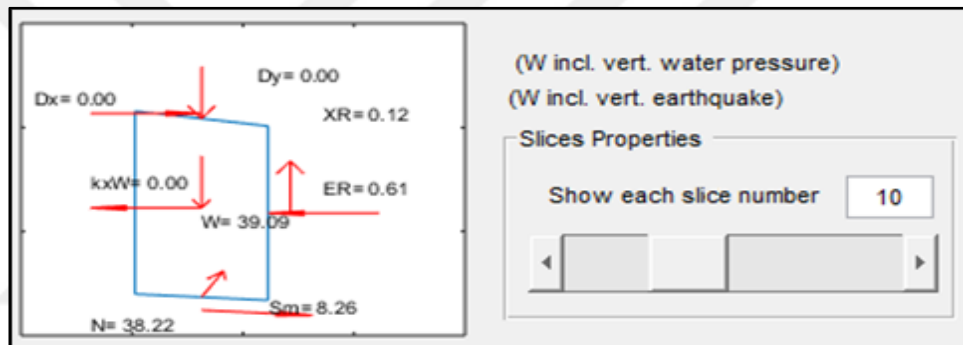
**Calculation Steps with Developed Software (SlopeME) Internal Forces for Case 4:**

Generalized Methods (GLE) are mentioned in Chapter 3.4. With the developed software (SlopeME), Case 4 "Internal Forces" was formed as follows.



**Figure 4.25 :** SlopeME output of internal forces for slice number 10: Bishop

Shown in Figure 4.25; In Bishop results, slice weight (W): 122.88 kN, slice base reaction force (N): 120.82 kN, slice base friction force (Sm): 36.66 kN, total lateral force in slice (ER-EL): -29.03 kN and total friction force on the slice edge (XR-XL): calculated as 0 kN.



**Figure 4.26 :** SlopeME output of internal forces for slice number 10: M&P

As shown in 4.26 in the figure; In M&P results, slice weight (W): 39.39 kN, slice base reaction force (N): 38.22 kN, slice base friction force (Sm): 8.26 kN, total lateral force on slice (ER-EL): -0.61 kN and total friction force (XR-XL) at the slice edge: was calculated as -0.12 kN.

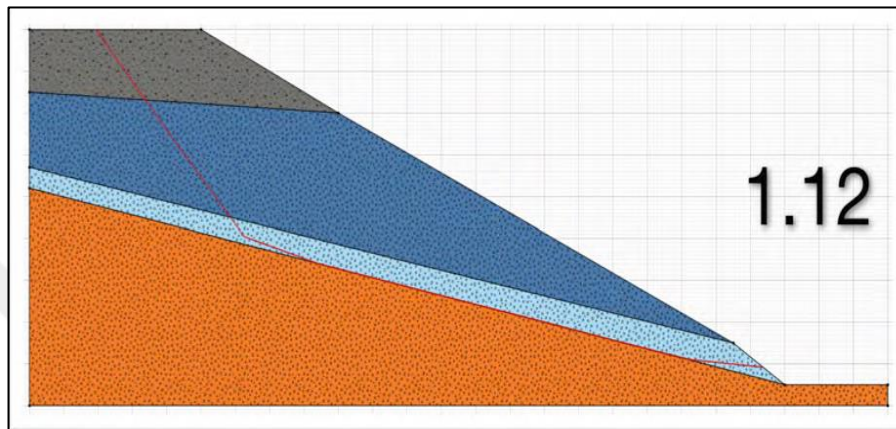
The relationship between E and X is described in Chapter 3.4.4. For slice 10, the value of the half-sine function and the X force is calculated as follows;  $f(x) = 0.79$  (function for semi-sinus) and  $\lambda = 0.25$  (from the balance of moment and force);  $X = W * \lambda * f(x)$ .

$$X = 0.61 * 0.25 * 0.79 = 0.12 \text{ kN (calculated horizontal forces for a slice)}$$

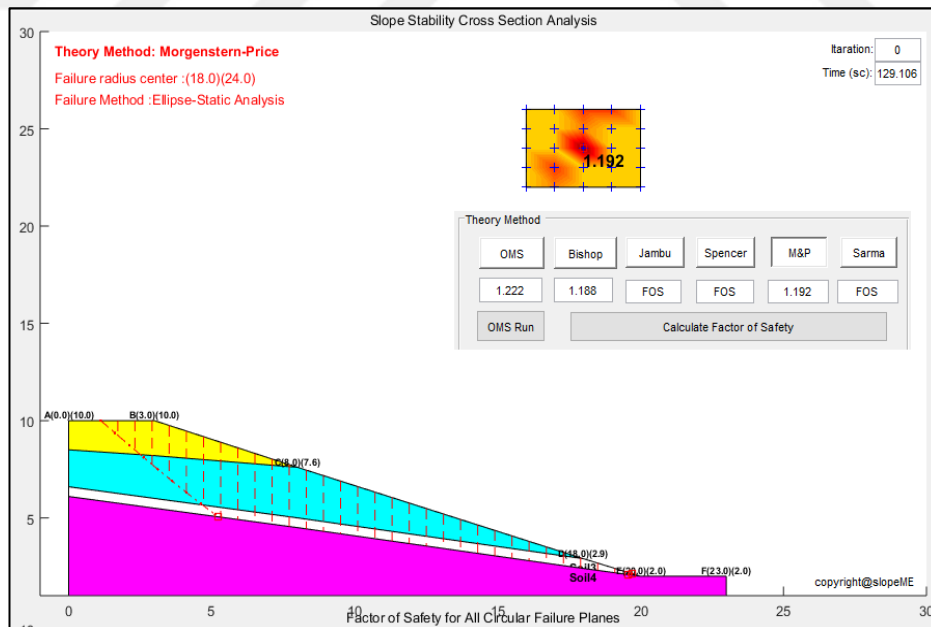


**Comparison of (SlopeME) and bSLOPE Results For Case 4:**

4 different situations have been examined above. In fact, the software developed has a lower safety factor. When this happens, it turns out that the software developed is more secure. However, it does not always have to be that way. Because in Limit Equilibrium Methods, finding the most critical fracture surface is based on the data end relationship. In other words, the grid spacing created as a possibility directly affects the results.



**Figure 4.27 :** SLOPE/W output of FOS: Case 4  
Source: (bSLOPE 2012).



**Figure 4.28 :** SlopeME output of FOS: Case 4.

Since it is left to the user in the step interval in the grid, it affects the sensitivity in finding the breaking circle. As the number of iterations increases, the processing time increases. Thanks to the advantage of using a computer, this time is minimized. Another issue is the force interaction between slices. The assumptions and assumptions here directly affect FOS. When all these are considered, the result that comes out with Case 4 is the result that many software wants to achieve.



## 5. CONCLUSIONS AND RECOMMENDATIONS

Software and capabilities used in the market have also been researched. Calculation methods that can be used were compared. The advantages and disadvantages of the limit equilibrium method are given in previous titles. Also, reference is made to the finite element method. It was created with MATLAB code, which is a mathematical software on the study pad. It is aimed to be an easy-to-use and convenient interface that will be offered to engineering service if it is a software suitable for the purpose. There was very little work on this.

The GLE (Generalized Limit Equilibrium Method) calculation principles are presented in this thesis using Matlab code developed for slope stability calculations. In the developed Matlab code, in the geometry part, modeling can be made in accordance with all geometries. Furthermore, any number of soil layers can be added. In the software available on the market, modeling is done as graphic drawing. It is aimed that the software will include a graphical interface in the future. Modeling works on the following principles, and it is created by entering the X and Y coordinates at the change points of the upper ground layer. That is, it is assumed that there is a borehole at the ground change points. At each ground change point, the borehole can easily be marked as the presence or absence of groundwater level without renewing the geometer. After the modeling is completed, the user chooses the number of slices. The user chooses the failure surface to be non-circular or circular. The user selects the start and end range at the Toe point, and the iterations start here with trial and error. Also, the user should choose the number of steps and choose the iteration. Iteration steps; It can be in the desired size, such as 1m, 0.5m.

The software will iterate to find the most unfavorable FOS along the rectangular range created to find the failure circle's center. There are many "For loops" for FOS iteration in Matlab code. Special formulations have been developed for all formulas in GLE. In order to evaluate all possibilities, a FOS is obtained with the OMS (Ordinary Method of Slices) method. Then iterations are made for the Tolerance range selected for Bishop, Spencer, Janbu, and M&P, and definitive results are

found. The tolerance range is presented to the user in the software interface, and the desired sensitivity can be selected. Software available on the market has an extension format for saving files. In the developed Matlab coded software, it is only saved as a cell data file. This file extension is given as ".xls".

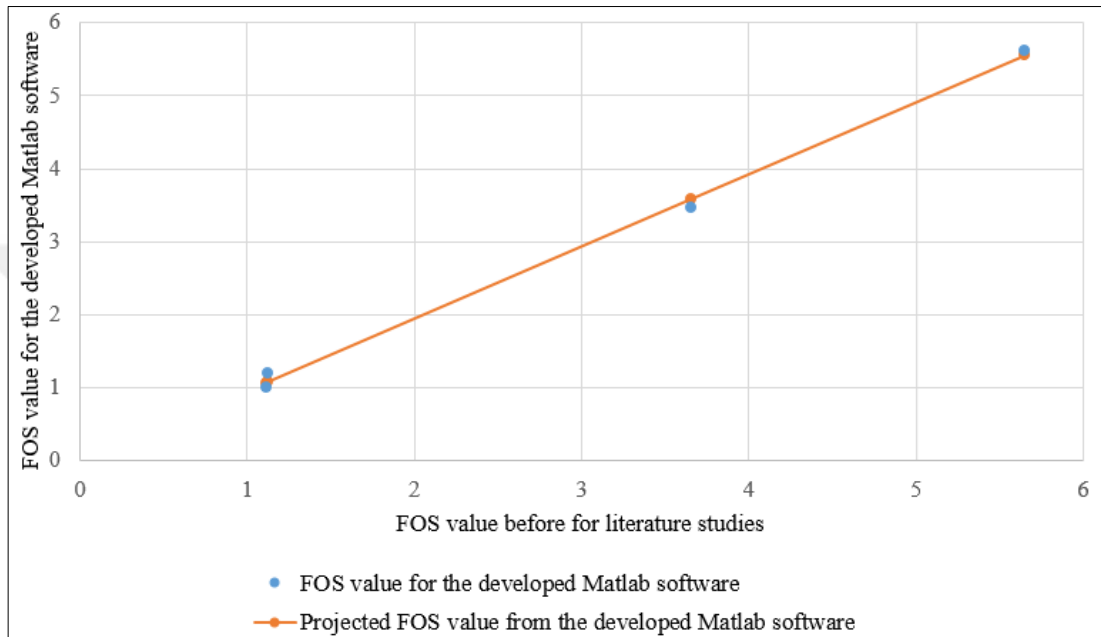
Sample slope problems were first taken from Atarigiya 2012, thesis work. For Case3, the model with GWL (Groundwater Level) in the Slope / W user manual was selected. For Case4, the multi-layer model in the bSlope user manual was selected. The FOS values, which were calculated before and whose results are known, were compared with the developed Matlab code results. This thesis's main purpose for future studies is to numerically model and calculate Slopes with Matlab code, which contains completely unique formulations. All geometries are remodeled in software developed with Matlab code. The FOS results were evaluated using the method of Morgenstern-Price (1965). "Semi-sinus" has been chosen as the function relation between the inter-slices  $X / E$ . As can be seen from the analysis, depending on the geotechnical parameters and geometries chosen, the safety factors are close to each other. As it is known, the properties of the soil parameters and the geometric variability affect the safety factor.

**Table 5.1** : Summary of FOS outputs.

Cases	FOS value before for literature studies	FOS value from the developed Matlab software	Amount of Difference (%)
Case 1	5.649	5.611	0.67%
Case 2	3.659	3.472	5.11%
Case 3	1.112	0.991	10.88%
Case 4	1.12	1.192	6.43%
Standard deviation for all cases	2.198296765	2.176416091	1.00%

**Table 5.2 : Regression statistics.**

Regression Parameters	
Multiple R	0.99874479
R <sup>2</sup>	0.99749115
Adjustable R <sup>2</sup>	0.99623672
Standard error	0.13485571
Observation (for 4 cases)	4



**Figure 5.1 :** Line alignment drawing for FOS.

The following results may have been obtained in this study:

1. In Table 5.1, the slope stability safety factor calculated for case1, case2, and case3 is greater than the safety factor calculated with the developed Matlab code. However, while the slope stability safety factor is 1,120 only in case4, the safety factor calculated with the Matlab code is 1,192. Case4 may be due to recurrence assumptions or convergence of interaction assumptions of slope slices. These differences may be the iteration interval adopted to find the center of the break circle or the iteration precision in the inter-slice X / E function relationship. Results are very similar.
2. The fact that the geometries are completely different from each other is an important comparison factor for the percentage of success in obtaining the FOS

value. This comparison is important in establishing the Academic value of the software developed.

3. Most software in the market was that the interface was complex and difficult to understand. In the developed Matlab code software, the interface was shown to be simple and understandable.

4. The developed software has reached similar standard deviation results as given in Table 5.1. It also reached a regression coefficient ( $R^2$ ) given in Table 5.2 (99%). As can be seen in Figure 5.1, the fit graph is quite convergent.

5. The exclusion of this study is that the Developed Matlab code may be suitable for all geometries for the slope stability solution. It aims to make comparisons and research with FEA (Finite Element Analysis) 2D and 3D.

6. This thesis aims to develop software for slope stability. There are ongoing studies to increase the reliability of the developed software and to use it more effectively by engineers when it is put into use. The number of iterations determining the fracture surface will be increased. Slope stability will be checked in earthquake movements. Improvement modules will be added for situations that do not provide slope stability. Finally, when these improvements are applied to the developed software, user-friendly software that can be used in academic research and publications will be obtained. The next stages aim to present the software to the practitioners with the software license.

## REFERENCES

- Abramson, L.W.**, (1996). Slope Stability and Stabilizations methods, Wiley, New York.
- Anaçali İ. & Şirin A.** (2015). Heyelan Tanımlama ve Veri Oluşturma Kılavuzu, Karayolları Genel Müdürlüğü, Ankara.
- Atarigiya, B. D.**, (2012). Numerical Modeling and Simulation of the Stability of Earth Slopes. University Of Ghana: Master Thesis.
- Avşar Ö.**, (2004). Landslide Stabilization in Weathered Tuffite Northern Turkey, Thesis of Master, Middle East Technical University, Natural and Applied Sciences, Ankara.
- Bishop, A.W.** (1955). The Use of the Slip Circle in the Stability Analysis of Slopes. London, England: Géotechnique 5(1).7-17
- Broms, B. B.**, (1964a). Lateral Resistance of Piles in Cohesive Soils, ASCE Journal of Soil Mechanics and Foundations Division, 90(SM2):27-63.
- Broms, B. B.**, (1964b). Lateral Resistance of Piles in Cohesive Soils, ASCE Journal of Soil Mechanics and Foundations Division, 90(SM3):123-156.
- Broms, B. B.**, (1983). Earth Pressures on Piles in a Row Due to Lateral Soil Movements, Soils and Foundations, 37(1):1-12.
- Bromhead, E. N.**, (1986). The Stability of Slope. Surrey University Press, A.B.D
- bSLOPE** (2012). Geotechnical Engineering Report No. UCB/GT/12-01. Berkeley, CA, 94720.
- Chen Z. & Shao C.** (1988). Evaluation of minimum factor of safety in slope stability analysis. Can. Geotech. J. , 20(1). 104-119.
- Cheng, Y. M., & Lau, C. K.** (2008, Dec 2008). Slope stability analysis stabilization; new methods and insight. SciTech Book News, 32.
- Cruden D. M. & Varnes D. J** (1993). Landslide Types and Processes, Transportation Research Board, National Academy of Sciences, 247, 36-75.
- Coduto, D.P.** (2006). Geotechnical Engineering Principles and Applications. Ankara: Gazi Kitap Evi.
- Coulomb, C.A.** (1776).”Essai sur une application des regles des maximis et minimis a quelques problemes de statique relatifs a l’architecture”. Memoires de l’ Academie Royale Pres Drivers Savants. Vol. 7.
- Çamlıbel, A.N.**, (1982). Yamaç Stabilesinin Düşey Kazıklarla İyileştirilmesi, Doktora Tezi, İstanbul Üniversitesi.

- Leman Çavumirza** (2018). Şev Stabilitesi Analizi Ve Kartepe-Uzuntarla (Kocaeli) Örneği, Kocaeli Üniversitesi.
- Das and Sobhan**, (2012). Principles of Geotechnical Engineering book.
- Das, M.B.**, (2006). Principles of Geotechnical Engineering, Thomson.
- Dawson, E. M. & Roth, W.H. & Drescher, A.** (1999). Slope Stability Analysis by Strength Reduction. Geotechnique, Vol. 49, No. 6, pp. 835-840
- Duncan, J.M.** (1996). State of art: limit equilibrium and finite-element analysis of slopes. Journal of Geotechnical Engineering, Vol. 122, No. 7.577-596
- Feng, H. Y.** (1994). "Cracking and fracture behavior of soil." Fracture Mechanics Applied to Geotechnical Engineering. ASCE, Geotechnical Special Publication.
- Fellenius, W.** (1927). Erdstatische Berechnungen mit Reibung and Kohasion. Berlin: Ernst.
- Hack, R.**, (2002). An evaluation of slope stability classification. Proc. ISRM EUROCK'2002, Portugal, Madeira, Funchal, 25-28 November 2002. Eds: C. Dinis da Gama & L. Ribeira e Sousa, Publ. Sociedade Portuguesa de Geotecnia, Av. do Brasil, 101, 1700-066 Lisboa, Portugal. pp. 3 – 32.
- Hammouri, N.A. & Husein Malkawi & A.I. & Yamin, M.M.A.** (2008). Stability analysis of slopes using the finite element method and limiting equilibrium approach, Bulletin of Engineering Geology and the Environment, 67 (4), 471-478.
- Hammah, R.E. & Curran, J.H. & Yacoub T. & Corkum, B.** (2004). Stability Analysis of Rock Slopes using the Finite Element Method. EUROCK 2004 & 53rd Geomechanics Colloquium. Schubert (ed.).
- Hamza T. & Raghuvanshi. T.K.**, (2017). GIS-based Landslide Hazard Evaluation and Zonation - A case from Jeldu District, Central Ethiopia, Journal of King Saud University – Science, 29(2),151- 165.
- Hoek, E. & Bray, J.W.**, (1981). Rock Slope Engineering (Revised Third Edition). Institute of Mining and Metallurgy, London, pp. 358.
- Hossain, M. M.**, (2011). Stability analysis of anchored rock slopes against plane failure subjected to surcharge and seismic loads. Retrieved from <http://ro.ecu.edu.au/theses/139> on December 18' 2020.
- GEO-SLOPE International Ltd** (2012). Stability Modeling with SLOPE/W. GEO-SLOPE International Ltd., Calgary, Alberta, Canada.
- Griffiths, D.V. & Lane P.A.** (1999). Slope Stability Analysis by Finite Elements, Geotechnique, Vol. 49, No. 3, pp. 387-403
- Gitirana, Jr. & F. N. G. & Fredlund, D. G.** (2005)a. The application of unsaturated soil mechanics to the assessment of weather-related geo-hazards, Proceedings of the Sixteenth International Conference on Soil Mechanics and Foundation Engineering, Osaka,
- Gitirana, Jr. & F. N. G. & Fredlund, D. G.** (2005)b. Evaluation of the variability of unsaturated soil properties, Proceedings of the Fifty-Eighth Canadian Geotechnical Conference, Saskatoon, SK, Vol. 2.



- Gitirana, Jr. & de F. N. G.** (2005). Weather-related geo-hazard assessment model for railway embankment stability, Ph.D. Thesis, University of Saskatchewan, Saskatoon, SK.
- Goodman, R.E. & J.W. Bray.,** (1976). Toppling of Rock slopes Proc. ASCE Conf. Rock Eng. for Foundations and Slopes, Boulder.
- Kasim, K.A. & Adhami, B. & Nazir, R. & Moayedi, H.** (2012). Slope stability and sheet pile and contiguous bored pile walls. EJDE vol 17.pp. 1-26.
- Kim, J. & Salgado, R. & Lee, J.** (2002). Stability analysis of complex soil slopes using limit analysis. Journal of Geotechnical and Geoenvironmental Engineering, ASCE, Vol. 128, No. 7, pp. 546-557.
- Krahn, J.** (2004). Stability modelling with SLOPE/W. Geo-Slope International Ltd., Calgary: Alberta.
- Kulhawy, F.H.,** (1969). Finite Element Analysis of stresses and movements in embankments during construction.
- Lupini J. & Skinner A. & Vaughan P..** (1981). The drained residual strength of cohesive soils, Géotechnique 31(2), 181-213.
- Matlab,** <https://en.wikipedia.org/wiki/MATLAB>, accessed July 15, 2020
- Morgenstern, N. R. & Price, V. E.** (1965). The analysis of the stability of general slip surfaces, Geotechnique, Vol. 15, No.1.79-93
- Önalp A.** (1983). İnşaat Mühendislerine Geoteknik Bilgisi 2, 1. Baskı. Trabzon: K.T.Ü Yayınları.
- Knut E. P.** (1955). The Early History of Circular Sliding Surfaces. Volume 5, Issue 4, December 1955, pp. 275-296.
- Rankine, W.** (1857). On the stability of loose earth. Philosophical Transactions of the Royal Society of London, Vol. 147.
- Rendulic, L.,** (1935). Der hydrodynamische spannungsausgleich in zentral entwässerten Tonzylindern, Wasserwirtschaft und Technik, 250–253p.
- Raghuvanshi, T.K. & Solomon, N.** (2005). A Sensitivity Analysis of a Natural slope having Planar mode of failure. Journal of Ethiopian Association of Civil Engineers. 4 (1), 27 – 40.
- Raghuvanshi, T.K. & Ibrahim, J. & Ayalew, D.,** (2014). Slope stability susceptibility evaluation parameter (SSEP) rating scheme – an approach for landslide hazard zonation. J. Afr. Earth Sci. 99, 595– 612.
- Rendulic, L.,** (1935). Ein Beitrag zur Bestimmung der Gleitsicherheit, Bauingenieur 16(19/20), 230–233.
- Sert S.,** (2019). Plaxis 2d Temel Eğitim Kursu. IMO İstanbul Şubesi.
- Sharma, S. & Raghuvanshi, T. & Anbalagan, R.,** (1995). Plane failure analysis of rock slopes. Geot. & Geol. Engg, 13, 105 – 111.
- Shao et al.** (2015). Rainfall intensity and slope gradient effects on sediment losses and splash from a saline–sodic soil under coastal reclamation. Germany: Catena 128.54-62

- Singh, T.N. & Gulati, A. & Dontha, L. et al.** (2008). Evaluating cut slope failure by numerical analysis-a case study. London: Nat Hazards 47.263.
- Skempton, A. W.** (1964). Long term stability of clay slopes. Fourth Rankine Lecture: Geotechnique 14(2).77-101.
- Stead, D. & Eberhardt, E. & Coggan, J.S.,** (2006). Developments in the characterization of complex rock slope deformation and failure using numerical modelling techniques. Eng. Geo. 83, 217– 235.
- Stark T.D. & Eid H. T.** (1994). Drained Residual Strength of Cohesive Soils, J. of Geot. Engineering 120(5), 856-871.
- Stark T. D. & Choi, H., & McCone S.** (2005). Drained shear strength parameters for analysis of landslides, J. of Geot. and Geoenv. Engineering 131(5), 575-588.
- Spencer, E.** (1967). A Method of Analysis of the Stability of Embankments Assuming Parallel Interslice Forces, Géotechnique, Vol. 17, No. 1.
- Taylor, D. W. & T. M. Leps** (1939). "a comparison of results of direct shear and cylindrical compression test". Proc. A.S.T.M.
- TBDY** (2018). Türkiye Bina Deprem Yönetmeliği. Türkiye: Çevre Şehircilik Bakanlığı.
- Tekin, A.** (2011). Sonlu Elemanlar Ve Limit Denge Yöntemleri Ile Şev Stabilitesi Analizi. İstanbul, İÜ: Master Thesis.
- Terzaghi, K.** (1950). Mechanisms of landslides, Engineering Geology (Berkey) Volume. USA: Geological Society of America.
- Tolon, M.** (2007). Artificial Neural Network Approaches For Slope Stability. İstanbul, İstanbul Technical University, Master Thesis.
- Tolon, M. & Serpengüzel D. N.** (2008). Slope Stability During Earthquakes: A Neural Network Application, Special Publication of Characterization, Monitoring, and Modeling of Geosystems. American Society of Civil Engineers Geo Congress, Num.179, Pages: 878–885.
- Tolon, M. & Serpengüzel D. N.** (2010). Slope Stability during Earthquakes: A Neural Network Application. International Review on Computers and Software, IRECOS, Special Section on Advanced Artificial Neural Network Approaches with Applications to System Management, Vol.5, Number.4, Pages:454–459.
- Taylor, D. W.,** (1948), Fundamentals of Soil Mechanics. New York: John Wiley, Page 700.
- Varnes, D.J,** (1978), Landslides, Analysis and Control, Special Report 176, pp 20-47, R.L. Scuster and R.J. Krizek, Ed., Transportation Research Board, Highway Research Council.
- Yıldız, E. & Tolon, M.,** (2020). Innovative Numerical Approaches based on Traditional Slope Stability Analysis Methods: A Preliminary Study, MAS 12th International European Conference on Mathematics, Engineering, Natural & Medical Sciences, 18-19 July 2020, Izmir, Turkey, ISBN:978-625-7139-16-8, pages:226-232.

**Yu H. & Salgado R. & Sloan W. & and Kim J.** (1999). Limit analysis versus equilibrium for slope stability. USA: J. Geotech. Geoenviron. Eng. ASCE 124-1.1-11

### **Internet Resources**

**Url-1** <<https://geotechpedia.com/Software/Category/171/Slope-Stability>>, Read the Date: 01.01.2020.

**Url-2** <<http://www.ggsd.com>>, Read the Date: 01.01.2020.

**Url-3** <<https://tr.wikipedia.org/wiki/MATLAB>>, Read the Date: 01.01.2020.



## **APPENDICES**

### **APPENDIX A: Summary of Developed Matlab Code with Main Headings**



## Appendix A (Summary of Developed Matlab Code with Main Headings)

```
% --- Executes on button press in pushbutton2.
function pushbutton2_Callback(hObject, eventdata, handles)
% hObject      handle to pushbutton2 (see GCBO)
% eventdata    reserved - to be defined in a future version of MATLAB
% handles      structure with handles and user data (see GUIDATA)

%% Create Box Containing Centers of Circles
clc;
axes(handles.axes1)
hold on
step2=round(str2double(get(handles.rcenter, 'String')),1)
.
.
.
.

%% Bütün tabloların sayısal verilerin çekmek için özel isim listesi
table = get(handles.uitable1, 'Data');
.
.
.
.

%Iterasyon adım sayısı
step=str2double(get(handles.edit5, 'String'))

%Ellips yöntemdeki katsayı
cf=str2double(get(handles.edit1, 'String'))

[rows columns] = size(table);
.
.
.
.
end

%water slopes
table4 = get(handles.uitable4, 'Data');
.
.
.
.
end

    %dış yük bilgileri bitti

% Calculate Intersection (X,Y Coordinates) of Circles and Top of
Slope
%Bir önceki hesabın verilerini kullanıyoruz
xend=str2double(get(handles.edit4, 'String'));
ct=find(x<xend ,1, 'last') %topuktaki kırılma yeri
CT=x(1, ct)
```

```

.
.
.
.
.

cp=find(x<xsa ,1,'last') %tavandaki kırılma yeri
CP=x(1,cp)
    %çemberin kestiği doğru yeri buluyoruz
    intercpt=slope(1,cp)*(0-x(1,cp))+y(1,cp);
.
.
.
.
.

    %% Çemberleri çizdiriyoruz
    xe=xsa:0.5:xend;
.
.
.
.
end

%Taban ile keşisen yeri buluyoruz
[xi,yi] = polyxpoly(xe,ye,xee,yee);
.
.
.
.
.
% Intersection varsa kesilen yeri çıkaracak

if xi>0 | yi>0
.
.
.
.
.
End

%şimdi kesilen yeri çıkarmamız lazım
xe=xsa:0.5:xs1;
.
.
.
.
.

end

% Malzeme özelliklerini çağırma
[rows columns] = size(table2);
.
.
.
.
.

end

```



```

xss=xe
yss=(ybottom(r1,1)+yold)/2
Rs=sqrt((xe-B/2-i)^2+(j-yss)^2)*cosd(Alpha2-Alpha)
if xe<i
Rz=+sqrt((xe-B/2-i)^2+(j-yss)^2)*sind(+Alpha2-Alpha)
else
Rz=-sqrt((xe-B/2-i)^2+(j-yss)^2)*sind(Alpha2-Alpha)
end

%kırılma yüzeyinin hangi tabakaya denk geldiğini buluyoruz
pta=max(find(ytop1<=ybottom(r1,1),1,'first')-1,1);

%Fricitonal angle için layer no;
pta2(kc)=max(find(ytop1<=ybottom(r1,1),1,'first')-
1,1)
kc=kc+1

%M&P için sadece alınacak değerler
if str2double(get(handles.theory,'String'))==5
.
.
.
.
end

%M&P için bitti
%dış yük ve deprem etkisi nokta yükleri
if get(handles.checkbox18,'Value')==1 |...
yw>ytop(1,1)
.
.
.
.

else
xd1=0;xd2=0;yd1=0;yd2=0;
Omega=0; %dış yük açısı
Dx=0*cosd(Omega); %yatay yükler
Dy=0*sind(Omega); %düşey yükler
end
if ytopw>ytop(1,1) %göl etkisi alan
Ab=Ab+B
end %göl etkisi bitti
if get(handles.checkbox14,'Value')==1
kxW=str2double(get(handles.Fh,'String'))*W %yatay
yük
kyW=str2double(get(handles.Fv,'String'))*W %düşey
yük

else
kxW=0 %yatay yük
kyW=0 %düşey yük
end
%dış yük ve deprem etkisi bitti
% dış yük kuvvet dengesi
Dh=Dh+Dx
khW=khW+kxW
% dış yükler moment etkisi
d1=-i+((xd2-xd1)/2+xd1)
d2=j-((yd2-yd1)/2+yd1)
Dhd=Dhd+Dx*d2+Dy*d1

```



```

        khWe=khWe+kxW*(j-yss+sum(h)/2)
        W=W+kyW %düşey deprem yükü toplam ağırlığa ilave
edildi
        %dış yük etkileri bitti
        N1=W-(C(pta,1)*Bl*sind(Alpha)-
U*Bl*sind(Alpha)*tand(Phi(pta,1)))/FS+Dy
        N2=cosd(Alpha)+sind(Alpha)*tand(Phi(pta,1))/FS
        %Vertical force
        N=N1/N2
        ER=(C(pta,1)*Bl-
U*Bl*tand(Phi(pta,1)))*cosd(Alpha)/FS+...
        N*(tand(Phi(pta,1))*cosd(Alpha)/FS-sind(Alpha))-
kxW+Dx
        ERL=ER-EL
        %sarma etkisi sonuçlar
        if str2double(get(handles.theory,'String'))==6
        %şimdilik kohezyon etkisi ihmal çünkü karmaşık
sonuçlar çıkıyor
        XR=sum(C.*h)*0+(sum(ER.*tand(Phi)))*k
        XRL=XR-XL
        else %ohters
        XR=ER*fx*k
        XRL=XR-XL
        end
        %sonuçlar bitti
        N1=W-(C(pta,1)*Bl*sind(Alpha)-
U*Bl*sind(Alpha)*tand(Phi(pta,1)))/FS
        N=((N1+XRL)/N2)%iterasyon gerektirmeyen düzeltme
        Nb=Nb+N*Rz %N*Rz merkez çemberden kaçıklık Bedrock
ve elips için
        %Force Safety
        Ff1=Ff1+(C(pta,1)*Bl*cosd(Alpha)+(N-
U*Bl)*tand(Phi(pta,1))*cosd(Alpha))
        Ff2=Ff2+(N)*sind(Alpha)
        %Moment Safety
        N=((N1+XRL)/N2)
        Mp=Mp+(C(pta,1)*Bl*Rs+(N-U*Bl)*tand(Phi(pta,1))*Rs)
        Mo=Mo+W*(-xe+B/2+i)
        x1=[xe xe];
        y1=[ytop(1,1) ybottom(r1,1)]
        h1=line(x1,y1,'Color','red','LineStyle','--')
        %Raporlamaya geçiyoruz
        %rapor oluşturmak için tek lamda lazım
        if str2double(get(handles.edit58,'String'))==1&...
            k==str2double(get(handles.edit60,'String'))
.
.
.
.
.
        set(handles.uitable12,'Data',table12); %Rapor
tablosu
        end
        break;
        end
    end
    end
    [m,f]=mode(pta2) % frictional angle için en çok tekrar eden
layeri buluyoruz
    set(handles.edit66,'String',m)
    set(handles.edit67,'String',f)%bitti

```

```

%göllenme etkisi Ab daha önce hesaplamıştık alan
Abh= ((yw(1,end)-y(1,end))+(yw(1,end-1)-y(1,end-1)))/2
if yw(1,end)>y(1,end)
Ax=1/2*Abh^2*9.81*Ab
Axb=Ax*(j+Abh*2/3-yw(1,1))
else
Ax=0
Axb=0
end
%göllenme etkisi bitti
%burasıda sadece FOS hesapla ilgili
RM(ka)=Mp
AM(ka)=(Mo-Nb-Dhd+khWe-Axb)
FOS1(ka)=Mp/(Mo-Nb-Dhd+khWe-Axb)
RF(ka)=Ff1
AF(ka)=(Ff2-Dh+khW-Ax)
FOS2(ka)=Ff1/(Ff2-Dh+khW-Ax)
ka=ka+1

end
set(handles.edit52,'string',FOS1(1));%Newton rapson için
gerekli Bishop=FOS1(1)

%Lambda olanlar için hesap
if str2double(get(handles.theory,'String'))==4|... %spencer
seçimi
str2double(get(handles.theory,'String'))==5|... %M&price
seçimi
str2double(get(handles.theory,'String'))==6 %sarma
seçimi
Sp=find(FOS1<FOS2 ,1,'first') %lambdanın yeri (min ile max
arasında)
Spencer=FOS1(Sp)
set(handles.Nvalue,'String',Spencer)

if get(handles.checkbox14,'Value')==1&... %Deprem etkisinde
moment sabitlemek için
get(handles.togglebutton1,'Value')==1 % ve Circle ise
moment sabit
for n=1:numel(m)
FOS1(n)=FOS1(1)
Sp=1
Spencer=FOS1(Sp)
end
end %Deprem etkisi düzeltme bitti
%lambda grafik
m=kmin:step:kmax

.
.
.
.
.

end
% Update handles structure
axes(handles.axes1)
end

%sonuçlarla alakalı veriler
if str2double(get(handles.theory,'String'))==2
.
.

```

```
.  
.   
.   
    end  
    %% Plotting Factor of Safety values versus circles  
if get(handles.checkbox6, 'Value')==1  
.   
.   
.   
.   
end  
set(handles.text102, 'String', 'Calculate completed.')
```

guidata(



## **RESUME**

**Name-Surname : Ersin YILDIZ**

### **EDUCATION STATUS:**

**Undergraduate : 2011, Sakarya University, Engineering Faculty, Civil Engineering Department**

### **PROFESSIONAL EXPERIENCE AND AWARDS:**

After graduating in 2011, I worked in the private sector. I received training on the software programming language. For the last 6 years, I have been working as an engineer in the Geotechnical Applications Department in Pendik Municipality.

### **PUBLICATIONS, PRESENTATIONS AND PATENTS GENERATED FROM THE THESIS:**

Yıldız, E. & Tolon, M. (2020), *Innovative Numerical Approaches based on Traditional Slope Stability Analysis Methods: A Preliminary Study*, MAS 12th International European Conference on Mathematics, Engineering, Natural & Medical Sciences, Uluslararası Konferans, 18-19 / 07 / 2020, Izmir, Turkey, ISBN: 978-625-7139-16-8, pages 226-232.